RESEARCH REPORT 580-2

TRANSFER AND DEVELOPMENT LENGTH OF 15.2 MM (0.6 IN.) DIAMETER PRESTRESSING STRAND IN HIGH PERFORMANCE CONCRETE: RESULTS OF THE HOBLITZELL-BUCKNER BEAM TESTS

Shawn P. Gross and Ned H. Burns

CENTER FOR TRANSPORTATION RESEARCH
BUREAU OF ENGINEERING RESEARCH
THE UNIVERSITY OF TEXAS AT AUSTIN

JUNE 1995

Technical Report Documentation Page

1. Report No.	2. Government Accession No.	3. Recipient's Catalog No.
FHWA/TX-97/580-2		

4. Title and Subtitle	5. Report Date
TRANSFER AND DEVELOPMENT LENGTH OF 15.2 MM (0.6 IN.) DIAMETER PRESTRESSING STRAND IN HIGH PERFORMANCE CONCRETE: RESULTS OF THE HOBLITZELL-BUCKNER BEAM TESTS	June 1995
	6. Performing Organization Code
7. Author(s)	8. Performing Organization Report No.
Shawn P. Gross and Ned H. Burns	580-2
9. Performing Organization Name and Address	10. Work Unit No. (TRAIS)
Center for Transportation Research The University of Texas at Austin 3208 Red River, Suite 200 Austin, TX 78705-2650	11. Contract or Grant No. 9-580
12. Sponsoring Agency Name and Address	13. Type of Report and Period Covered
Texas Department of Transportation Construction/Research Section P.O. Box 5080 Austin, TX 78763-5080	Research Report (9/94— 6/95)
	14. Sponsoring Agency Code

15. Supplementary Notes

Project conducted in cooperation with the Federal Highway Administration.

16. Abstract

This study examines the transfer and development length of 15.2 mm (0.6 in.) diameter prestressing strand in high performance (high strength) concrete. Two 1067 mm (42.0 in.) deep rectangular beams, commonly called the Hoblitzell-Buckner beams, each with one row of 15.2 mm (0.6 in.) diameter strands at 51 mm (2.0 in.) spacing on center, were instrumented to measure the transfer and development length of the strands. Concrete strengths were 48.5 MPa (7040 psi) at transfer and 90.7 MPa (13,160 psi) at the time of development length testing. The strand surface condition was weathered or rusty.

Transfer length was determined from the concrete strain profile at the level of the strands at transfer. The average transfer length of the strands in the specimen beams was observed to be 14.3 inches. Code equations and other proposed equations were found to be conservative in comparison with the measured value.

Development length was determined from the results of four full-scale flexural tests on the Hoblitzell-Buckner beams with various embedment lengths. All four tests resulted in flexural failures, such that the development length of the strands was observed to be less than 78 inches. Measured values were compared to previous research results and proposed equations, including the AASHTO and ACI 318 code equations, which were found to be conservative in this case.

17. Key Words	18. Distribution Statement
Hoblitzell-Buckner beams, high performance concrete, transfer and development length	No restrictions. This document is available to the public through the National Technical Information Service, Springfield, Virginia 22161.

19. Security Classif. (of report)	20. Security Classif. (of this page)	21. No. of pages	22. Price
Unclassified	Unclassified	106	

Form DOT F 1700.7 (8-72) Reproduction of completed page authorized

TRANSFER AND DEVELOPMENT LENGTH OF 15.2 MM (0.6 IN.) DIAMETER PRESTRESSING STRAND IN HIGH PERFORMANCE CONCRETE: RESULTS OF THE HOBLITZELL-BUCKNER BEAM TESTS

by

Shawn P. Gross

and

Ned H. Burns

Research Report 580-2

Research Project 9-580
Design and Construction of Extra-High Strength Concrete Bridges

Conducted for the

TEXAS DEPARTMENT OF TRANSPORTATION

in cooperation with the

U.S. DEPARTMENT OF TRANSPORTATION
FEDERAL HIGHWAY ADMINISTRATION

by the

CENTER FOR TRANSPORTATION RESEARCH
Bureau of Engineering Research
THE UNIVERSITY OF TEXAS AT AUSTIN

June 1995

DISCLAIMERS

The contents of this report reflect the views of the authors, who are responsible for the facts and the accuracy of the data presented herein. The contents do not necessarily reflect the official views or policies of the Federal Highway Administration (FHWA) or the Texas Department of Transportation (TxDOT). This report does not constitute a standard, specification, or regulation.

There was no invention or discovery conceived or first actually reduced to practice in the course of or under this contract, including any art, method, process, machine, manufacture, design or composition of matter, or any new and useful improvement thereof, or any variety of plan, which is or may be patentable under the patent laws of the United States of America or any foreign country.

NOT INTENDED FOR CONSTRUCTION, BIDDING, OR PERMIT PURPOSES

Ned H. Burns, P.E. (Texas No. 20801)
Research Supervisor

IMPLEMENTATION

On October 26, 1988, the FHWA issued a memorandum that disallowed the use of 15.2 mm (0.6 in.) diameter strands in pretensioned applications, increased minimum strand spacing requirements, and increased the required development length for fully bonded strands to 1.6 times the AASHTO AND ACI 318 code requirements. The results of this research show that the transfer and development of 15.2 mm (0.6 in.) diameter strand *in high performance (high strength) concrete* is clearly adequate.

The results of this study, along with the results from other recent and ongoing studies around the country, show that the use of 15.2 mm (0.6 in.) diameter strand along with high performance concrete should be allowed in pretensioned applications. Furthermore, the current code provisions are shown to be quite conservative with respect to high concrete strengths, demonstrating the need to include concrete strength as a parameter in prediction equations for transfer and development length.

ACKNOWLEDGMENTS

The authors acknowledge the support of the TxDOT project director, Ms. Mary Lou Ralls (DES). Also appreciated is the support provided by the other members of the TxDOT Project Monitoring Committee, which included A. Cohen (DES), W. R. Cox (CMD), D. Harley (FHWA), G. D. Lankes (MAT), L. Lawrence (MAT), J. J. Panak (Retired), D. Van Landuyt (DES), J. P. Vogel (HOU), L. M. Wolf (DES), and T. M. Yarbrough (CSTR).

Research performed in cooperation with the Texas Department of Transportation and the U.S. Department of Transportation, Federal Highway Administration.

TABLE OF CONTENTS

CHAPTER 1. INTRODUCTION 1
1.1 Background and Problem Definition 1
1.2 Objective of the Research Program 1
1.3 Objective of this Study 2
1.4 High Performance Concrete versus High Strength Concrete 2
1.5 Organization of Presentation 3

CHAPTER 2. LITERATURE REVIEW 5
2.1 Introduction 5
2.2 Nature of Bond Stresses 5
2.3 Definitions 8
2.4 Effect of Variables 9
2.5 Previous Research 11
2.6 Equations for Transfer and Development Length 14

CHAPTER 3. TEST PROGRAM 17
3.1 Introduction and Scope of Tests 17
3.2 Specimen Design and Designation 17
3.3 Material Properties 20
3.4 Specimen Fabrication 22
3.5 Instrumentation for Transfer Length Measurements 26
3.6 Development Length Test Setup 27
3.7 Instrumentation for Development Length Tests 30
3.8 Development Length Test Procedure 34

CHAPTER 4. TEST RESULTS 37
4.1 Introduction 37
4.2 Transfer Length Measurements 37
4.3 Development Length Test Results 42

CHAPTER 5. DISCUSSION OF TEST RESULTS 55
5.1 Introduction 55
5.2 Transfer Length Measurements 55
5.3 Development Length Tests 59
5.4 Effect of Variables 63

CHAPTER 6. SUMMARY AND CONCLUSIONS 65
6.1 Summary 65
6.2 Conclusions 65

REFERENCES 67

APPENDIX A—CONTRACTOR DRAWINGS FOR HOBLITZELL-BUCKNER BEAMS 71
APPENDIX B—MATERIAL PROPERTY PLOTS 75
APPENDIX C—DEVELOPMENT LENGTH TEST SETUPS 81
APPENDIX D—MOMENT-CURVATURE SECTION ANALYSIS 87
APPENDIX E—NOTATION 93

SUMMARY

This study examines the transfer and development length of 15.2 mm (0.6 in.) diameter prestressing strand in high performance (high strength) concrete. Two 1067 mm (42.0 in.) deep rectangular beams, commonly called the Hoblitzell-Buckner beams, each with one row of 15.2 mm (0.6 in.) diameter strands at 51 mm (2.0 in.) spacing on center, were instrumented to measure the transfer and development length of the strands. Concrete strengths were 48.5 MPa (7040 psi) at transfer and 90.7 MPa (13,160 psi) at the time of development length testing. The strand surface condition was weathered or rusty.

Transfer length was determined from the concrete strain profile at the level of the strands at transfer. The average transfer length of the strands in the specimen beams was observed to be 14.3 inches. Code equations and other proposed equations were found to be conservative in comparison with the measured value.

Development length was determined from the results of four full-scale flexural tests on the Hoblitzell-Buckner beams with various embedment lengths. All four tests resulted in flexural failures, such that the development length of the strands was observed to be less than 78 inches. Measured values were compared to previous research results and proposed equations, including the AASHTO and ACI 318 code equations, which were found to be conservative in this case.

CHAPTER 1. INTRODUCTION

1.1 BACKGROUND AND PROBLEM DEFINITION

For several decades, prestressed concrete has been an efficient, economical design option for highway structures. With the use of modern, higher strength materials — specifically high performance concretes and 15.2 mm (0.6 in.) diameter prestressing strand—the benefits of prestressed concrete can be enhanced further. Longer spans and larger girder spacing may result in significantly more efficient structures. Before these materials become the standard in practice, however, more must be learned about their *interaction* in prestressed concrete members.

Prestressing strand and concrete in a pretensioned, prestressed member interact through *bond*. Bond is the mechanism through which tension in a strand is transferred to compression in the concrete. The entire concept of prestressed, pretensioned concrete as a structural material is thus based on this bond between the strand and concrete. Without bond, no transfer of forces would occur and the member would not act integrally.

As modern high strength materials are adopted for use in prestressed concrete, higher forces must be transmitted between the strand and the concrete. As a result, the demand on bond is magnified. For the implementation of these modern materials to be effective at the structural-member level, their interaction at the level of bond must first be understood.

On October 26, 1988, the Federal Highway Administration (FHWA) issued a memorandum that disallowed the use of 15.2 mm (0.6 in.) diameter strand in pretensioned applications, increased minimum strand spacing requirements, and increased the required development length for fully bonded strands to 1.6 times the AASHTO and ACI 318 code requirements. The memorandum was issued because the code requirements for bond were based on tests using materials that were effectively outdated, and because recent research results (10) had questioned the conservatism of the code (15).

As a result of the FHWA memorandum, numerous researchers have studied prestressing bond, transfer length, and development length, over the last half decade. This study specifically addresses the use of high performance concrete and 15.2 mm (0.6 in.) diameter strands and their effect on transfer and development length.

1.2 OBJECTIVE OF THE RESEARCH PROGRAM

This study is part of a research project entitled "Design and Construction of Extra High Strength Concrete Bridges," funded by the FHWA and the Texas Department of Transportation (TxDOT). The objective of the research program is to develop guidelines for the design and construction of high strength prestressed concrete bridges. The project revolves around the construction of two adjacent high strength highway bridges in Houston, Texas, namely, the northbound and southbound Louetta Road Overpass on Texas State Highway 249.

The design utilizes the new Texas Type U54 beam and 15.2 mm (0.6 in.) diameter prestressing strand at 50 mm (1.97 in.) spacing. The benefits of the U54 beam are discussed by Ralls et al. (22). The use of high performance concrete with 15.2 mm (0.6 in.) diameter strands allows for greater prestressing forces and, therefore, longer spans than may be accommodated by current standard materials. Required compressive strengths at transfer for the structural girders range from 47.6 MPa (6,900 psi) to 60.7 MPa (8,800 psi). Required 56-day compressive strengths range from 67.6 MPa (9,800 psi) to 90.3 MPa (13,100 psi). Details of the design process used for the Louetta Road Overpass are presented by Barrios (2).

A pilot study was performed to verify the adequate performance of the design beams at transfer. Results of the pilot study were very positive and are discussed in detail by Barrios (2). The current study was then performed to examine the development length of 15.2 mm (0.6 in.) diameter strands at 51 mm (2.0 in.) spacing in high performance concrete under ultimate flexural loads. An extensive quality control program is underway to monitor the fabrication of the actual structural beams. Beams are currently being instrumented for camber, strain, and temperature measurements during the casting process. Long-term performance will be monitored before and after completion of the structure. Guidelines and recommendations for the design and construction of high strength concrete bridges will be developed.

1.3 OBJECTIVE OF THIS STUDY

The purpose of this study is to determine the development length of 15.2 mm (0.6 in.) diameter prestressing strand at 51 mm (2.0 in.) spacing in high performance concrete. Full-scale rectangular beams were cast at a prestressing plant and instrumented to determine the transfer length of the strands. Beams were tested in flexure to determine if the ultimate strength of the strands could be developed by bond. The required development length for the strands was determined from the results of the flexural tests.

1.4 HIGH PERFORMANCE CONCRETE VERSUS HIGH STRENGTH CONCRETE

Simply defined, high performance concrete is any concrete that exhibits beneficial strength and/or durability properties. Beneficial strength properties may include compressive strength, tensile or flexural strength, modulus of elasticity, and creep and shrinkage characteristics. Beneficial durability properties may include low permeability, good abrasion resistance, and good freeze-thaw characteristics. A concrete does not have to have both good strength characteristics and good durability characteristics to be considered a high performance concrete, though these strength and durability properties are often inseparable.

The terms *high strength concrete* and *high performance concrete* are used somewhat interchangeably throughout the report. This is not meant to imply that all high performance concretes exhibit high strength (although all high strength concretes are high

performance concretes). The terms are used interchangeably because the content of this report is primarily concerned with the strength aspects of high performance concrete. Throughout this report, both terms are simply meant to refer to a concrete that has high strength.

1.5 ORGANIZATION OF PRESENTATION

Chapter 1 has presented a brief introduction to the study described in this report. Chapter 2 provides background material on the subject of transfer and development length of pretensioned members. The test program is described in detail in Chapter 3, and the results are presented in Chapter 4. Chapter 5 discusses the results of the test program. A summary of the study and a list of conclusions are provided in Chapter 6.

CHAPTER 2. LITERATURE REVIEW

2.1 INTRODUCTION

This chapter is intended to provide a brief theoretical background on transfer and development length of pretensioned, prestressed concrete members. First, a general overview of bond stresses is presented. Transfer and development length are then defined and the many variables that affect them are discussed. Selected experimental research programs from the past 40 years are summarized, and a list of the many proposed equations for transfer and development length is provided.

2.2 NATURE OF BOND STRESSES

2.2.1 Bond Mechanisms

There are three mechanisms by which the concrete and steel strand bond to one another in pretensioned, prestressed concrete members: adhesion, Hoyer's effect (wedge action), and mechanical interlock. Each mechanism is discussed briefly below:

Adhesion—There is a small adhesive effect between the prestressing strand and surrounding concrete that contributes to bond in pretensioned members. This adhesion is present only prior to any relative slip that may occur between the strand and the concrete. Therefore, this component of bond is often neglected.

Hoyer's effect (wedge action)—As a strand is tensioned, its diameter and cross-sectional area reduce an amount determined by Poisson's ratio of the strand. Upon transfer, the strand near the end of a pretensioned beam tries to return to its original unstressed state. However, the surrounding concrete prevents the lateral expansion of the strand back to its original diameter and area. This restraint, in the form of a normal (radial) force on the strand, induces a frictional force along the longitudinal axis of the strand. This frictional force opposes any relative movement between the strand and surrounding concrete. Since Hoyer's effect may be visualized as the strand wedging itself against the surrounding concrete to prevent slip, it is often referred to as *wedge action*.

Mechanical interlock—Seven-wire strands consist of six small wires wound around one center wire to form a helical shape. Because of this helical shape, a component of the normal force between the outer wires of the strand and the surrounding concrete acts along the axis of the strand. This component acts to resist slip between the strand and concrete. This mechanism is extremely similar to the pullout resistance provided by patterned deformations on reinforcing bars in reinforced concrete. Mechanical interlock will develop in pretensioned members only if twisting of the strand is prevented (23). When strand twist

is not restrained, the strand will simply slide through the member, as normal forces will not be developed.

2.2.2 Transfer Bond Stresses

A plot of stress and strain in the transfer zone is illustrated in Figure 2.1. For standard seven-wire prestressing strand, the stress and strain profiles are linear in the transfer zone. The increase in steel stress, from zero at the beam end to the effective prestress f_{se} at the end of the transfer zone, must be developed by *transfer bond stresses.*

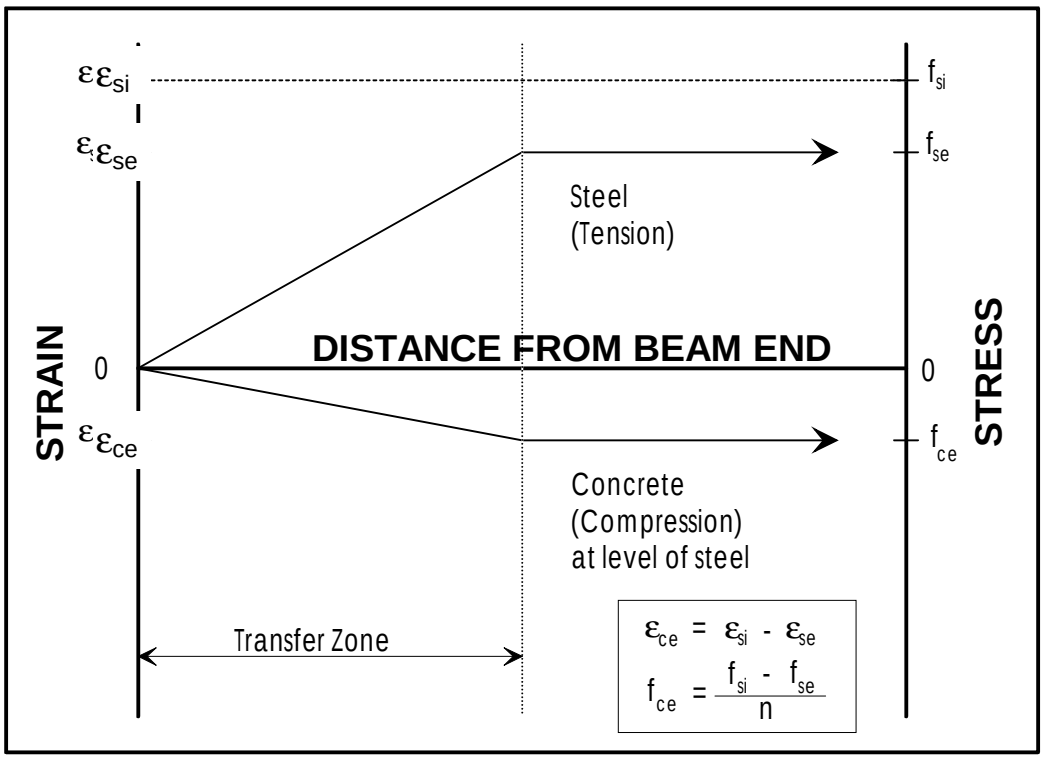

Figure 2.1 Stress and strain in the transfer zone

Bond stresses, by definition, are directly proportional to the rate of change, or derivative, of the steel stress. Thus, in the transfer zone, bond stresses must be uniform, because the steel stress varies linearly. This uniform bond stress in the transfer zone must be developed by the three mechanisms discussed in Section 2.2.1.

Since strain compatibility between the strand and concrete does not occur in the transfer zone, adhesion does not contribute to bond in the transfer zone. Hoyer's effect will serve to anchor the strand near the beam ends, as the large reduction in steel stress (from f_{si} to the steel stress line in Figure 2.1) induces sufficient wedge action. Further into the transfer zone, the steel loses a smaller proportion of its initial stress, and the contribution of

Hoyer's effect is reduced. Mechanical interlock is effective here, because Hoyer's effect closer to the end prevents strand twist. At the inner end of the transfer zone, mechanical interlock is fully effective and accounts for nearly the entire transfer bond stress.

2.2.3 Flexural Bond Stresses

Flexural bond stresses are those bond stresses required to develop an increase in strand tension caused by applied loads. Prior to flexural cracking, increases in strand tension are very small, and the resulting flexural bond stresses are very low. Once flexural cracking occurs, the concrete contributes zero tensile resistance, and the strand stress increases dramatically at the crack locations, as shown in Figure 2.2. High bond stresses must develop adjacent to cracks, where the rate of change of steel stresses is very high. When a limiting value of bond stress is reached, slip between the strand and concrete will occur over a finite distance to relieve the high bond stresses. These ideas were first proposed by Janney (13) and confirmed in tests by Hanson and Kaar (12).

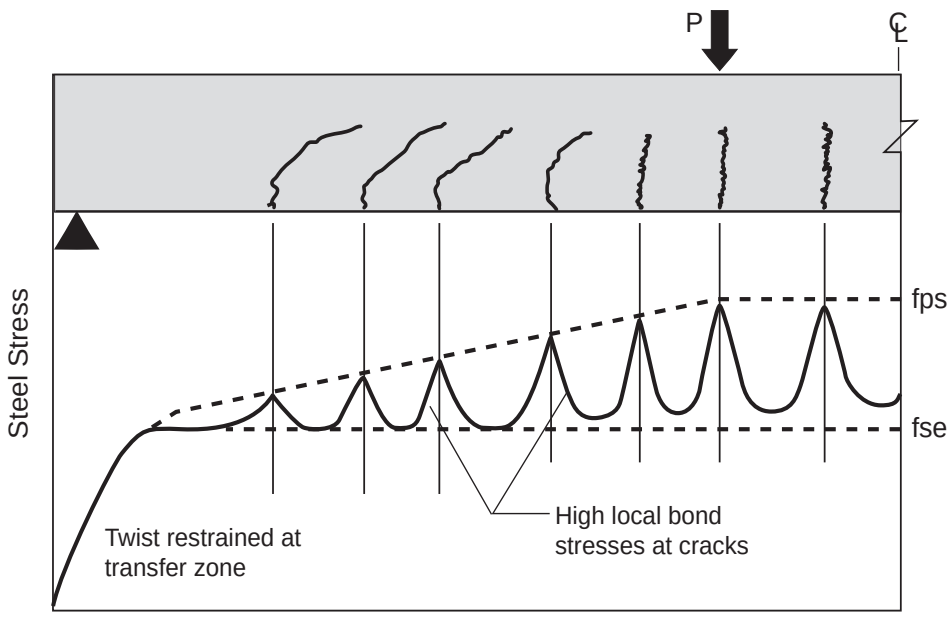

Figure 2.2 Pretensioned steel stresses in a cracked beam (23)

As moments caused by applied loads increase, flexural cracking propagates from the load point toward the beam ends in a simply supported member. With each successive flexural crack, there is an increase in strand tension accompanied by high bond stresses. Janney (13) first characterized this behavior as a wave of high flexural bond stresses, which propagates from the center of the member toward the ends under increasing applied loads.

2.2.4 General Bond Failure

Janney (13) suggested that a general bond failure would occur when the wave of high flexural bond stresses reaches the transfer zone of a pretensioned member. An increase in strand tension in the transfer zone after release will cause Hoyer's effect to be reduced. As a result, twist restraint may not be adequate to develop full mechanical interlock between the strand and concrete. The probable scenario is a sudden bond failure.

Russell and Burns (23) noted that anchorage failure also occurs when web-shear cracks in the transfer zone propagate to the level of the strand. Similar failures were reported by Burdette et al. (7) and by Mitchell et al. (19). The ultimate failure mechanism in these cases is the same as that for flexural cracking in the transfer zone: an increase in strand tension in the transfer zone results in a loss of anchorage from Hoyer's effect.

In general, any significant increase in strand tension in the anchorage zone will result in a general bond failure. Since large increases in strand tension may be the result of either flexural or shear cracking, the prediction model for general bond failure is stated by Russell and Burns (23) as follows:

> If cracks propagate through the anchorage zone of a strand, or immediately next to the transfer zone, then failure of the strand anchorage is imminent.

2.3 DEFINITIONS

Transfer length, flexural bond length, development length, and embedment length are defined below and illustrated in Figure 2.3.

2.3.1 Transfer Length

Transfer length is defined as the length of bond required to develop the effective prestress force, f_{se}, in the strand. Alternatively, transfer length may be defined as the length of bond required to transfer the fully effective prestress force from the strand to the concrete.

2.3.2 Flexural Bond Length

Flexural bond length is defined as the length of bond required to develop an increase in strand tension, from f_{se} to f_{ps}, caused by applied loads. Note that f_{ps} is the stress in the strand at the ultimate strength of the member.

2.3.3 Development Length

Development length is defined as the total length of bond required to develop the steel stress f_{ps} at the ultimate strength of the member. Development length is the algebraic sum of transfer length and flexural bond length.

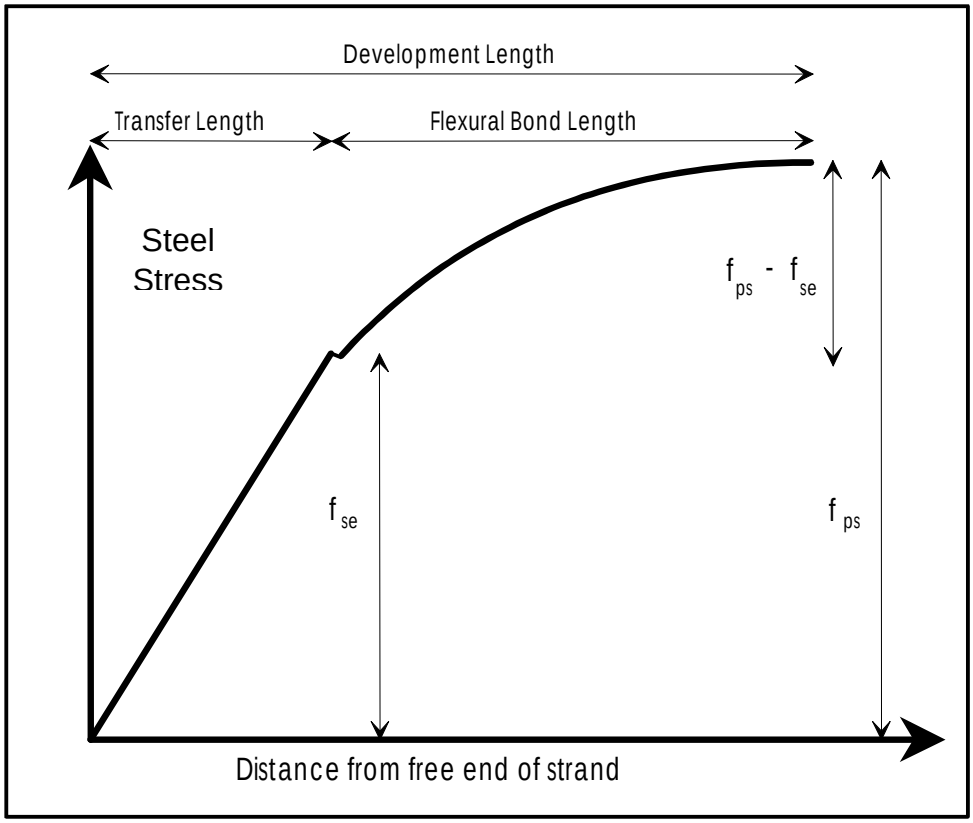

Figure 2.3 Variation of steel stress with distance from free end of strand (6)

2.3.4 Embedment Length

Embedment length is defined as the length of bond from the critical section to the beginning of bond. The critical section is the location at which the steel stress is maximum and usually occurs at the point of maximum moment. The beginning of bond occurs at the end of the member for a fully bonded strand, and at the end of debonding for a debonded strand.

In order to prevent a general bond failure, the available embedment length must be larger than the required development length:

$$L_e \geq L_d$$

2.4 EFFECT OF VARIABLES

The transfer and development length of prestressing steel is affected by many parameters (26), including:

1. Type of steel, e.g., wire, strand/stress-relieved, low relaxation
2. Steel size (diameter)
3. Steel stress level
4. Surface condition of steel—clean, oiled, rusted, epoxy coated
5. Concrete strength
6. Type of loading, e.g., static, repeated, impact
7. Type of release, e.g., gradual, sudden
8. Confinement
9. Time-dependent effects (losses)
10. Consolidation and consistency of concrete around steel
11. Cover and spacing

The effects of some of these variables are discussed below.

2.4.1 Strand Diameter

Many studies (7, 8, 12, 14, 16, 19, 23) have investigated the variation of transfer and/or development length with strand diameter. All of these studies, with one exception (7), have shown that transfer and development lengths increase for larger strand diameters. Kaar et al. (14) determined that the variation in transfer length is nearly linear with respect to strand diameter. This linear relationship is incorporated into many of the proposed equations for transfer and development length presented in Section 2.6.

2.4.2 Concrete Strength

In 1963, Kaar et al. (14) reported little influence of concrete strength on transfer lengths for up to 12.7 mm (0.5 in.) diameter strands. Concrete strengths at transfer in that test program ranged from 11.4 to 34.5 MPa (1,660 to 5,000 psi). More recently, the relationship between transfer and development lengths and concrete strength has been investigated for high strength concretes. Castrodale et al. (9) observed transfer lengths approximately 30% shorter for concrete with f'_{ci} = 64.8 MPa (9,400 psi), compared to concrete with f'_{ci} = 35.2 MPa (5,100 psi). Mitchell et al. (19), in tests with f'_{ci} ranging from 21.0 to 50.0 MPa (3,050 to 7,250 psi), and f'_c ranging from 31.0 to 88.9 MPa (4,500 to 12,900 psi), concluded that both transfer and development lengths decrease with increasing concrete strength. More recent equations developed for transfer and development length incorporate these conclusions.

2.4.3 Strand Surface Condition

The effect of strand surface condition is probably the most important variable affecting transfer length, yet it is the most difficult to determine (23). Strands may be lightly rusted, well rusted, epoxy coated with grit, oiled, or indented. Each of these conditions will affect the coefficient of friction—and thus the bonds—between the strand and the concrete. The variation in transfer and development lengths with strand surface

conditions has been noted by many researchers (7, 10, 11, 12, 13, 16, 23). In general, well-rusted and epoxy-coated strands with grit have significantly shorter transfer and development lengths than clean strands. Likewise, the presence of oils on the surface of a strand will substantially increase transfer and development lengths.

2.4.4 Type of Release

It is generally accepted that a sudden transfer of prestress caused by flame cutting or sawing will result in longer transfer lengths. This trend was reported by Kaar et al. (14), who noted a 20% to 30% increase in transfer length for flame-cut strands. Likewise, Hanson (11) reported an average increase in transfer length of 4 in. for flame-cut strands.

2.4.5 Effective Prestress Force

Transfer length will logically increase with a higher effective prestress force, f_{se}, since a higher strand stress must be developed in the transfer zone. Flexural bond length will correspondingly decrease for a higher f_{se}, since the additional strand tension to be developed at the critical section will be lower. Most proposed equations presented in Section 2.6 assume that the decrease in flexural bond length will be larger than the increase in transfer length for a given increase in f_{se}. As a result, the development length decreases with increasing effective prestress forces.

2.4.6 Strand Spacing

Only recently, and after the 1988 FHWA memorandum discussed in Section 1.1, has the effect of strand spacing on transfer and development length been examined. Russell and Burns (23) reported no difference in measured transfer lengths for 15.2 mm (0.6 in.) diameter strands at 51 and 57 mm (2.0 and 2.25 in.) spacings. Burdette et al. (7) reported similar findings for 12.7 mm (0.5 in.) diameter strands at 44 and 51 mm (1.75 and 2.0 in.) spacings. Naturally, there is a minimum spacing for a given strand diameter at which the splitting resistance of the concrete will be exceeded. Further testing is required to determine this minimum spacing for larger diameter strands. However, it is important to note that splitting was not observed in the tests of 15.2 mm (0.6 in.) diameter strands at 51 mm (2.0 in.) spacing by Russell and Burns (23).

2.5 PREVIOUS RESEARCH

Numerous experimental research programs have investigated the transfer and development of prestressing strand. Selected research programs are summarized briefly below.

2.5.1 Hanson and Kaar (12)—Portland Cement Association Laboratories (1959)

The work of Hanson and Kaar at the Portland Cement Association (PCA) Laboratories in the late 1950s created the framework for much of today's development

length testing. Twenty-four rectangular prisms, each containing one to six Grade 250 stress-relieved strands, were tested in a series of flexural tests. The main variables in the test series were strand diameter (6.4, 9.5, and 12.7 mm, or 1/4, 3/8, and 1/2 in.) and embedment length. Secondary variables included concrete strength and strand surface condition.

Hanson and Kaar's work verified the wave of high bond stress theory proposed by Janney (13) by measuring strand stresses (strains) at various stages before and after flexural cracking. Based on an analytical model developed from measured strand stresses, minimum suggested embedment lengths that could prevent bond slip were proposed: 70 in., 106 in., and 134 in. for 6.4, 9.5, and 12.7 mm (1/4, 3/8, and 1/2 in.) diameter strand, respectively. Although these recommendations are generally considered to be overconservative, the results of Hanson and Kaar's test program became the basis for the ACI 318 and AASHTO code equation for development length (6, 24).

2.5.2 Cousins, Johnston, and Zia (10)—North Carolina State University (1986)

Cousins, Johnston, and Zia studied the effects of epoxy coating on the transfer and development of prestresssing strand. Single-strand rectangular prisms were instrumented to measure transfer length, and later tested in flexure with various embedment lengths in order to determine a development length. Strand diameters were 9.5, 12.7, or 15.2 mm (3/8, 1/2, or 0.6 in.), and strand surfaces were either left uncoated or epoxy coated with grit impregnated in the surface to improve bonding characteristics.

Although Cousins, Johnston, and Zia established a pattern of significant reduction in transfer and development lengths for epoxy-coated strands, their most significant findings may have been their measurements on uncoated strands. They reported average transfer lengths of 34, 50, and 56 in., and development lengths of 57, 119, and 132 in., for 9.5, 12.7, or 15.2 mm (3/8, 1/2, and 0.6 in.) strands, respectively. These measured values were significantly larger than values predicted by the AASHTO and ACI 318 code equations. This apparent lack of conservatism in the code equations was a factor that ultimately led to the FHWA memorandum discussed in Section 1.1 (15).

2.5.3 Burdette, Deatherage, and Chew (7)—Univ. of Tenn., Knoxville (1991)

Burdette, Deatherage, and Chew measured transfer and development lengths on twenty full-scale AASHTO Type I beams with large strand diameters (12.7, 14.3, and 15.2 mm, or 1/2, 9/16, and 0.6 in.). Average transfer lengths of 32, 35, and 24 in. were measured for 12.7, 14.3, and 15.2 mm (1/2, 9/16, and 0.6 in.) strands, respectively. The smaller measured transfer length for 15.2 mm (0.6 in.) strand contradicts the general trend in the literature of transfer length increasing with strand diameter. Approximate development lengths for 12.7, 14.3, and 15.2 mm (1/2, 9/16, and 0.6 in.) strand sizes were 80, 105, and 85 in. Based on the data, the researchers proposed conservative modifications to the existing AASHTO and ACI 318 code equations.

This research program also investigated the influence of strand spacing on transfer and development length. Comparable results were noted for 12.7 mm (0.5 in.) strands spaced at 44 and 51 mm (1.75 in. and 2.0 in.).

2.5.4 Russell and Burns (23)—The University of Texas at Austin (1993)

Russell and Burns performed an extensive study on transfer length of 12.7 mm (0.5 in.) and 15.2 mm (0.6 in.) diameter strands. The effects of strand diameter, strand spacing, confinement, cross-sectional size, strand debonding, and many other variables were examined. Specimens were rectangular prisms with gradual release of pretensioning. The average transfer length of 12.7 mm (0.5 in.) diameter strands was 30 in., and the average transfer length of 15.2 mm (0.6 in.) diameter strands was 41 in. Strand spacing and confinement were observed to have no effect on transfer length. Shorter transfer lengths were noted for smaller strand diameters, larger cross sections, and debonded strands.

Nineteen full-scale AASHTO-type girders and nine rectangular beams were tested to determine development length of 12.7 mm (0.5 in.) and 15.2 mm (0.6 in.) diameter strand. The reported values of development length for the AASHTO-type beams were 72 and 84 in., for 12.7 mm (0.5 in.) and 15.2 mm (0.6 in.) diameter strands, respectively. Many of the bond failures in the AASHTO-type beams were precipitated by shear failures, demonstrating the possibility that shear may have a significant influence on the bond requirements in a pretensioned beam. For the rectangular specimens, the reported development lengths were 96 in. for 12.7 mm (0.5 in.) diameter strands, and less than 78 in. for 15.2 mm (0.6 in.) diameter strands. The surface of the 12.7 mm (0.5 in.) diameter strand in the rectangular beams may have been contaminated by oil prior to casting, contributing to the longer-than-expected development length.

Russell and Burns also proposed a new form of development length equation, which limits the applied loads such that cracking is prevented in the transfer zone.

2.5.5 Mitchell, Cook, Khan, and Tham (19)—McGill University (1993)

Mitchell et al. studied the influence of high strength concrete on transfer and development length. Twenty-two single-strand prisms were cast with 9.5, 12.7, and 15.7 mm (3/8, 1/2, and 0.62 in.) diameter strands. Concrete strengths at transfer ranged from 21.0 to 50.0 MPa (3,050 to 7,250 psi), and 28-day concrete strengths ranged from 31.0 to 88.9 MPa (4,500 to 12,900 psi). The results showed a definite decrease in transfer and development length for high concrete strengths. The average transfer length for 15.7 mm (0.62 in.) diameter strands was 30 in. for f'_{ci} = 20.7 MPa (3,000 psi) and 19 in. for f'_{ci} = 47.9 MPa (6,950 psi). Approximate development lengths for 15.7 mm (0.62 in.) diameter strands were greater than 73 in. for f'_c = 31.0 MPa (4,500 psi) and 30 in. for f'_c = 65.0 MPa (9,430 psi). Mitchell et al. proposed revised transfer and development length equations to account for the influence of concrete strength.

2.5.6 Barrios and Burns (2)—The University of Texas at Austin (1994)

As part of this current research program, Burns and Barrios measured transfer length on five full-scale, high strength specimens at a prestressing plant. Three rectangular slab-type specimens and two Texas Type U54 beams with concrete strengths at transfer ranging from 54.3 to 63.0 MPa (7,880 to 9,130 psi) were instrumented. The measured transfer length on the rectangular slab-type specimens was less than 27 in. for fully bonded strands and 18 to 24 in. for debonded strands. The exact transfer length for the U54 beams was difficult to determine because of the effects of staggered debonding and the transition from a solid end block to the beam cross section 457 mm (18 in.) from the end of the specimen. A finite element analysis by Baxi and Burns (3) showed the transfer length of the U-beams to be 18 inches.

2.6 EQUATIONS FOR TRANSFER AND DEVELOPMENT LENGTH

2.6.1 AASHTO and ACI 318 Code Equations

The AASHTO (24) and ACI 318 (6) codes are nearly identical in their requirements for transfer and development of prestressing strand. Both codes require a minimum development length, which is calculated by a simple equation. Note that both codes use the standard unit of *inches* for development length. The AASHTO Code provisions are as follows:

9.28.1 Three- or seven-wire pretensioning strand shall be bonded beyond the critical section for a development length, in inches, not less than

$$\left(f^*_{su} - \tfrac{2}{3} f_{se}\right) \cdot D$$

where D *is strand diameter in inches, and* f^*_{su} *and* f_{se} *are expressed in kip per square inches.*

9.28.2 Investigation may be limited to cross sections nearest each end of the member that are required to develop their full ultimate capacity.

This code equation was derived by Alan Mattock and is based on the results of transfer and development tests by Hanson and Kaar (12) and Kaar et al. (14) at the PCA in the late 1950s and early 1960s (25). The expression presented above may be rewritten as follows:

$$\frac{f_{se}}{3} \cdot D \quad + \quad \left(f^*_{su} - f_{se}\right) \cdot D$$

where the first term represents the transfer length of the strand and the second term represents the additional flexural bond length required for development of the strand (6). Transfer length and flexural bond length are defined in Section 2.3 and illustrated in Figure 2.3.

The code equation for required development length is clearly flexural in nature. The accompanying provision, however, implies that any critical section nearest the end of a member that may develop the design strength of the strand, regardless of its nature (flexure, shear, axial loads), should be investigated. The possibility of shear cracking as a precipitator of bond failure is discussed in Section 2.2.4.

The shear provisions of each code (AASHTO Section 9.20.4/ACI 318 Section 11.4.4) assume a transfer length of 50 strand diameters for purposes of computing V_{cw}, the resistance to web-shear cracking of the concrete alone. This assumption is merely a simplification of the transfer length portion of the development length equation, based on a strand stress after losses of 1030 MPa (150 ksi) (25). With the Grade 270 prestressing strand used today, this simplification becomes slightly less conservative.

2.6.2 Other Proposed Equations

Several authors (5, 7, 10, 18, 19, 23, 26) have presented equations for transfer and development length of prestressing strand. A list of proposed equations may be found in Table 2.1. All of the equations compute the transfer or development length in *inches.*

The majority of these equations are empirical in nature, and take the form of the code equations presented in the previous section. Some have attempted to incorporate the effect of concrete strength, while others have modified coefficients in an attempt to make the equations more conservative. Buckner (5) has proposed a modification to the code equations based on a minimum strand strain at failure. Cousins, Johnston, and Zia (10) developed an analytical model that accounts for strand surface condition. Russell and Burns (23) presented a relationship based on preventing cracking in the transfer zone.

Since so many variables affect transfer and development length of prestressing strand, it is clearly difficult to develop equations that are applicable and accurate for all cases. This may account for the large number of proposed equations and models on this subject.

Table 2.1 Transfer and Development Length Equations

Author(s)	Yr.	TL Equation	DL Equation
AASHTO/ACI 318[1]	1963	$L_t = \frac{f_{se}}{3} \cdot D$ $L_t \approx 50 \cdot D$	$L_d = L_t + \left(f^*_{su} - f_{se}\right) \cdot D$
Martin and Scott[2]	1976	$L_t = 80 \cdot d_b$	$f_{ps} \le \frac{L_e}{80 \cdot d_b}\left(\frac{135}{d_b^{1/6}} + 31\right) \quad L_e \le 80 \cdot d_b$ $f_{ps} \le \frac{135}{d_b^{1/6}} + \frac{0.39 \cdot L_e}{d_b} \quad L_e > 80 \cdot d_b$

Author(s)	Yr.	TL Equation	DL Equation
Cousins, Johnston and Zia[3]	1990	$L_t = \frac{\left(U'_t \cdot \sqrt{f'_{ci}}\right)}{2 \cdot B} + \frac{f_{se} \cdot A_{strand}}{\pi \cdot d_b \cdot U'_t \cdot \sqrt{f'_{ci}}}$	$L_d = L_t + \left(f_{ps} - f_{se}\right) \cdot \left(\frac{A_{strand} / \left(\pi \cdot d_b\right)}{U'_d \cdot \sqrt{f'_c}}\right)$
Russell and Burns[4]	1993	$L_t = \frac{f_{se}}{2} \cdot d_b$	$M_{cr} > L_t \cdot V_u$ Fully Bonded $\frac{L_b + L_t}{Span} \le \frac{1}{2} \cdot \left[1 - \sqrt{1 - \frac{M_{cr}}{M_u}}\right]$ Debonded
Mitchell et al.[5]	1993	$L_t = \frac{f_{si} \cdot d_b}{3} \cdot \sqrt{\frac{3}{f'_{ci}}}$	$L_d = L_t + \left(f_{ps} - f_{se}\right) \cdot d_b \cdot \sqrt{\frac{4.5}{f'_c}}$
Burdette, Deatherage, and Chew	1994	$L_t = \frac{f_{si}}{3} \cdot d_b$	$L_d = L_t + 150 \cdot \left(f_{ps} - f_{se}\right) \cdot d_b$
Buckner (FHWA)	1994	$L_t = \frac{1250 \cdot f_{si} \cdot d_b}{E_c} \approx \frac{f_{si}}{3} \cdot d_b$	$L_d = L_t + \lambda \cdot \left(f_{ps} - f_{se}\right) \cdot d_b$ $\lambda = \left(0.6 + 40\varepsilon_{ps}\right)$ or $\left(0.72 + 0.102 \frac{\beta_1}{\omega_p}\right)$ $\left(1.0 \le \lambda \le 2.0\right)$

1 in. = 25.4 mm

Note: Notation changed in some cases to provide consistency between equations.
All equations are in standard units of inches for transfer and development length

(1) *Second equation for TL is from shear provisions of AASHTO 9.20.4 ACI 318 11.4.*

(2) *Martin and Scott's DL equations limit f_{ps} as a function of L_e.*

(3) *B = 300 psi/in. on average; U'_t and U'_d are functions of strand surface conditions.*

(4) *Russell and Burns' DL criteria are based on preventing cracking in transfer zone.*
L_b = Length of debonding for debonded strands.

(5) *f'_{ci} and f'_c in units of ksi.*

CHAPTER 3. TEST PROGRAM

3.1 INTRODUCTION AND SCOPE OF TESTS

The main portion of the test program consisted of four experimental tests performed on full-scale rectangular prestressed concrete beams. The goal of the test program was to determine the development length of the prestressing strands in the specimens. Specimens were designed to be identical, while the test setup was designed to be variable for each of the four tests. Specific characteristics of the test specimens included:

1) 15.2 mm (0.6 in.) diameter prestressing strands
2) high performance concrete (high concrete strengths)
3) minimal strand spacing and cover
4) fully bonded strands

The original rectangular section was designed in May 1993 by Jim Hoblitzell of the Federal Highway Administration (FHWA). Dale Buckner, of the Virginia Military Institute and author of an analysis of recent transfer and development research for the FHWA (5), suggested slight modifications to the section in June 1993. Two identical beams, commonly referred to as the Hoblitzell-Buckner beams, were then cast in December 1993 at Texas Concrete Company in Victoria, Texas. Both beams were shipped to the Phil M. Ferguson Structural Engineering Laboratory at The University of Texas at Austin in January 1994 for structural testing. A series of four experimental tests, one on each beam end, began in April 1994.

A second portion of the test program involved the measurement of the transfer length of the 15.2 mm (0.6 in.) diameter strands. The same two beams fabricated for the development length tests were instrumented during the casting process in Victoria, Texas. Measurements were made to determine the strain profile in the concrete at the level of the strands at transfer for each of the four specimen ends. The constructed strain profile was then used to determine the transfer length of the strands.

This chapter discusses the specimen design and fabrication, as well as the instrumentation and test setup, for both transfer length measurements and development length tests.

3.2 SPECIMEN DESIGN AND DESIGNATION

3.2.1 Specimen Design

The specimen cross section was designed to permit the examination of the transfer and development of 15.2 mm (0.6 in.) diameter prestressing strands with minimal spacing and cover. A single row of six strands was selected with 51 mm (2.0 in.) spacing on center

and 51 mm (2.0 in.) cover, resulting in a cross-sectional width of 356 mm (14 in.). This minimum width section design allowed for the examination of the critical case of high splitting stresses along the plane of prestressed reinforcement, and did not limit a bond failure to the pullout of individual strands.

Another objective of the section design was to ensure that the strain in the prestressing steel at flexural failure was at least the guaranteed minimum elongation of the strand, taken to be 0.035 or 3.5%. A 1,067 mm (42 in.) deep section was arbitrarily chosen. The original design called for a concrete compressive release strength of 41.4 MPa (6,000 psi) and a 28-day strength of 55.2 MPa (8,000 psi). For this concrete strength, the steel strain at failure was calculated to be approximately 0.025. In order to raise the neutral axis, compression steel in the form of three #9 bars was added to the cross section at a depth of 51 mm (2.0 in) from the top of the beam. A calculated steel strain of approximately 0.033 resulted and was deemed adequate. The inclusion of compression steel also greatly simplified the installation of shear stirrups for the contractor. As discussed in Section 3.3.2, the actual concrete strength at testing was greater than 90 MPa (13,050 psi), raising the neutral axis even higher and increasing the calculated steel strain at failure above 0.040. A sketch of the specimen cross section is shown in Figure 3.1.

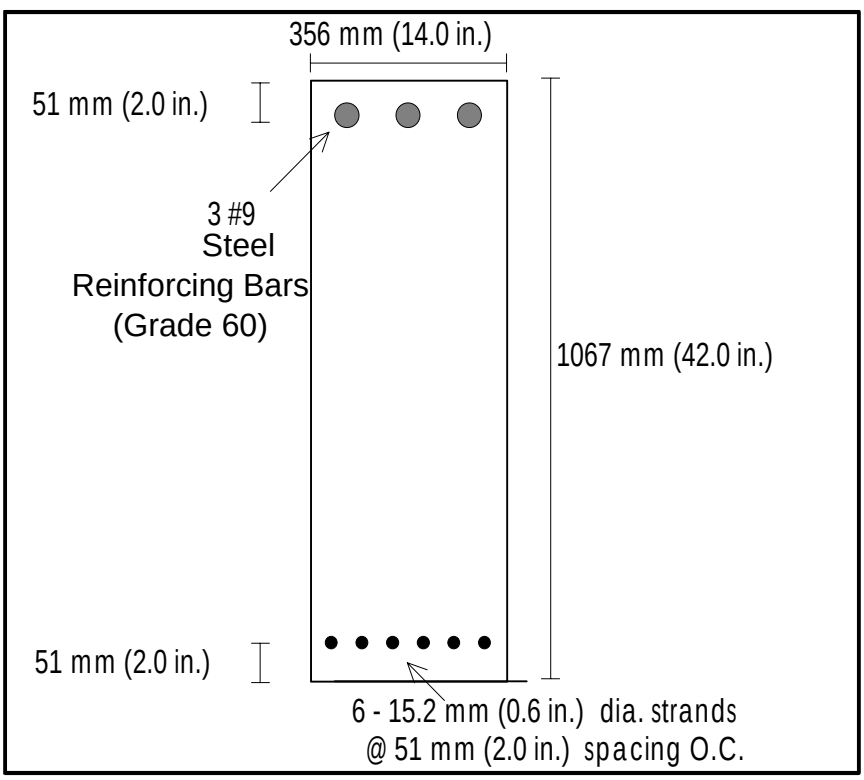

Figure 3.1 Specimen cross section

The selection of a rectangular section had two major advantages. First, the rectangular section permitted the use of simple formwork by the contractor, as discussed in Section 3.4.3. More importantly, the rectangular section eliminated any potential for web-shear cracking because of its wide web. As discussed in Section 2.2.4, web-shear cracking near beam ends can precipitate general bond failure.

Each beam was designed to be 13.56 m (44.5 ft) in length, so that both ends of each beam could be tested individually. Approximate lengths of cracked sections were calculated to verify that an adequate length of uncracked beam would remain for a second test on the opposite beam end. Nominal shear reinforcement for each beam consisted of Grade 60 U-shaped #4 bars at 457 mm (18 in.) spacing along the beam length and two additional stirrups at the beam ends. Note that only minimum shear reinforcement was required because of the wide web of the rectangular section. Additional anchorage zone reinforcement, in the form of Grade 60 #3 bars that completely circle the six strands, was included to resist splitting stresses resulting from the transfer of prestress force. Prestressing strands were fully bonded along the length of each beam. The contractor drawings for the test beams may be found in Appendix A.

3.2.2 Specimen and Test Designation

The two identical specimen beams were designated D1 and D2 at casting. Each specimen end was then identified based on its orientation during casting. For example, specimen D1S was the south end (during casting) of beam D1.

Each test was designated in three parts, as summarized in Table 3.1. The first part is the number of the experimental test. The second part is the beam end designation, as discussed above. The third part is the embedment length for that test, in the standard unit of *inches*. Embedment length was defined in Section 2.3.4.

Table 3.1 Experimental test designations

Test Designation	**Test Number**	**Beam End**	**Embedment Length (*in.*)**
1-D1N-163	1	D1N	163
2-D1S-119	2	D1S	119
3-D2N-102	3	D2N	102
4-D2S-78	4	D2S	78

3.3 MATERIAL PROPERTIES

3.3.1 Pretensioning Strands

The pretensioning reinforcement used in the test specimens was 15.2 mm (0.6 in.) diameter Grade 270 low-relaxation seven-wire strand. The 15.2 mm (0.6 in.) diameter strand is the largest diameter strand currently produced by strand manufacturers. The nominal cross-sectional area is 140 mm^2 (0.217 $in.^2$), which is 41.8% larger than the 98.7 mm^2 (0.153 $in.^2$) nominal area of 12.7 mm (0.5 in.) diameter strand. This permits a significant increase in the load-carrying capacity of each strand. However, an increased load capacity results in a higher bond stress per unit length of strand. These higher bond stresses raise the potential for both anchorage slip and splitting cracks parallel to the strand. This increased potential for bond failures when using 15.2 mm (0.6 in.) diameter strands is the fundamental purpose of this study. Bond and bond stresses are discussed in greater detail in Section 2.2.

The strand used in the test specimen beams was manufactured by Shinko Wire America, Inc. The strand was part of a shipment of five large coils of 15.2 mm (0.6 in.) diameter wire to Texas Concrete Company, the contractor who fabricated the test specimens. The strand manufacturer performed tensile tests on two strand samples from the shipment. Two additional strand samples were tested at the Construction Materials Research Group at The University of Texas at Austin. The results of all tests are summarized in Table 3.2. The load-elongation plots for each test may be found in Appendix B. The modulus of elasticity of the strand is taken to be 193 GPa (28,000 ksi).

Table 3.2 Tensile tests on prestressing strands

Test	Shinko #1	Shinko #2	CMRG #1	CMRG #2	AVG
Breaking Load kN (kip)	269 (60.5)	267 (60.0)	270 (60.7)	274 (61.5)	270 (60.7)
Breaking Stress MPa (ksi)	1922 (278.8)	1906 (276.5)	1929 (279.7)	1954 (283.4)	1928 (279.6)
Load at 1% Elongation kN (kip)	258 (58.0)	258 (58.0)	235 (52.9)	244 (54.8)	249 (55.9)
Stress at 1% Elongation MPa (ksi)	1843 (267.3)	1843 (267.3)	1681 (243.8)	1741 (252.5)	1777 (257.7)
Total Elongation	9.0%	8.2%	N/A	N/A	8.6%

The strand condition prior to casting was weathered or rusty. The coil from which the strand was drawn had clearly been exposed to significant rain and moisture at the prestressing plant for some time before the casting of the test specimens. This strand condition was observed to be typical of most of the strand at the plant. As discussed in

Section 2.4.3, the strand condition is one of many variables that affects transfer and development length

3.3.2 Concrete

Concrete for the test specimens was batched and mixed on site at the prestressing plant in Victoria, Texas. The original design of the test beams required a concrete release strength of 41.4 MPa (6,000 psi) and a 28-day design strength of 55.2 MPa (8,000 psi). The contractor elected to use its own standard 55.2 MPa (8,000 psi) mix design for the casting of the test specimens. This mix design is summarized in Table 3.3. Because conditions were cold and rainy at the time of casting on December 17, 1993, the contractor ultimately elected to reduce the water content of the mix. The slump of the initial batch measured 6.5 inches.

A set of companion 102 x 204 mm (4 x 8 in.) cylinders was cast from a concrete batch corresponding to each beam. Cylinders were moist cured and tested for compressive strength and modulus of elasticity at various intervals. Complete plots of cylinder compressive strengths and moduli of elasticity against time are located in Appendix B. A summary of critical values may be found in Table 3.4. It is important to note that the compressive strengths at the time of testing were 90.3 to 91.2 MPa (13,090 to 13,220 psi), more than 63% higher than the 28-day design strength of 55.2 MPa (8,000 psi). These high strengths classify the concrete as high performance concrete.

Table 3.3 Concrete mix design

Material	**Quantity** kg/m^3	**Quantity** (lb/yd^3)
Type III Cement	362	(611)
Water	123	(207)
Coarse Aggregate (3/4” Rock)	1159	(1954)
Fine Aggregate (Sand)	775	(1307)
Pozzolith 100XR (Retarder)	577 mL	(19.5 oz.)
Admixture LL-400-N (HRWR)	3.84 L	(130.0 oz.)

Table 3.4 Summary of concrete compressive strengths

Time	**Design Requirements** MPa (psi)	**Beam D1 Cylinders** MPa (psi)	**Beam D2 Cylinders** MPa (psi)
Release (16 hours)	41.4 (6,000)	48.5 (7,040)	48.5 (7,040)
28 days	55.2 (8,000)	81.4 (11,810)	82.0 (11,890)
Testing (116 days)	N/A	90.3 (13,090)	N/A
Testing (139 days)	N/A	N/A	91.2 (13,220)

3.4 SPECIMEN FABRICATION

The test specimens were fabricated December 16–18, 1993, at Texas Concrete Company in Victoria, Texas. The stressing operations and mild steel placement were performed on the first afternoon. Formwork was erected the second morning and beams were cast that afternoon. Formwork removal and the release of prestress took place the next day.

3.4.1 Pretensioning Procedure

The six strands were pretensioned according to the standard method used by the contractor. Each strand was first cut to an approximate length, anchored at the dead end (north end) of the bed using a strand chuck, and was then stretched the length of the bed. Strands were individually tensioned at the live end (south end) of the bed to a specified elongation of 316 mm (12.43 in.) using a hydraulic jack. This calculated elongation is derived from the common strength of materials equation:

$$\delta = \frac{PL}{AE}$$

where

δ = the total elongation between end anchorages,

P = the force in one strand,

L = the length of the strand between end anchorages,

A = the area of one strand, and

E = the modulus of elasticity of the strand.

Strands were stressed an extra 9.5 mm (3/8 in.) in order to account for the slip resulting from anchorage of the strand. Calculations were based on a desired force per strand of 195.5 kN (43.95 kip). The actual force per strand, as calculated during stressing operations, was 196.6 kN (44.21 kip). This is an overstress error of 0.6%, which is well within acceptable tolerance.

3.4.2 Mild Steel Placement

Following the stressing operation, shear and anchorage zone reinforcement was placed. Stirrups were first tied to the row of stressed strands. The compression steel, consisting of three #9 bars, was then tied to the stirrups along the length of the beam. To finalize the mild steel fabrication, anchorage zone reinforcement was placed at the ends of each beam. Figure 3.2 is a photograph of the mild steel reinforcement in one of the test beams.

3.4.3 Formwork

Steel rectangular forms owned by the contractor were used for the specimen fabrication. After the bottom of the prestressing bed was lubricated with form oil, each side form was lowered into place by crane. Once the side pieces had been placed, they were tied together every few feet using small cross pieces. End forms consisted of simple plywood cutouts placed at each beam end prior to the stressing of the strands.

Figure 3.2 Mild steel reinforcement

3.4.4 Placement and Curing of Concrete

Concrete for the specimens was mixed at the on-site batching plant and transported in 4-cubic yard buckets to the prestressing bed. Concrete was placed in the beams and vibrated internally. The entire casting required four batches; the first two batches were placed in beam D2, and the second two batches were placed in beam D1. Concrete for companion cylinders was sampled from the second and fourth batches. The bed arrangement and concrete placement are shown in Figure 3.3.

The concrete was cast between 2:00 p.m. and 2:30 p.m. on December 17, 1993. The weather conditions during casting were cold and rainy, with a temperature of approximately 7°C (45°F). Because of the rain, temporary shelters were held over the beams by cranes during the casting operation.

After casting was completed, the beams were covered with burlap and heavy cotton blankets. Beams were then steam cured overnight to ensure that the required release strength would be obtained the following day.

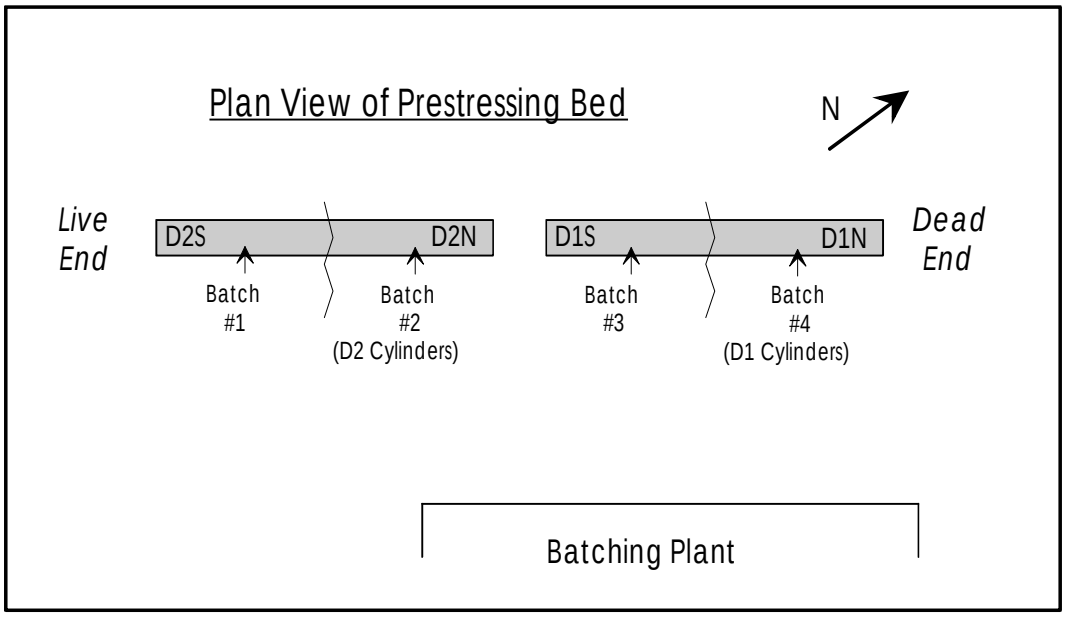

Figure 3.3 Bed arrangement and concrete placement

3.4.6 Release of Prestress Force

After the instrumentation of the beams for transfer length measurements was completed and initial measurements were taken, the release of prestress force began. Since the beams contained only six strands, the contractor elected to flame-cut rather than slowly detension the strands. As a safety precaution, large concrete blocks were placed over the exposed strand at the dead end of the bed. This prevented any violent movement of the strands upon release of the prestress force. The strands were first cut simultaneously at the dead and live ends of the bed, beginning with the outside strands and moving progressively inward. Strands were then cut at the location between the two beams. Note that no splitting cracks were observed upon transfer of prestress.

Approximate stresses immediately after transfer were computed using a simple elastic analysis with transformed section properties, and are compared to allowable stresses from ACI 318 Section 18.4 (6) in Table 3.5. An immediate elastic shortening loss of 46.3 MPa (6.72 ksi) or 3.30% at the ends, and 34.7 MPa (5.03 ksi) or 2.47% at midspan, was included in the calculations. Computed stresses exceeded ACI allowable tensile stresses at the top fiber, both at the end and at midspan. However, no flexural cracking resulting from the transfer of prestress force was observed during an inspection of the beams shortly after

transfer. The lack of cracking was probably caused by the presence of compression steel and a factor of safety against cracking inherent in the ACI allowable stresses. According to Carrasquillo et al. (8), the modulus of rupture for high strength concrete is between $8\sqrt{f'_c}$ and $12\sqrt{f'_c}$. Camber, measured on each side of both beams at midspan using a steel ruler, is compared to predicted values in Table 3.6.

Table 3.5 Fiber stresses immediately after transfer

Location	**Computed Stress from Elastic Analysis** [(1)] MPa (psi)	**Allowable Stress from ACI 318** [(2)] MPa (psi)
Top Fiber at Ends	-4.73 (-686)	-3.63 (-527)
Bottom Fiber at Ends	10.74 (1,557)	31.94 (4,632)
Top Fiber at Midspan	-1.94 (-282)	-1.82 (-264)
Bottom Fiber at Midspan	7.94 (1,152)	31.94 (4,632)

(1) Assumed E_{ci} = 41.4 GPa (6,000 ksi) at transfer in computing elastic losses.
(2) Based on cylinder strength of f'_{ci} = 53.2 MPa (7,720 psi) at transfer.
Notes: Compressive stresses are positive, tensile stresses are negative.
Stresses were computed using transformed section properties.

Table 3.6 Camber immediately after transfer

Calculated Midspan Camber	**5.8 mm (0.23 in.)**
Measured Midspan Camber	
Beam D1 East Side	3.3 mm (0.13 in.)
Beam D1 West Side	4.8 mm (0.19 in.)
Beam D2 East Side	2.3 mm (0.09 in.)
Beam D2 West Side	5.6 mm (0.22 in.)
AVERAGE	**4.1 mm (0.16 in.)**

One month after release, a tensile crack was observed on each beam end approximately 178 mm (7.0 in.) above the level of the strands. Each crack extended roughly 102 to 152 mm (4 to 6 in.) along each side face of the beam before closing. This crack, which is not structurally significant, is typical of many prestressed concrete beams, and results from a significant principal tensile stress acting perpendicular to the prestressing force as a result of the flow of compressive stresses in the end region (20). A typical tensile crack may be seen at a beam end in Figure 3.4.

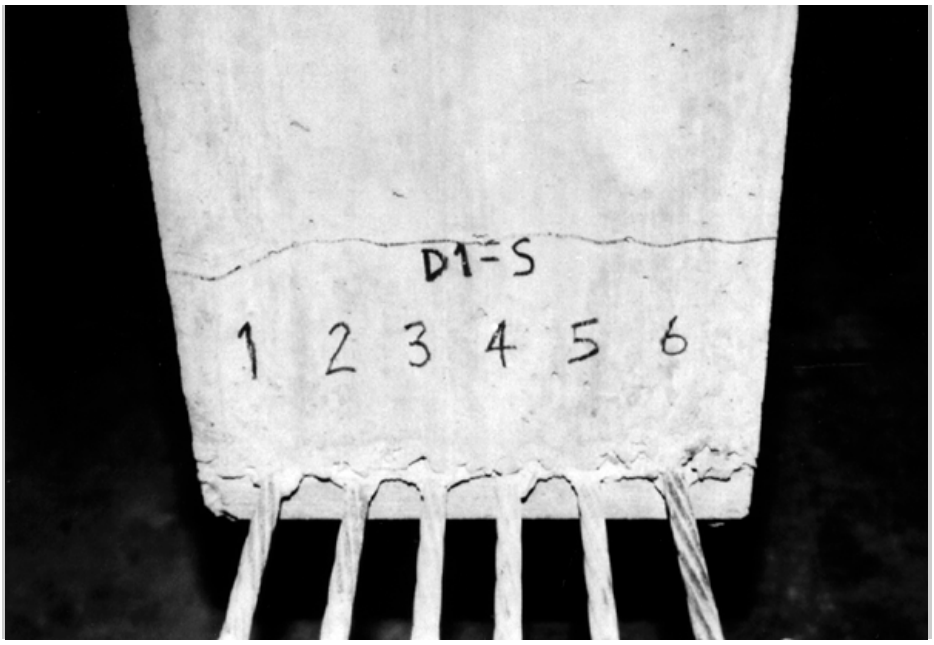

Figure 3.4 Tensile crack at beam end

3.5 INSTRUMENTATION FOR TRANSFER LENGTH MEASUREMENTS

3.5.1 Overview of the DEMEC Mechanical Strain Gauge System

Instrumentation for transfer length measurements at beam ends utilized the DEMEC Mechanical Strain Gauge System manufactured by the Hayes Manufacturing Company in England. This instrumentation process has been used in previous research at The University of Texas at Austin (1, 2, 9, 23), and is described in detail in this section.

DEMEC target points consist of stainless steel discs approximately 6.4 mm (0.25 in.) diameter, with a machined gauge point centered on the disc. The DEMEC gauge is placed in between two discs approximately 200 mm (7.87 in.) apart, and the precise distance between the points is measured. One division on the DEMEC's dial gauge indicator corresponds to a distance of 0.002 mm (7.87 x 10^{-5} in.). Measurements made at different time periods may be compared, and an incremental strain may be calculated. The overall accuracy of the DEMEC system has been reported to be approximately 16 microstrains (1).

3.5.2 Installation of DEMEC Target Points

DEMEC target points were placed along the side faces of the end regions of the test beams immediately after the removal of the forms. Points were spaced at 50 mm (1.97 in.)

intervals along the level of the strand for a distance of 1.83 m (6.0 ft.) from the beam ends. Approximate point locations were first marked out on all sides using a tape measure. A group of four points was then placed using 5-minute epoxy gel and a standard placement bar supplied by the gauge manufacturer. The epoxy was allowed a minimum of 10 minutes to set before the following group of points was installed. This installation procedure ensured that distances between each set of points for a single reading remained approximately 200 mm (7.87 in.). A total of 304 DEMEC points were installed in about 2 hours.

3.5.3 Initial and Final Measurements

Prior to the transfer of prestress force, initial measurements were taken using the DEMEC gauge. As seen in Figure 3.5, readings were taken between each set of points approximately 200 mm (7.87 in.) apart. Each reading for a set of points was taken twice (consecutively) to ensure accuracy. If readings were not within two gauge divisions, equivalent to approximately 16 microstrains, a third reading was taken. Readings were recorded manually on a data sheet and later transferred to a computer spreadsheet for data reduction.

Shortly after the release of prestress force, final measurements were taken between each set of points. The same procedure utilized in the initial measurements was followed. The difference between the initial and final measurements was then used to compute the strains resulting from the transfer of prestressing force. The method of data reduction is discussed in Section 4.2.1.

3.5.4 End Slip Measurements

In order to measure the relative movement between the strand and the concrete at the beam ends, strands were marked with tape and fluorescent paint a distance of 152 mm (6.0 in.) from each beam end, as shown in Figure 3.6. After the transfer of the prestress force, the distances between the marked location on each strand and the beam end were remeasured using a steel ruler. Each measurement was taken to the nearest 0.8 mm (1/32-in.). The difference between the initial and final lengths was recorded on a data sheet. The results of the end slip measurements are presented in Section 4.2.2.

3.6 DEVELOPMENT LENGTH TEST SETUP

Development length testing was performed in April and May 1994 at the Ferguson Structural Engineering Laboratory at The University of Texas at Austin. The setup for each test included a simply supported span with a cantilevered end, as shown in Figure 3.7. Beams were supported by large concrete blocks upon which elastomeric bearing pads were placed. The supports placed the beams approximately 2 feet above the testing floor. Load was applied by the 2,670-kN (600-kip) capacity Riehle testing machine to a spreader beam centered along the simply supported region of the test beam. The weight of the spreader beam and its bearing plates was approximately 3.78 kN (850 lb). Half of the total applied

load was transmitted to the specimen beam at each of the bearing locations of the spreader beam, creating a constant *applied* moment region. Note that the total moment in this section is not constant because of the dead load moments resulting from the beam's weight.

Figure 3.5 Reading of DEMEC points

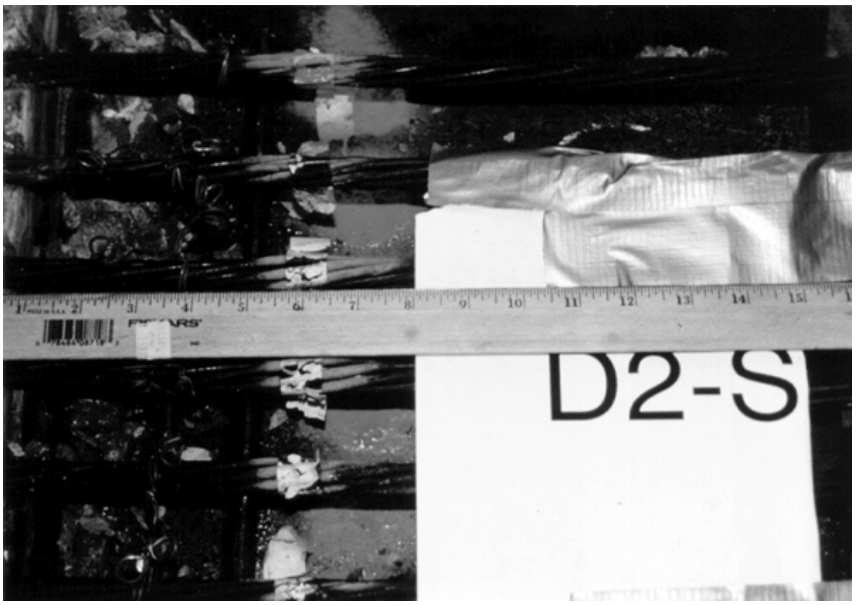

Figure 3.6 End slip measurements at transfer

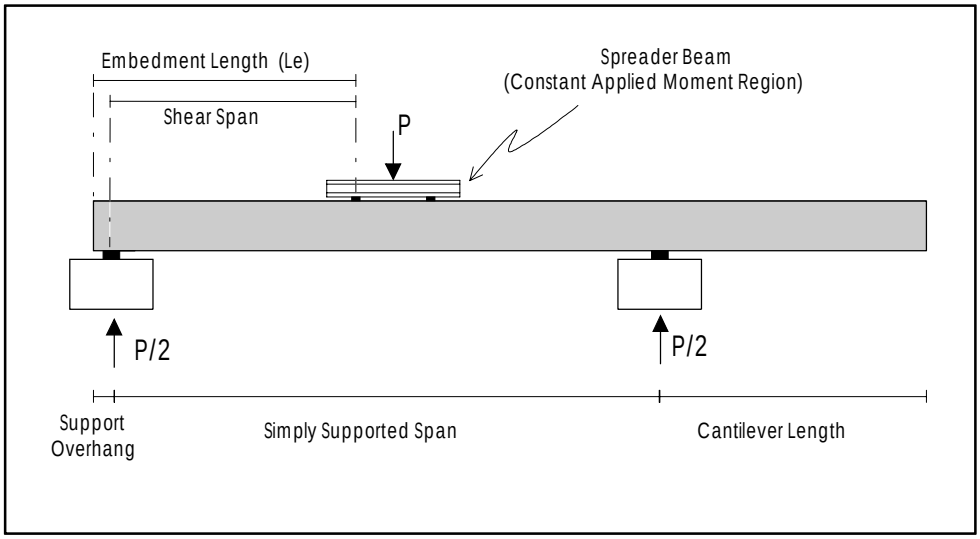

Figure 3.7 Development length test setup

The following parameters were varied for each test:

1) Length of the simply supported span
2) Length of the cantilever overhang
3) Length of the shear span
4) Length of the constant applied moment region
5) Embedment length of the strand

Parameters for each test are summarized in Table 3.7. The parameters were carefully chosen to ensure the structural integrity of the unloaded beam end (i.e., to guarantee that two experimental tests could be performed on each beam). The embedment length for each test was varied based on the type of failure observed in the previous test. An arbitrary value of 163 in. was chosen for the first experimental test.

Table 3.7 Development length test setup parameters

Test	**Simply Supported Span** m (ft)	**Cantilever Length** m (ft)	**Shear Span** m (ft)	**Constant Applied Moment Region** m (ft)	**Embedment Length** (in.)
1-D1N-163	9.14 (30.0)	4.27 (14.0)	3.96 (13.0)	1.22 (4.0)	(163)
2-D1S-119	7.01 (23.0)	6.40 (21.0)	2.90 (9.5)	1.22 (4.0)	(119)
3-D2N-102	6.71 (22.0)	6.71 (22.0)	2.44 (8.0)	1.83 (6.0)	(102)
4-D2S-78	5.49 (18.0)	7.92 (26.0)	1.83 (6.0)	1.83 (6.0)	(78)

For Test 4-D2S-78, the cantilever length exceeded the simply supported length by 2.44 m (8.0 ft). This setup caused a large "overturning" moment owing to the weight of the overhang, and a temporary support was required at the overhang end to prevent tipping. The temporary support was removed as soon as the applied load caused the free beam end to deflect upward.

A photograph of a typical test setup may be seen in Figure 3.8. Sketches for all four test setups may be found in Appendix C.

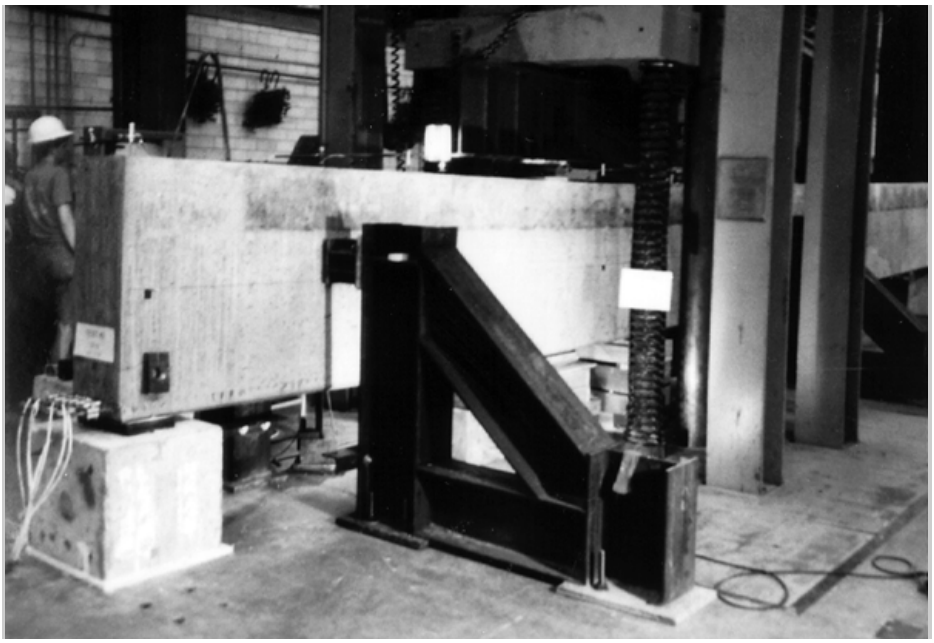

Figure 3.8 Typical development length test setup

3.7 INSTRUMENTATION FOR DEVELOPMENT LENGTH TESTS

Instrumentation for each development length test was designed to monitor the following:

1) Applied load
2) Deflections at several points, including midspan and supports
3) Concrete top fiber strains in the constant applied moment region
4) Strand end slip

Each type of instrumentation is discussed in detail below. Figure 3.9 shows locations of instrumentation in the constant applied moment region. Figure 3.10 is a photograph of the instrumentation in this region.

3.7.1 Data Acquisition System

Measurements from all electronic gauges were taken using a computerized data acquisition system comprised of a Hewlett-Packard scanner and an IBM personal computer. Each channel was electronically scanned for a voltage reading as desired. All voltage readings were later converted to engineering units by the HPDAS2 conversion program written by Alex Tahmassebi. Data were formatted for use in a spreadsheet and stored in a disk file.

3.7.2 Load and Deflection Measurements

Applied load was measured using a load cell that is part of the Riehle testing machine. The load cell was connected to the data acquisition system described in Section 3.7.1. Calibration of the load cell was performed approximately one month before testing began.

Deflection measurements were taken throughout each experimental test using linear potentiometers, or linear pots. Linear pots were placed at the six locations shown in Figure 3.9: two at midspan of the simply supported span, one at each quarter point of the simply supported span, and one directly above each support. Each linear pot was supported from a stand and was set to bear on a smooth mirror epoxied to the surface of the beam, as shown in Figure 3.11. Each gauge was connected to the data acquisition system and scanned at various intervals during the test.

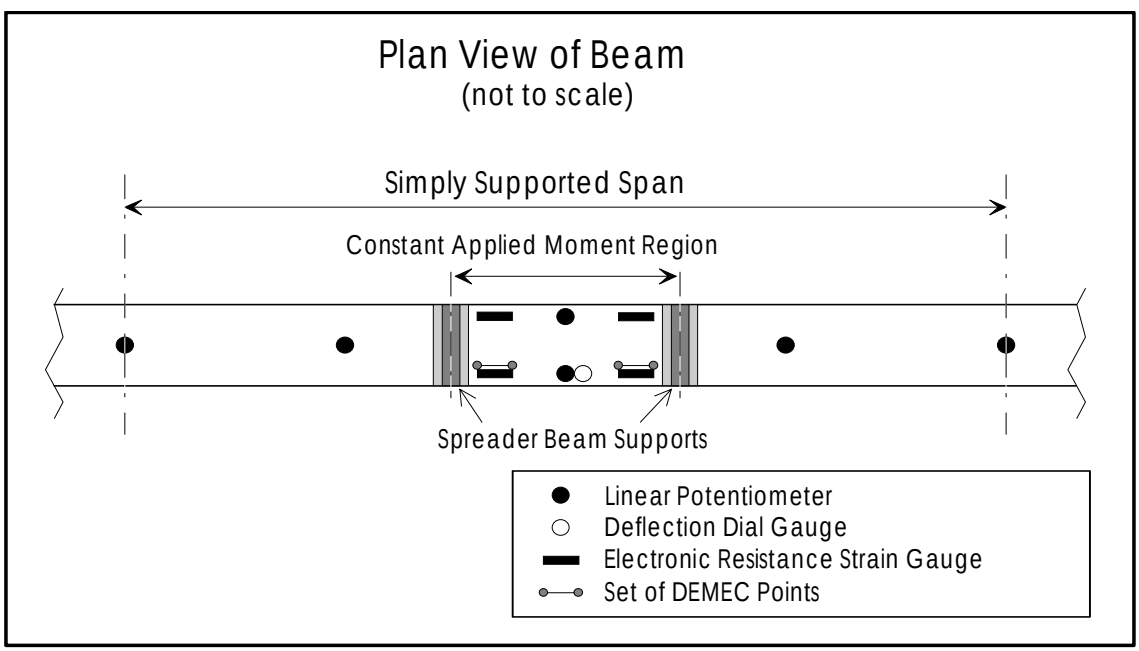

Figure 3.9 Instrumentation locations

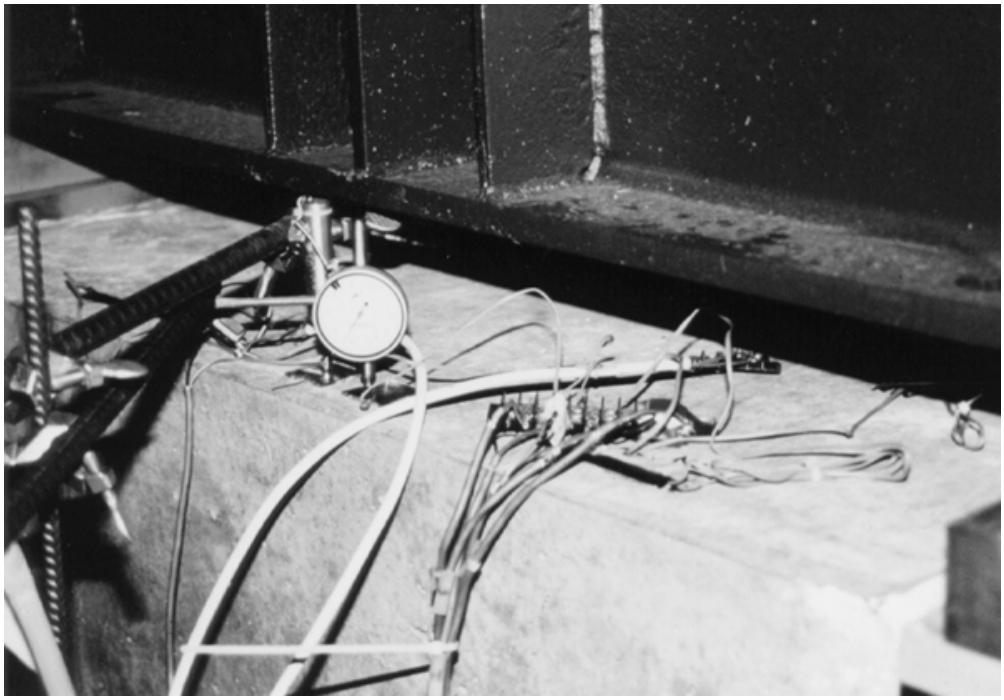

Figure 3.10 Instrumentation in constant applied moment region

A dial gauge was placed at midspan of the member and monitored throughout the test. This gauge provided a backup to the linear pots and, more significantly, was used to control loading during the later stages of each test.

Initial camber measurements prior to the application of load were taken using a surveyor's level. At both supports and at midspan, the location of the gross section centroid was marked at exactly 21 in. from the bottom surface. A steel ruler was held flush to the beam at each location, with the bottom of the ruler at the centroidal mark. The ruler was read to the nearest 1/32-in. at each location and the midspan camber was calculated from the three readings. This level system was also used at various intervals during the test as a backup deflection measuring system.

3.7.3 Measurement of Concrete Top Fiber Strains

Top fiber concrete strains were measured in the constant applied moment region throughout each test. These measured strains served as a guide to determine when to stop testing, as it was desirable not to crush concrete. The measured strains were also used to estimate the strand elongation at any point during the test on the basis of a strain compatibility analysis. Two types of strain measurements were made: DEMEC Mechanical Strain Gauge measurements and electric resistance strain gauge (ERSG) measurements. Gauge locations are shown in Figure 3.9.

Two sets of DEMEC target points were placed in the constant applied moment region centered approximately 30 mm (12 in.) from each load point. Installation and reading of points were performed using the same procedure described in Section 3.5. Initially, a DEMEC Mechanical Strain Gauge reading was taken manually at every second load increment. At higher loads, a DEMEC reading was taken at every load increment.

ERSGs were mounted to the top surface of the beam at four locations in the constant applied moment region. As shown in Figure 3.9, two gauges corresponded directly to the location of sets of DEMEC points, and two gauges corresponded to similar locations on the opposite side of the top surface. ERSGs were connected to the data acquisition system and scanned at each load increment.

3.7.4 End Slip Measurements

End slip measurements were taken during testing using linear pots. A linear pot was anchored to each strand a few inches from the end of the beam, as seen in Figure 3.12. Small mirrors were epoxied to the concrete surface to provide smooth bearing locations for each gauge. Each linear pot was connected to the data acquisition system and read at each load interval. If the strand slipped with respect to the beam end, the linear pot reading would show the magnitude of the relative displacement.

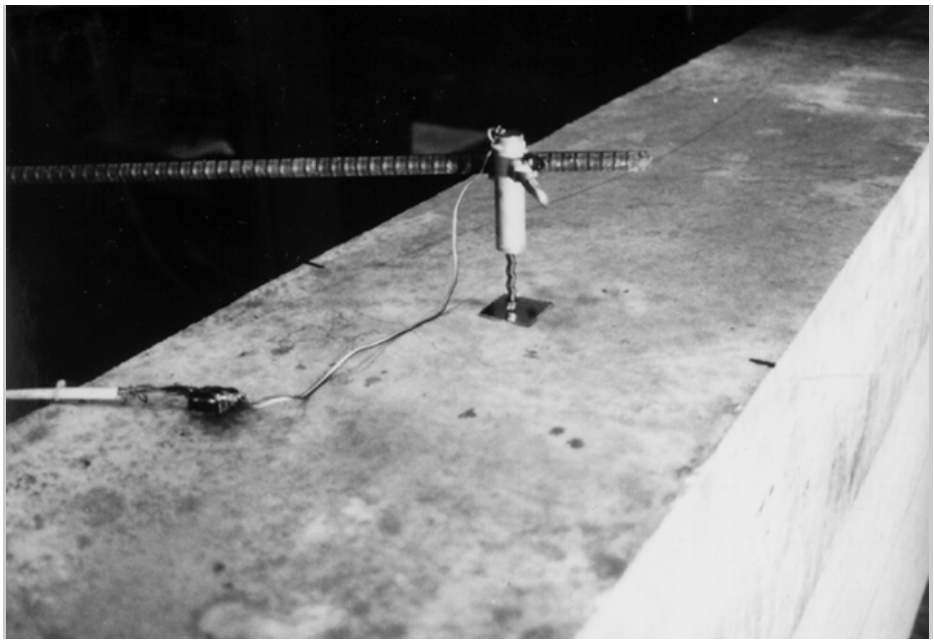

Figure 3.11 Linear potentiometer

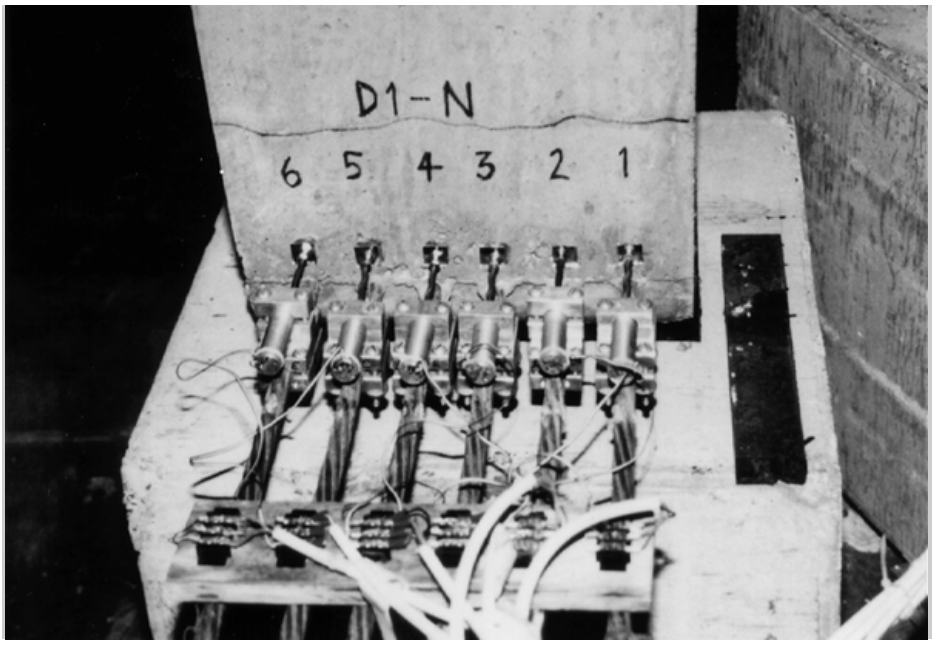

Figure 3.12 End slip instrumentation

3.8 DEVELOPMENT LENGTH TEST PROCEDURE

Once instrumentation had been installed, initial readings were taken before any load was applied to the specimen. The initial readings consisted of scanning all electronic gauges, recording initial DEMEC and deflection dial gauge readings, and determining the initial camber using a surveyor's level.

Load was then applied to the specimen in small increments of 44 to 89 kN (10 to 20 kip), up to the formation of the first flexural cracks. At each load stage, all gauges were scanned by the data acquisition system. DEMEC, deflection dial gauge, and surveyor's level deflection readings were taken manually at approximately every second load stage.

After first flexural cracking, load was applied in smaller increments of less than 22 kN (5 kip). All electronic gauges were again scanned at each load stage. DEMEC, deflection dial gauge, and surveyor's level deflection measurements were recorded at approximately every second load stage. As flexural and or splitting cracks developed at each load stage, they were marked on the member.

Once the member stiffness became sufficiently small, load was applied in deflection increments. Load was applied until the member had incrementally deflected 2.5 to 5.1 mm (0.10 to 0.20 in.), as measured by the dial gauge at midspan. Electronic gauges were scanned, DEMEC and deflection dial readings were taken, and crack propagation was marked at each load increment.

The test continued in this manner until a bond or flexural failure resulted. A bond failure would show a significant loss in the member's load capacity, accompanied by an end slip of one or more strands. A flexural failure was acknowledged to have occurred when the maximum measured top fiber strain was at least 0.00225. This top fiber strain corresponds to a strand elongation of at least 3.49%, and is clearly indicative of ductile member behavior. It was desired that spalling of concrete at the top fiber be minimized, both for safety purposes and to preserve the integrity of the beam. This would allow a second experimental test to be formed on the opposite end of the beam.

Once a bond or flexural failure had occurred, the specimen was unloaded in three or four load increments. All electronic and manual measurements were made at each unloading stage. Upon completion of unloading, a detailed crack pattern of the member was sketched and all instrumentation was removed. Measurements from the data acquisition system were loaded onto a floppy disk and stored for later manipulation. A single experimental test typically took 7 to 8 hours.

CHAPTER 4. TEST RESULTS

4.1 INTRODUCTION

The results of both the transfer length measurements and the development length tests are included in this chapter. Methods of data reduction are discussed along with the presentation of the data. All data in this chapter are found in the form of graphical plots.

4.2 TRANSFER LENGTH MEASUREMENTS

4.2.1 Method of Data Reduction

Strain measurements were taken at transfer on each of the four beam ends according to the procedure outlined in Section 3.5.3. Raw data values were manually input into a computer spreadsheet and manipulated according to the procedure described in this section. The data reduction scheme for measured strains is illustrated in Figure 4.1.

First, the two readings for each measurement on a set of DEMEC points were averaged. This average was found for both initial and final readings, and the difference between the two averages at every set of points was then multiplied by a gauge factor of 8.1 to produce a differential strain. This differential strain is the *average* strain between the two given DEMEC points caused by the transfer of prestress force. For simplification, the strain at the *midpoint* of any set of two points was assumed to be equivalent to this average value. The differential strain values from one beam face were then averaged with their corresponding values on the opposite beam face, resulting in a measured strain value at any given distance from the beam end.

The measurements are then smoothed to reduce large amounts of variability in the data. The smoothing process utilizes a running average of three consecutive points and may be summarized by the equation below (23):

$$\text{Strain}_i = \frac{\text{Strain}_{i-1} + \text{Strain}_i + \text{Strain}_{i+1}}{3}$$

It may be shown that the combined effect of data smoothing and a 200 mm (8 in.) gauge length for raw measurements is that the reported strain at a single point is actually a weighted average of the strain over a 300 mm (12 in.) interval centered around that point. Strain closer to the actual point is weighted more heavily than strain at the edges of the interval. The effect of smoothing data may be seen in Figure 4.2, which shows the strain profile for beam end D2S in both smoothed and unsmoothed form. Because of the smoothing process, the first data point is 175 mm (6.91 in.) from the beam end, even though the first DEMEC point was located only 1 in. from the beam end.

4.2.2 Measured Strains at Transfer

The strain profiles at transfer for all four beam ends are shown in Figures 4.3, 4.4, 4.5, and 4.6. The idealized theoretical strain profile would show a linear increase in strain in the transfer zone, followed by a uniform strain plateau (neglecting small effects caused by self-weight moment). Three of the specimens showed a linear increase in strain in the transfer zone, but a uniform strain plateau was difficult to define because of variability in the measurements. The fourth specimen, D1S, showed no linear increase in strain beyond the first data point, which is approximately 175 mm (7 in.) from the beam end.

DEMEC Readings - Beam D2S (East Side)

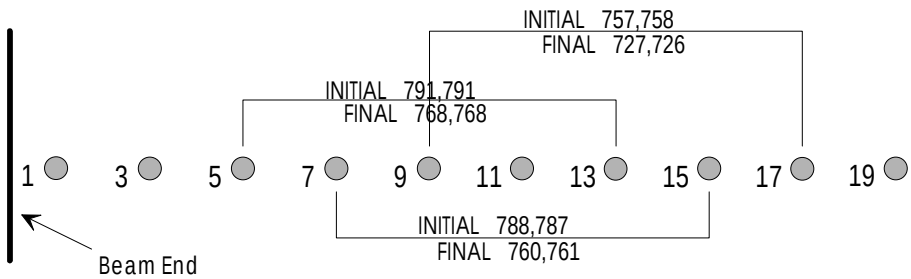

East Face
Strain @ Point 9 = 8.1[(791+791)/2 + (768+768)/2] = 186.3 microstrains
Strain @ Point 11 = 8.1[(788+787)/2 + (760+761)/2] = 218.7 microstrains
Strain @ Point 13 = 8.1[(757+758)/2 + (727+726)/2] = 251.1 microstrains

West Face (not shown)
Strain @ Point 9 = 8.1[(867+868)/2 + (848+848)/2] = 158.0 microstrains
Strain @ Point 11 = 8.1[(824+825)/2 + (791+791)/2] = 271.3 microstrains
Strain @ Point 13 = 8.1[(885+885)/2 + (849+850)/2] = 287.6 microstrains

Average Differential Strains
Point 9 = (186.3+158.0)/2 = 170 microstrains
Point 11 = (218.7+271.3)/2 = 242 microstrains
Point 13 = (251.1+287.6)/2 = 266 microstrains

Smoothed Strain at Point 11 = (170+242+266)/3 = 226 microstrains

Figure 4.1 Method of data reduction for strain readings

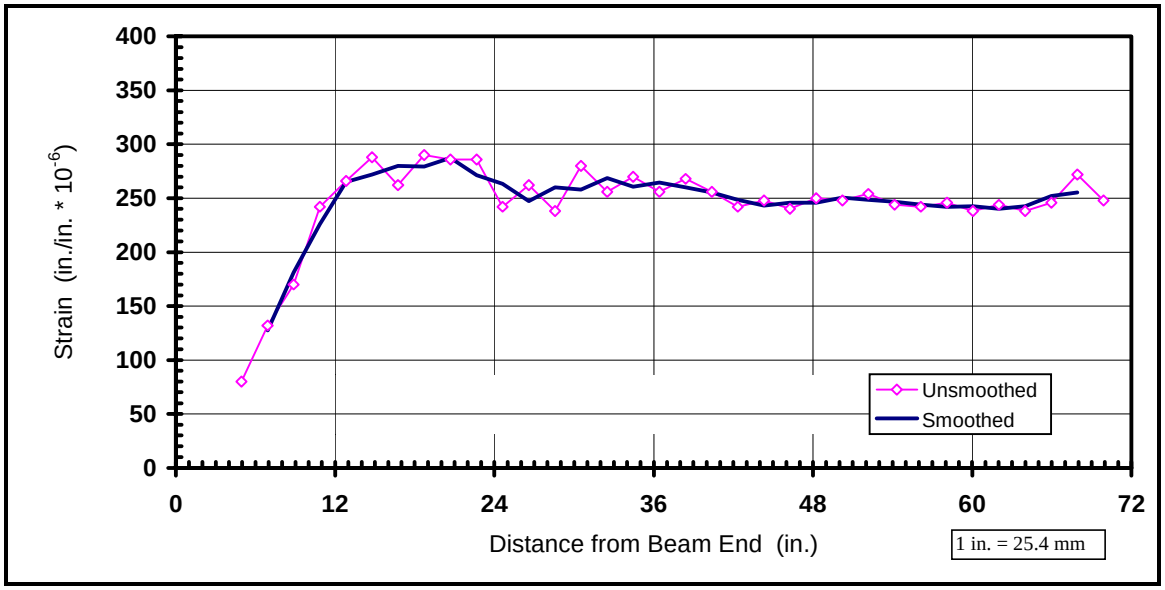

Figure 4.2 Effect of smoothing on strains for beam end D2S

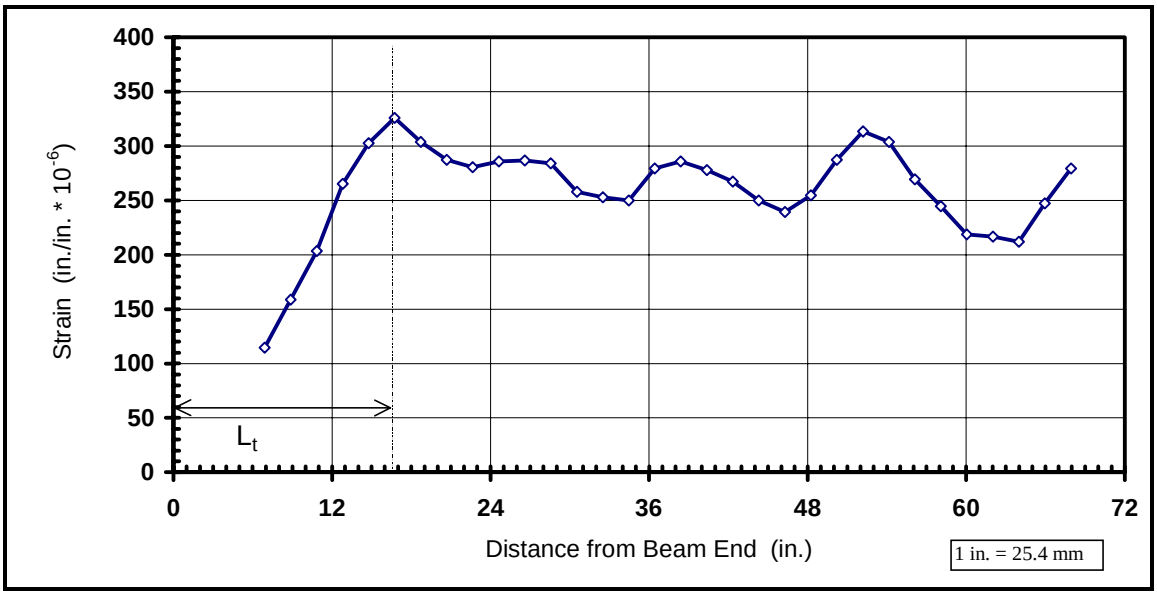

Figure 4.3 Smoothed strain profile for beam end D1N

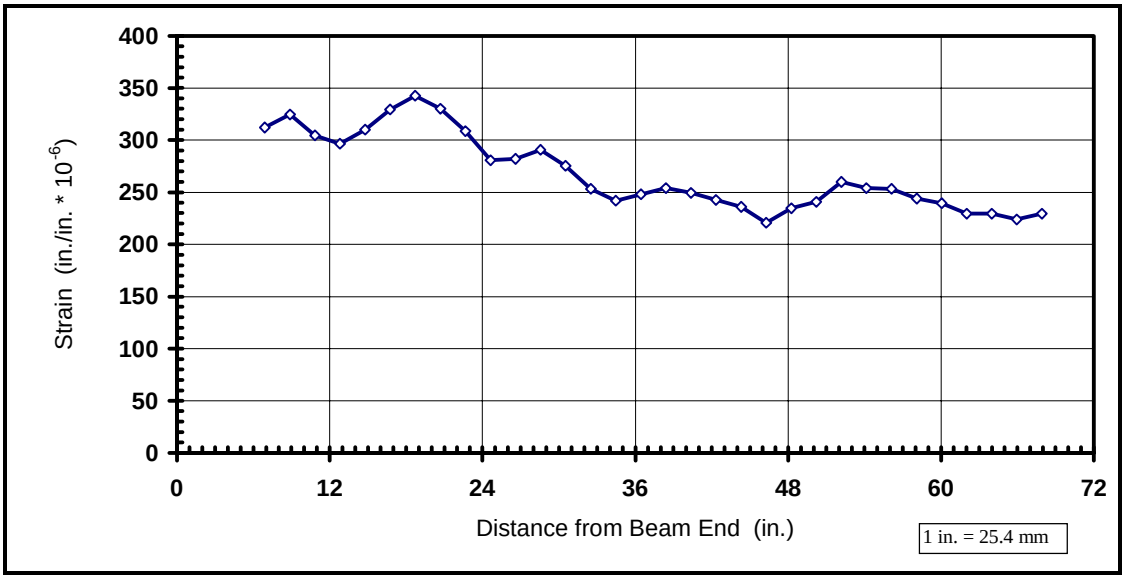

Figure 4.4 Smoothed strain profile for beam end D1S

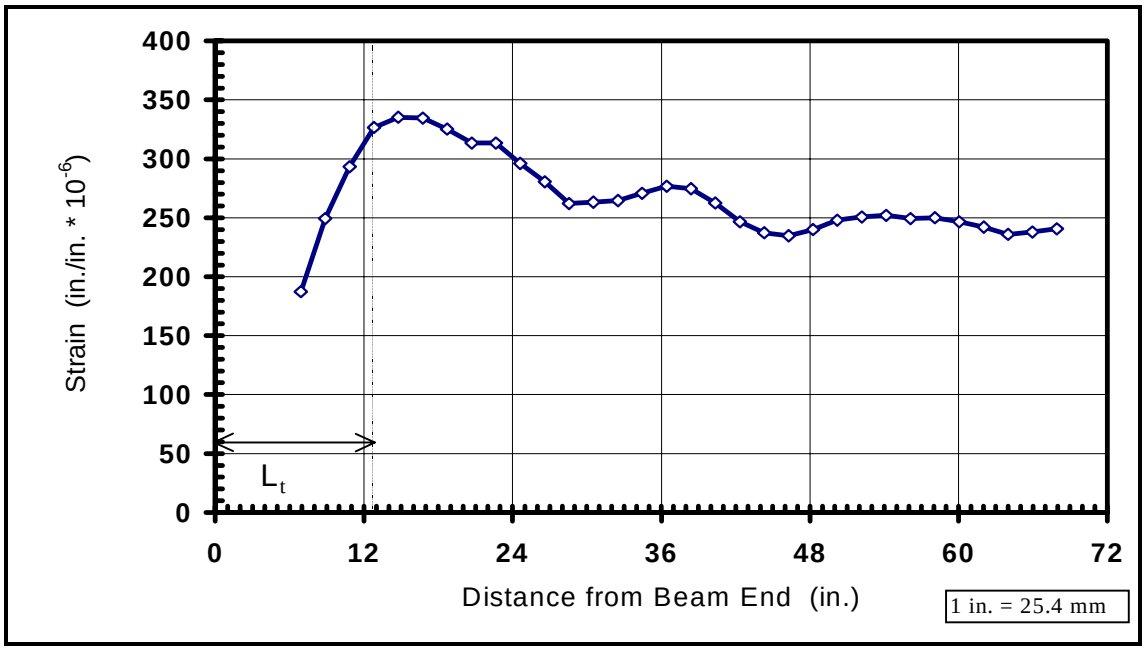

Figure 4.5 Smoothed strain profile for beam end D2N

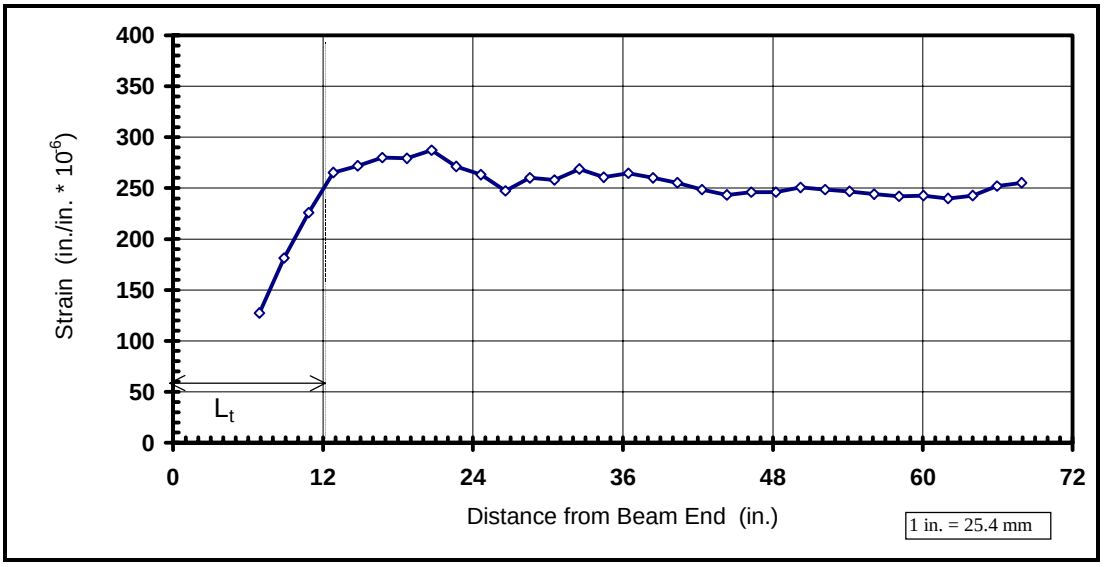

Figure 4.6 Smoothed strain profile for beam end D2S

4.2.3 Measured End Slip at Transfer

End slips were measured at transfer according to the procedure described in Section 3.5.4. Measured end slips are shown in Figure 4.7. The average measured end slip for all strands was 2.5 mm (0.098 in.).

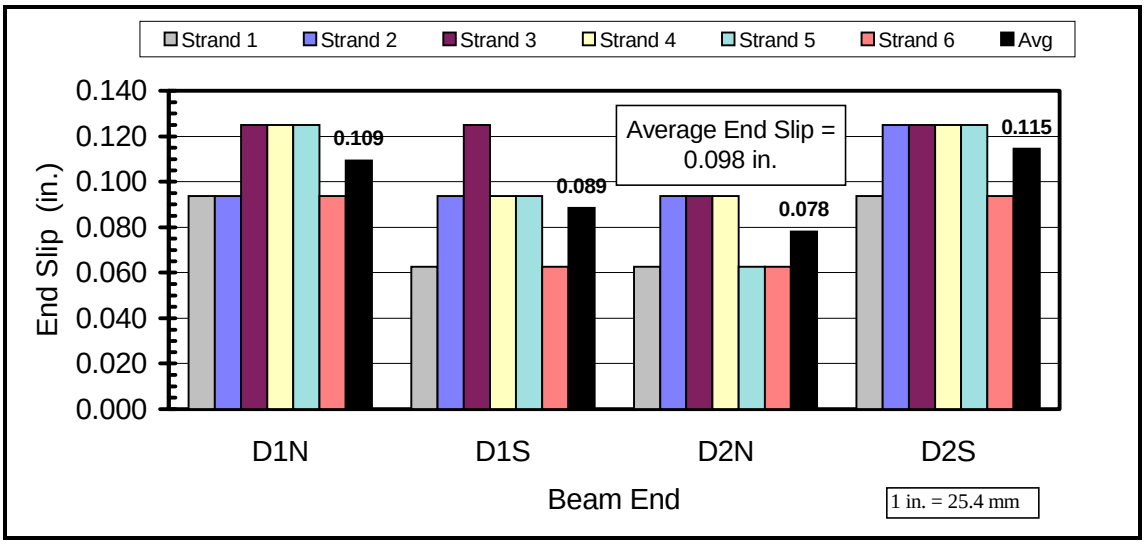

Figure 4.7 Measured end slips at transfer

4.3 DEVELOPMENT LENGTH TEST RESULTS

4.3.1 Introduction

The results of the four development length tests on the Hoblitzell-Buckner beams are presented in this section. The following observations and measurements are discussed for each experimental test and are defined below:

Failure Type—Each failure is classified as either a flexural or bond failure, based on the measurements of top fiber strains, strand end slips, and midspan deflections, as well as the observed cracking pattern.

Applied Load, Net Midspan Deflection, and Maximum Moment—The maximum applied load, not including the specimen self-weight or the weight of the test setup, is reported. Applied load is plotted against the net midspan deflection for each test. The net midspan deflection at any point during the test is defined as the measured midspan deflection (average of two gauge measurements at midspan) minus the measured initial camber and the average measured bearing deflection. The residual net deflection after unloading is also presented. The maximum total moment at the critical section, due to applied load and any positive or negative moment induced by the test setup and beam self-weight, is noted. In this series of tests, the critical section is always located at one end of the constant applied moment region.

Maximum Top Fiber Strain—The maximum concrete top fiber strain, as measured by the instrumentation discussed in Section 3.7.3, is reported. The stated value is the measured strain minus any initial tensile strain caused by prestressing, specimen self-weight, and weight of the test setup. The initial tensile strain was calculated using an elastic analysis with transformed section properties.

Approximate Maximum Strand Elongation—The approximate strand elongation at failure is calculated using strain compatibility principles with the measured maximum top fiber concrete strain and given material properties.

Strand End Slip—Any significant strand end slip, as measured according to Section 3.7.4, is noted.

Cracking Pattern—A sketch of the cracking pattern at the maximum applied load is presented. Critical crack dimensions, including the maximum crack width, are reported, and the load at first flexural cracking is noted. The distance from the last crack to the free end of the beam is also reported.

4.3.2 Test 1-D1N-163

Specimen D1N was tested with an embedment length of 4 m (163 in.), a simply supported span measuring 9.14 m (30 ft.), and a constant moment region measuring 1.22 m (4 ft.) in length. A flexural failure was observed in this test.

A plot of applied load versus net midspan deflection is shown in Figure 4.8. Load was applied until flexural cracking was first observed at which time the beam was completely unloaded. Upon reloading, the maximum applied load was 762.4 kN (171.7 kip) and the maximum net midspan deflection was 70.6 mm (2.78 in.). The corresponding maximum moment at the critical section was 1,577 kN-m (1163 ft-kip). After unloading, a residual net midspan deflection of 15.7 mm (0.62 in.) was measured.

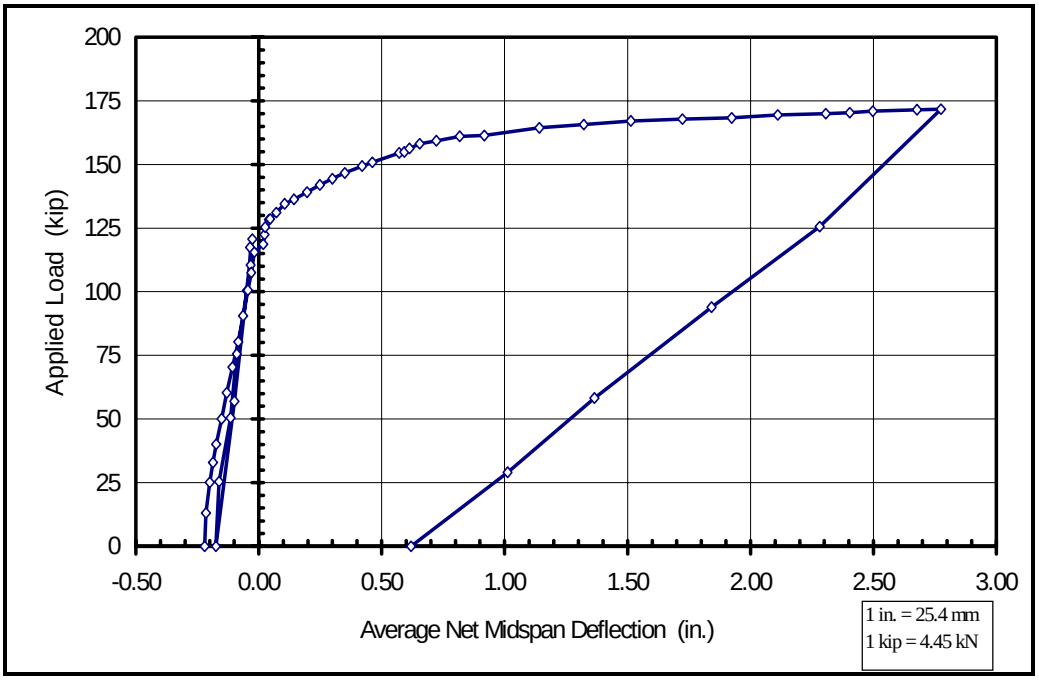

Figure 4.8 Load versus deflection for Test 1-D1N-163

The maximum top fiber concrete strain at the peak load was 0.00245, as measured by the electronic resistance strain gauge in the southwest corner of the constant moment region. The approximate strand elongation, based on this top fiber strain, was 3.90%. No significant end slip was measured on any of the six strands at any point during the test.

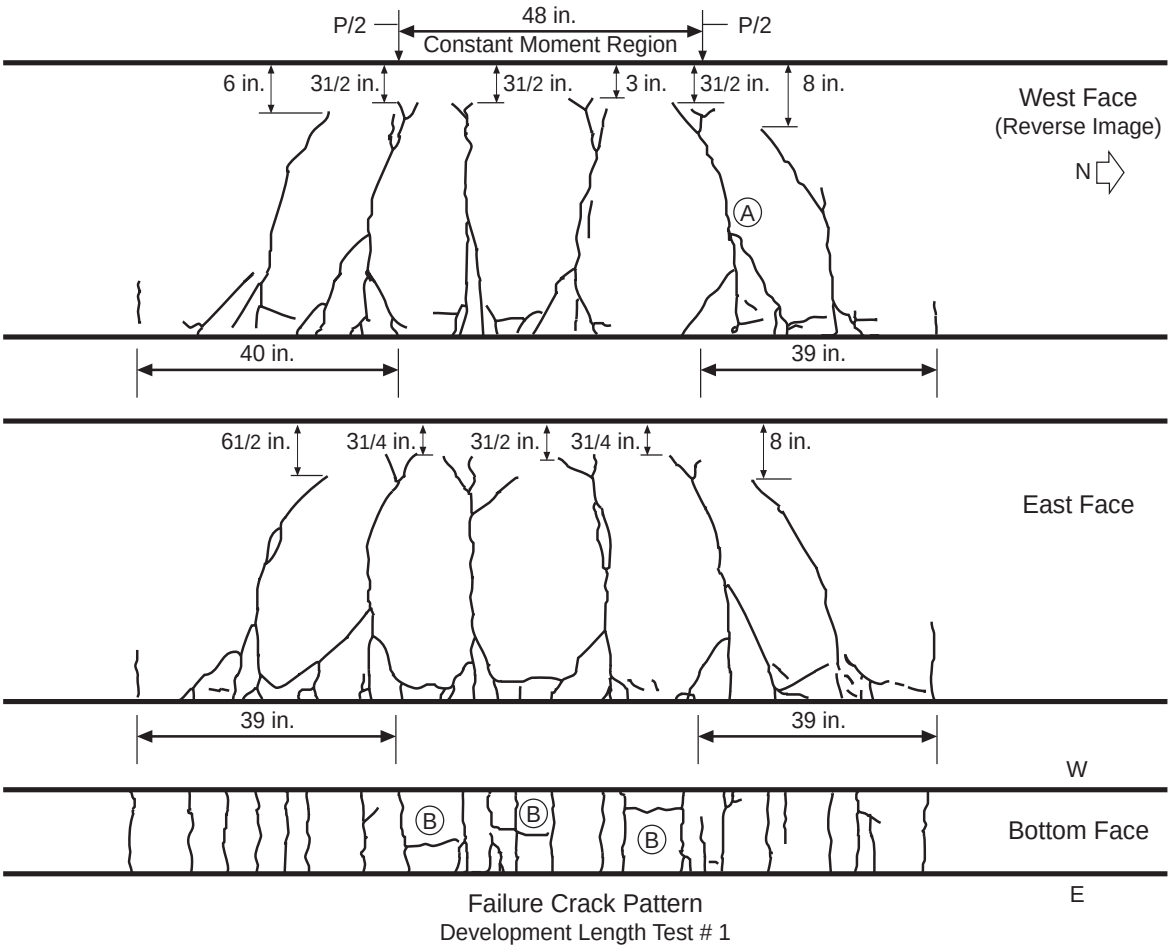

Figure 4.9 Cracking pattern for Test 1-D1N-163

Flexural cracking was first observed at a load of 489 kN (110 kip), with the first noticeable loss of member stiffness at 560 kN (126 kip). A sketch of the cracking pattern at ultimate load may be found in Figure 4.9. Cracking extended to within 3.12 m (123 in.) of the free end of the beam. The maximum crack width was 6.4 mm (0.25 in.). At the peak load, flexural cracks had propagated as high as 76 mm (3 in.) from the top fiber. Cracking was well distributed in and around the constant applied moment region. Three splitting cracks along the axis of the strand were observed on the bottom face of the beam near the peak load. Each of these splitting cracks occurred beneath one of the inner strands in the constant moment region. Measuring less than 300 mm (12 in.) in length, the splitting cracks had no noticeable impact on the beam behavior. A photograph of one of the three longitudinal splitting cracks may be found in Figure 4.10.

Figure 4.10 Longitudinal splitting crack on bottom face (Test 1-D1N-163)

4.3.3 Test 2-D1S-119

Specimen D1S was tested next with an embedment length of 2.98 m (119 in.). The test setup included a 7.01 m (23.0 ft) simply supported span and a 1.22 m (4.0 ft) constant applied moment region. This test resulted in a flexural failure.

The applied load versus net midspan deflection for this test is shown in Figure 4.11. A maximum load of 1,115 kN (250.6 kip) was applied to the specimen, resulting in a maximum net midspan deflection of 61.2 mm (2.41 in.). The maximum moment at the critical section was 1,597 kN-m (1178 ft-kip). A net deflection of 16.8 mm (0.66 in.) remained after unloading. A photograph of the test specimen under 1,093 kN (245.7 kip) applied load appears in Figure 4.12.

A top fiber concrete strain of 0.00242 was measured at the peak load using a DEMEC mechanical strain gauge in the northeast corner of the constant applied moment region. The approximate strand elongation based on this top fiber strain was 3.84%. Local concrete crushing was observed near the north load point at failure and is shown in Figure 4.13. None of the six strands showed a significant end slip during the test.

A sketch of the crack pattern for Test 2-D1S-119 is shown in Figure 4.14. First flexural cracking occurred at a load of 823 kN (185 kip). Cracking extended to within 1.85 m (73 in.) of the free end of the beam. The maximum crack width was measured to be 8.6 mm (0.34 in.), and flexural cracks propagated to 64 mm (2.5 in.) from the top fiber of the specimen. Cracking was well distributed in the constant moment region. A few splitting cracks, similar to those found in Test 1-D1N-163, were observed on the bottom face of the beam near the maximum applied load.

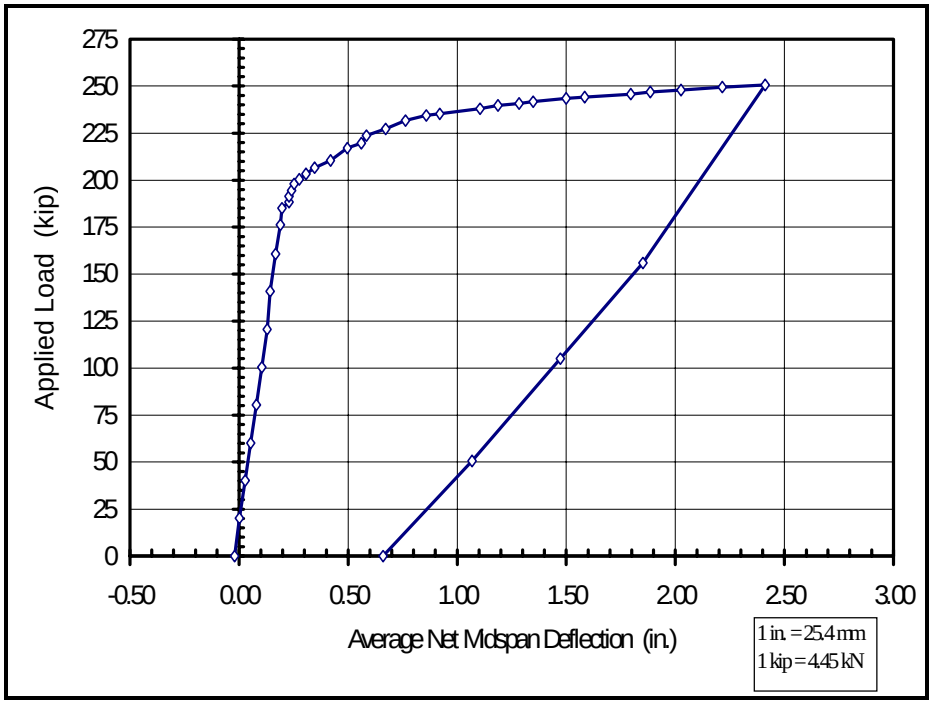

Figure 4.11 Load versus deflection for Test 2-D1S-119

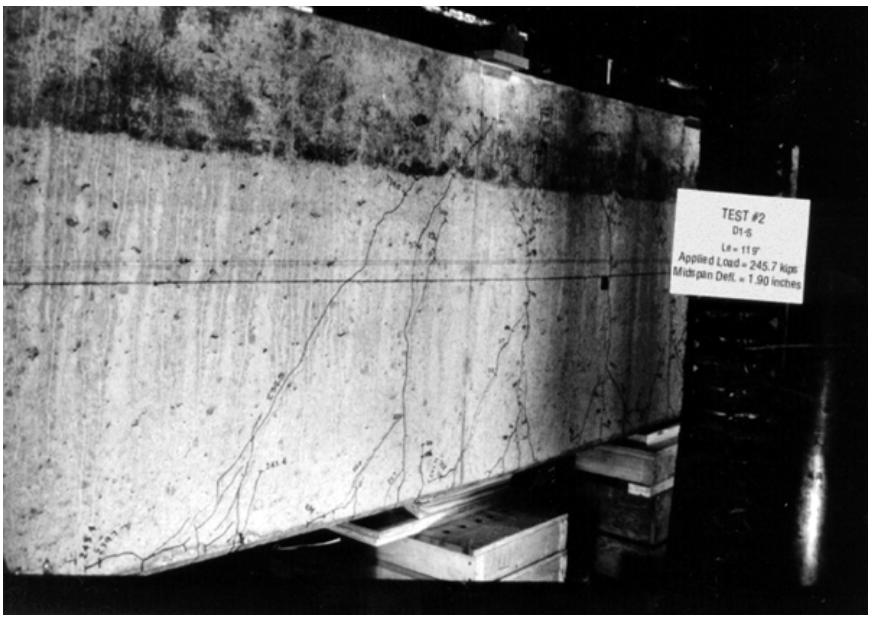

Figure 4.12 Test 2-D1S-119 at applied load of 245.7 kip

Figure 4.13 Local concrete crushing (Test 2-D1S-119)

4.3.4 Test 3-D2N-102

The third experimental test, Test 3-D2N-102, was performed using an embedment length of 2.55 m (102 in.) and also resulted in a flexural failure. The test setup utilized a simply supported span of 6.71 m (22 ft) and a constant applied moment region of 1.83 m (6 ft).

Figure 4.15 shows a plot of applied moment versus net midspan deflection for this test. A maximum load of 1,357 kN (305.1 kip) was applied to the specimen. The corresponding maximum net midspan deflection was 65.5 mm (2.58 in.). The maximum moment at the critical section was 1,633 kN-m (1,204 ft-kip). After complete unloading, the residual net midspan deflection was measured to be 18.8 mm (0.74 in.).

At the peak load, a top fiber concrete strain of 0.00227 was measured using a DEMEC mechanical strain gauge in the northeast corner of the constant applied moment region. Based on this top fiber strain, the approximate strand elongation was 3.54%. As shown in Figure 4.16, local concrete crushing was observed at the north load point at the peak load. No significant end slip was measured on any of the six strands.

Flexural cracking first occurred at an applied load of 992 kN (223 kip). Cracking extended to within 1.88 m (74 in.) of the free beam end. A maximum crack width of 7.9 mm (0.31 in.) was measured at the peak load, as shown in Figure 4.17. Flexural cracks propagated to 57.2 mm (2.25 in.) from the top fiber of the specimen at the maximum load. Flexural cracking was again well distributed in the constant moment region. Several local

longitudinal splitting cracks were observed on the bottom face at large applied loads, as shown in the sketched crack pattern in Figure 4.18.

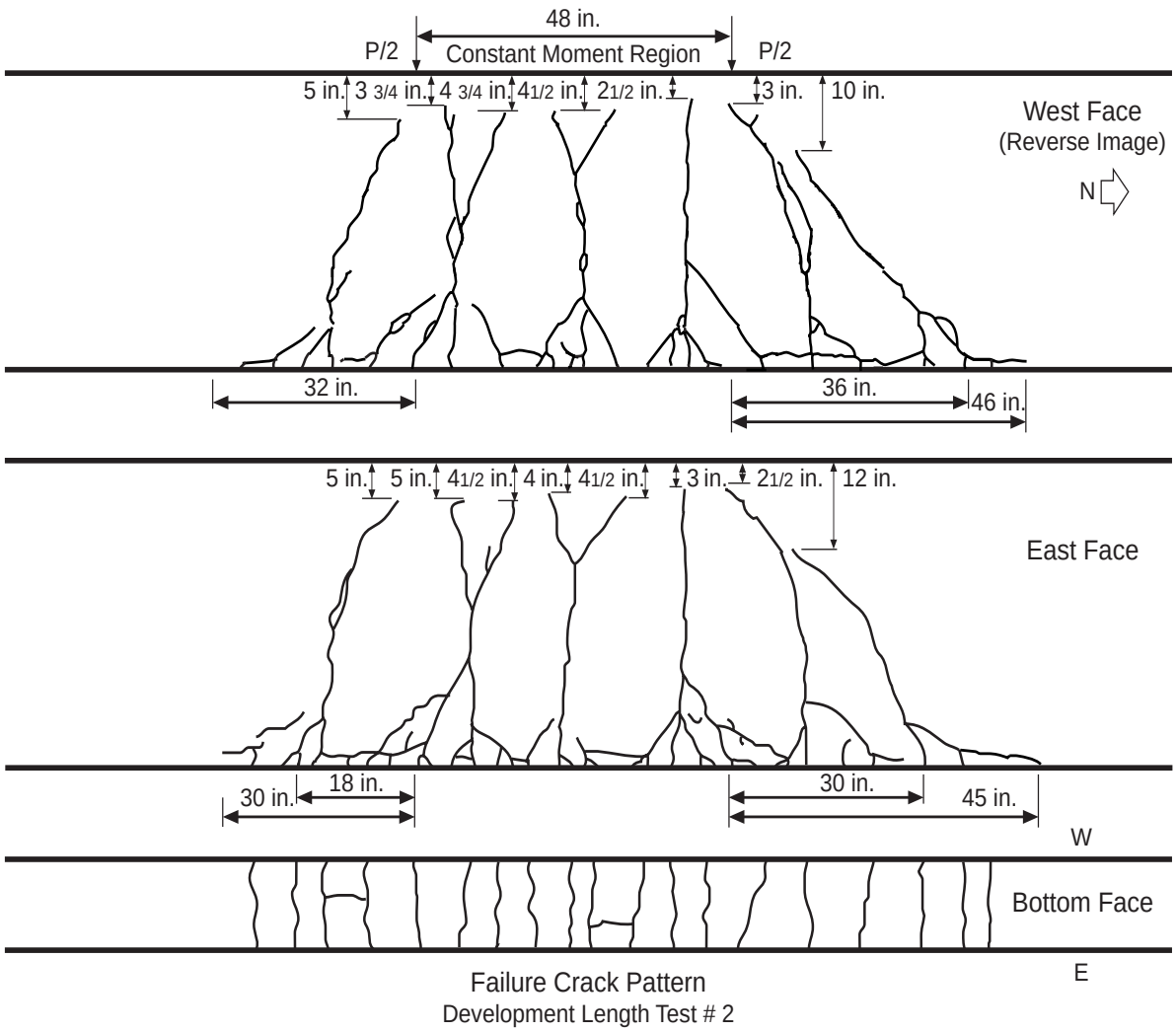

Figure 4.14 Cracking pattern for Test 2-D1S-119

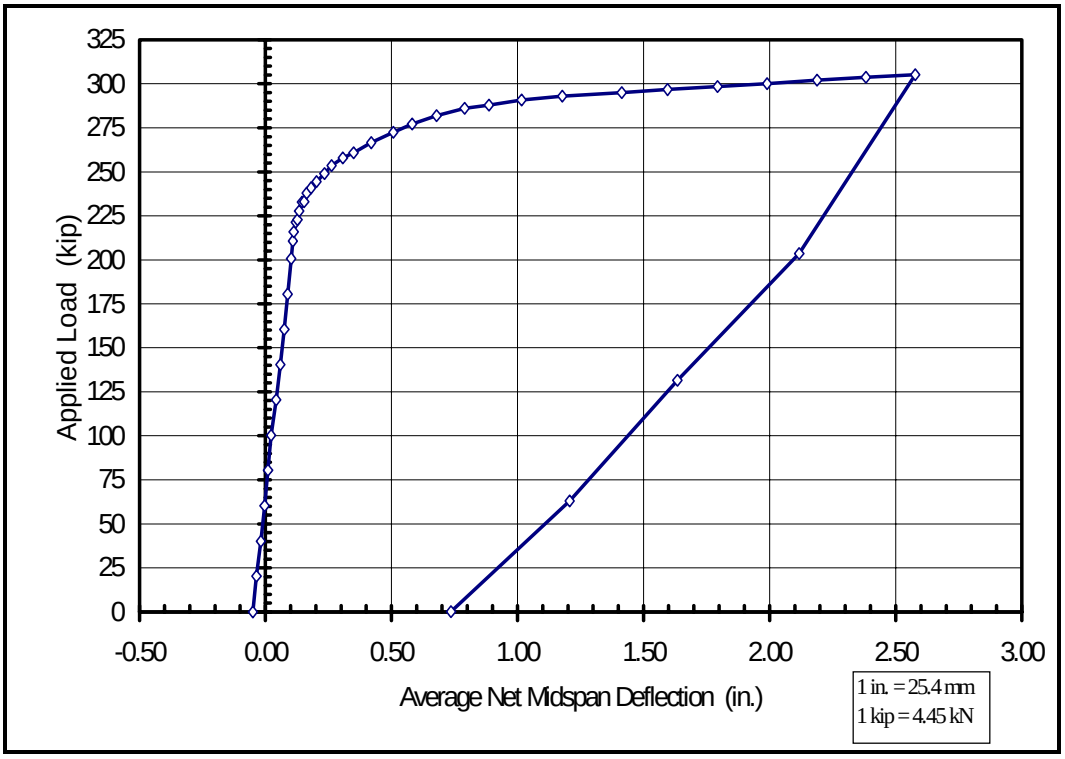

Figure 4.15 Load versus deflection for Test 3-D2N-102

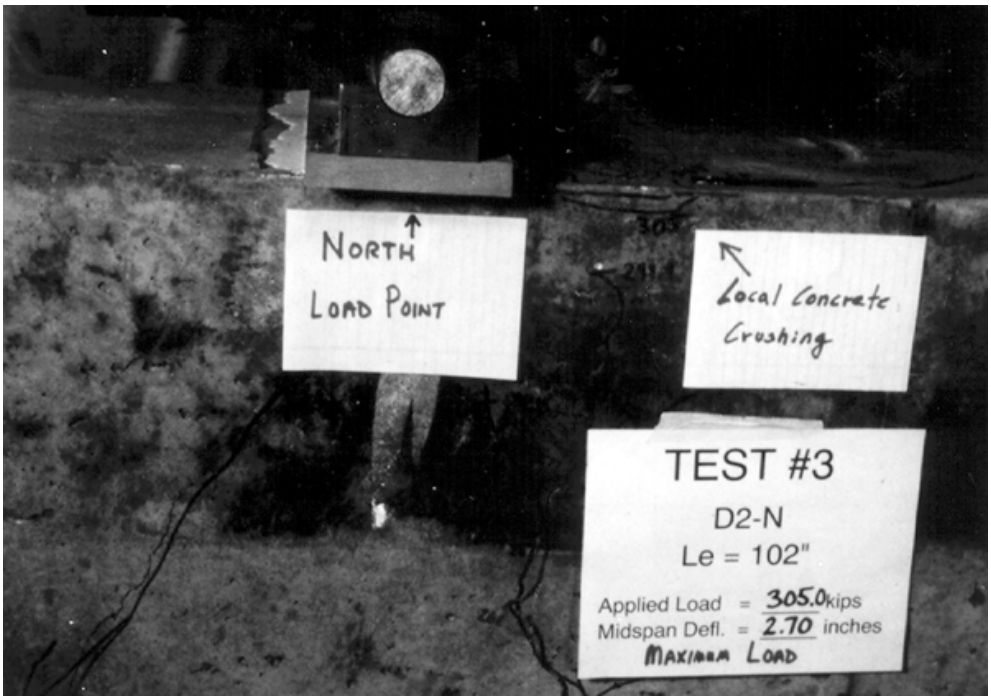

Figure 4.16 Local concrete crushing (Test 3-D2N-102)

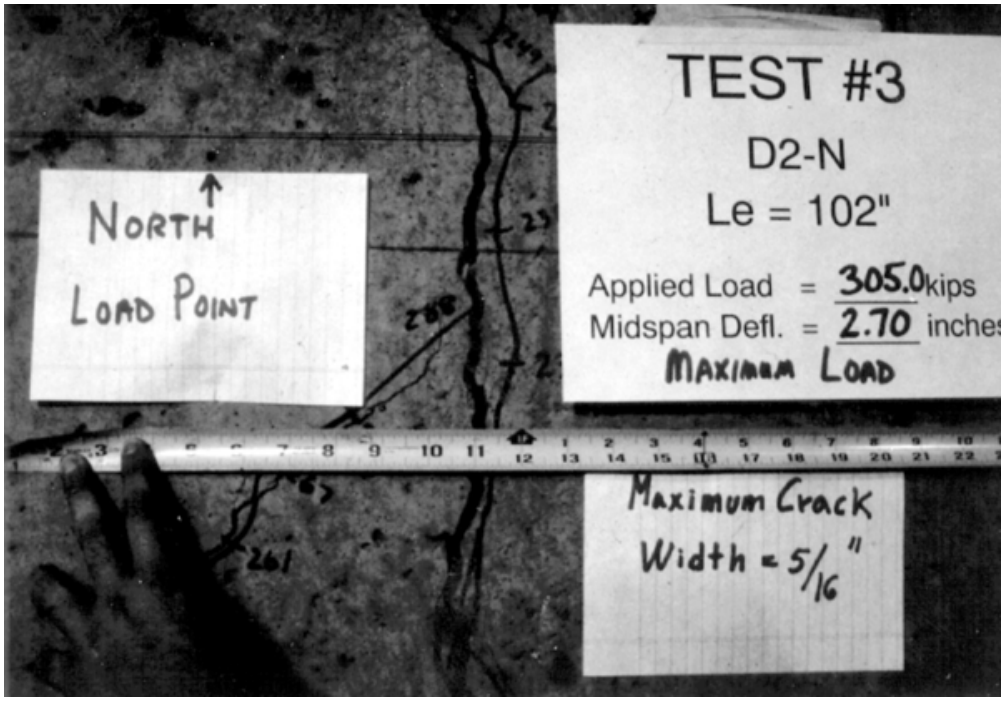

Figure 4.17 Maximum crack width (Test 3-D2N-102)

4.3.5 Test 4-D2S-78

The final test, Test 4-D2S-78, was performed using an embedment length of 78 in. The simply supported span measured 5.49 m (18 ft), and the constant applied moment region measured 1.83 m (6 ft). The test resulted in a flexural failure.

A plot of applied load versus net midspan deflection is shown in Figure 4.19. As discussed in Section 3.6, this test setup required a temporary support that initially made the beam continuous. As shown in the photograph in Figure 4.20, the beam was no longer continuous at an applied load of 1,668 kN (375 kip). The maximum applied load was 1,832 kN (411.8 kip), and the maximum net midspan deflection was 32.5 mm (1.28 in.). The corresponding maximum moment at the critical section was 1,615 kN-m (1191 ft-kip). A residual deflection of 5.3 mm (0.21 in.) was measured after unloading.

At the maximum load, a top fiber strain of 0.00243 was measured using a DEMEC mechanical strain gauge in the southeast corner of the constant moment region. The approximate strand elongation based on this top fiber strain was 3.87%. None of the six strands showed any significant end slip during the test.

A sketch of the crack pattern at ultimate load may be found in Figure 4.21. First flexural cracking occurred at a load of 1,339 kN (301 kip). Cracking extended to within 1.32 m (52 in.) of the free beam end. A maximum crack width of 6.4 mm (0.25 in.) was

measured, and flexural cracks propagated to 76 mm (3.0 in.) below the top fiber at the peak load. As in previous tests, flexural cracking was well distributed; fewer cracks occurred, however, because of the larger moment gradient inherent in the setup. Several splitting cracks were again observed along the bottom face of the beam at high applied loads.

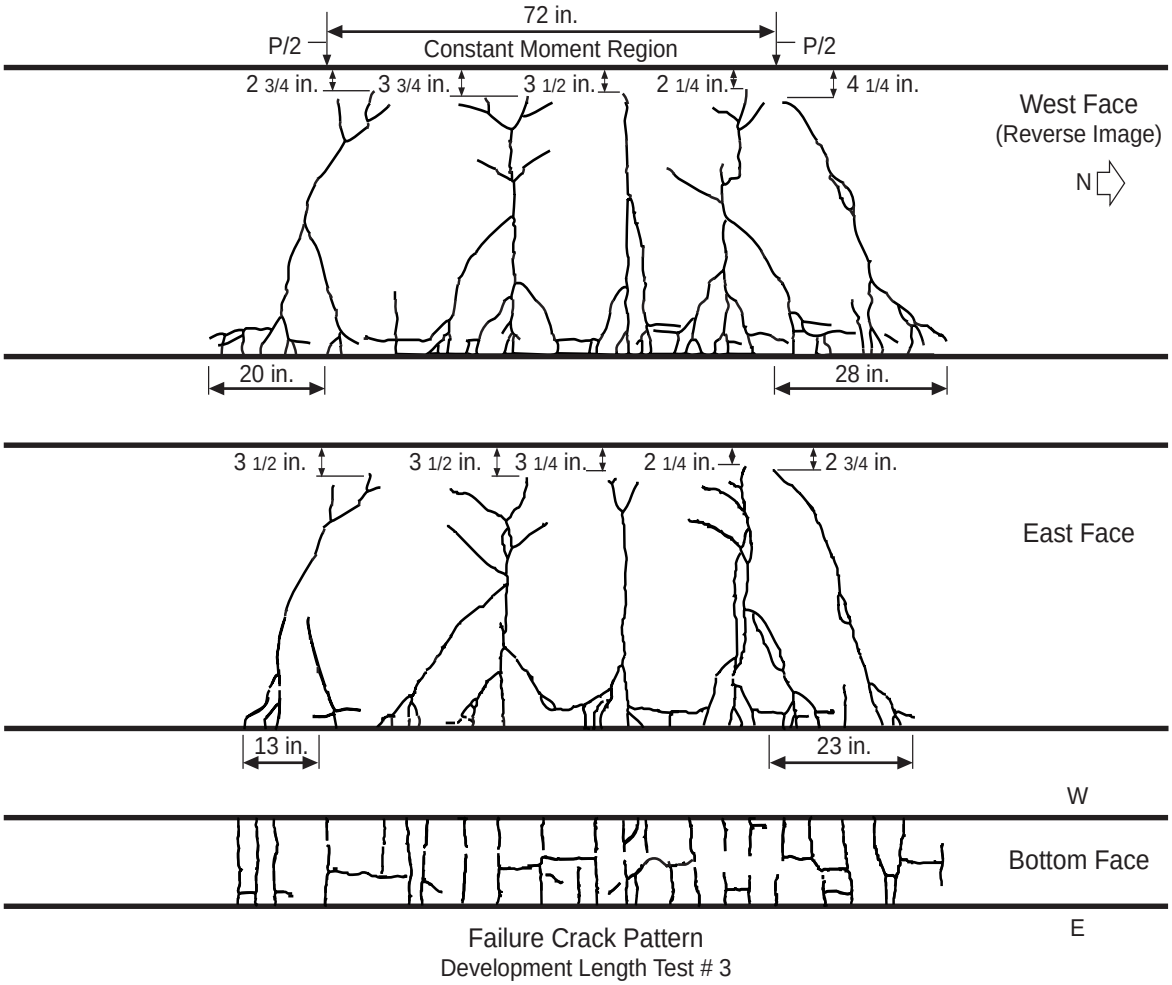

Figure 4.18 Cracking pattern for Test 3-D2N-102

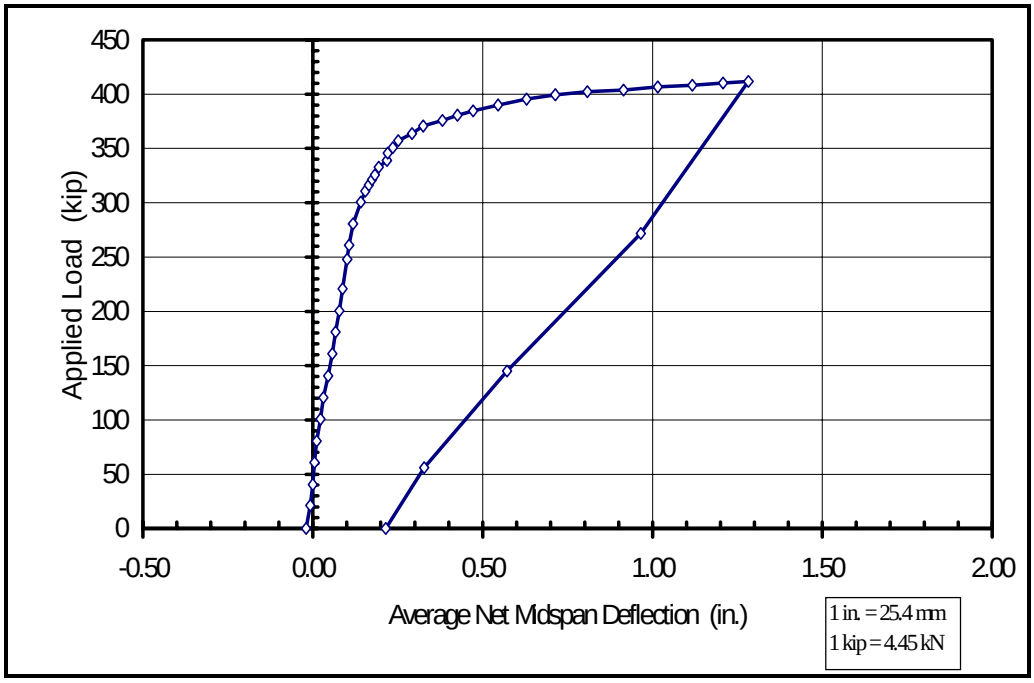

Figure 4.19 Load versus deflection for Test 4-D2S-78

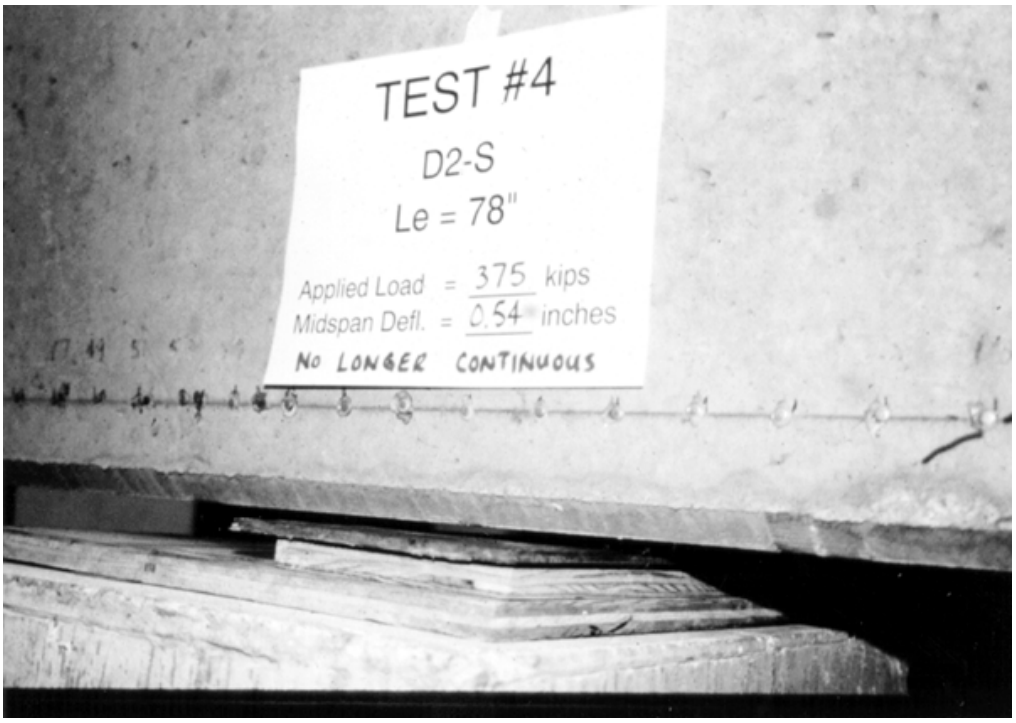

Figure 4.20 Temporary support (Test 4-D2S-78)

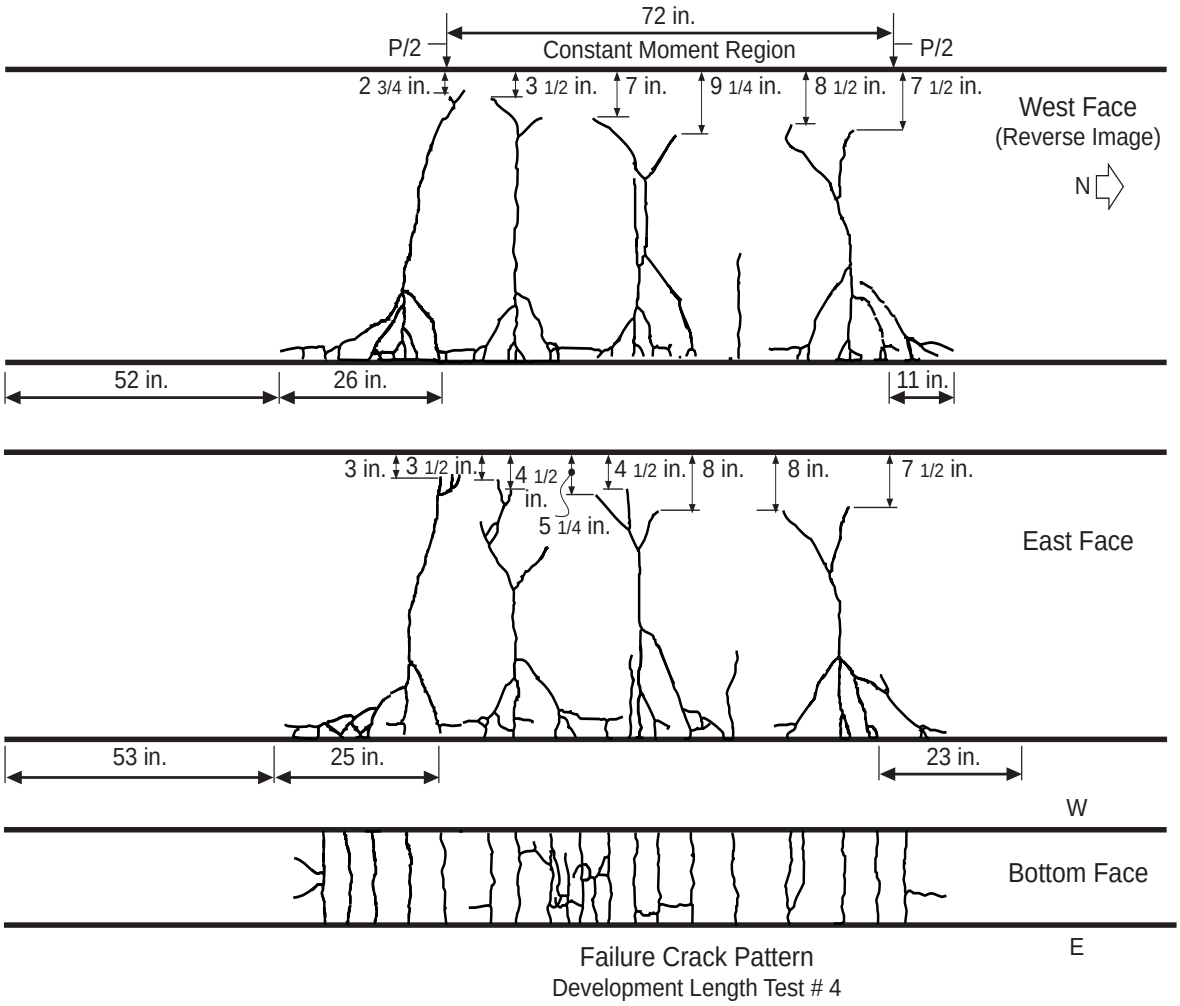

Figure 4.21 Cracking pattern for Test 4-D2S-78

4.3.6 Summary of Results

The results of the four experimental development length tests on the Hoblitzell-Buckner beams are summarized in Table 4.1. All four tests resulted in flexural failures with measured top fiber concrete strains above 0.00225 and approximate steel elongations above 3.5%. No significant end slip was measured in any of the four tests. Flexural cracks were well distributed in the constant moment region, and propagated to within 51 to 76 mm (2.0 to 3.0 in.) of the top fiber. Localized, discontinuous, longitudinal splitting cracks were common on the bottom face of each test specimen at high applied loads.

Table 4.1 Summary of development length test results

Test	**1-D1N-163**	**2-D1S-119**	**3-D2N-102**	**4-D2S-78**
Failure Type	Flexural	Flexural	Flexural	Flexural
Max. Applied Load kN (kip)	762.4 (171.7)	1,115 (250.6)	1,357 (305.1)	1,832 (411.8)
Moment at Critical Section kN-m (ft-kip)	1,577 (1,163)	1,597 (1,178)	1,633 (1,204)	1,615 (1,191)
Max. Net Midspan Deflection mm (in.)	70.6 (2.78)	61.2 (2.41)	65.5 (2.58)	32.5 (1.28)
Max. Top Fiber Strain mm/mm or in./in.	0.00245	0.00242	0.00227	0.00243
Approx. Strand Elongation	3.90%	3.84%	3.54%	3.87%

CHAPTER 5. DISCUSSION OF TEST RESULTS

5.1 INTRODUCTION

A brief analysis and discussion of the experimental results are presented in this chapter. Measured transfer and development lengths are compared to reported results from previous research. The results are also compared with values calculated from several proposed transfer and development length equations, including those found in the AASHTO and ACI 318 codes. The variables that affected the results of this study are discussed, and potential sources of error are listed.

5.2 TRANSFER LENGTH MEASUREMENTS

5.2.1 Determination of Transfer Length

A value for transfer length is generally determined from the constructed strain profile at each beam end. Methods for determining transfer length include the 95% Average Maximum Strain Method (11, 23), the 100% Average Maximum Strain Method (9, 16), and the Slope-Intercept Method (7, 19). All of these methods require a fairly well-defined uniform strain plateau, which was not present in the strain profiles for the beam ends in this study shown in Section 4.2.2. These methods were therefore inapplicable.

In this study, transfer lengths were determined by inspection of the strain profile for each beam end. The transfer length was determined as the length from the beam end at which the linearly increasing region of the strain profile ends. Strain profiles for each beam end may be found in Section 4.2.2. Transfer lengths are presented in units of *inches* for comparison with previous research and empirical equations presented in the literature.

The transfer length for beam end D1N was thus approximately 17 inches. For beam ends D2N and D2S, the transfer length was approximately 13 inches. The transfer length for beam end D1S was indeterminable owing to the lack of a linearly increasing strain region, though the transfer length is possibly less than 7 inches. The average transfer length, as reported in Table 5.1, is 14.3 inches.

Table 5.1 Transfer lengths for specimen beam ends

Beam End	**Transfer Length (in.)**
D1N	17
D1S	N/A [(1)]
D2N	13
D2S	13
Average Transfer Length	14.3

[(1)] *Transfer length for beam end D1S was indeterminable due to lack of a linearly increasing strain region.*

5.2.2 Discussion of End Slip Measurements

The measured end slip may be used to approximate transfer length. The elastic shortening of the strand over the 150 mm (6.0 in.) free length is subtracted from the measured end slip to determine the actual end slip. The transfer length can then be determined from the corrected end slip by the equation (23):

$$L_t = \frac{2 \cdot \text{Slip} \cdot E_{ps}}{f_{si}}$$

Transfer lengths based on the average measured end slips for each beam end reported in Section 4.2.3 were computed and are listed in Table 5.2. The average measured end slip of 2.5 mm (0.098 in.) relates to a computed transfer length of 14.8 inches. This value correlates extremely well with the average transfer length of 14.3 in. reported in Section 5.2.1. However, since end slips were made only to the nearest 0.8 mm (1/32-in.), the accuracy of this computation is somewhat marginal.

Table 5.2 Calculation of transfer length from measured end slips

Beam End	Measured End Slip	Actual End Slip [(1)]	$L_t = \frac{2 \cdot \text{Slip} \cdot E_{ps}}{f_{si}}$
D1N	0.109	0.065	17.9
D1S	0.089	0.045	12.4
D2N	0.078	0.034	9.3
D2S	0.115	0.071	19.5
AVERAGE	0.098	0.054	14.8

[(1)] *Actual end slip = (Measured end slip) – (elastic shortening)*

$$\text{Elastic Shortening} = \frac{f_{si} \cdot \text{Free Length}}{E_{ps}} = \frac{(203.7\ \text{ksi})(6\ \text{in.})}{28000\ \text{ksi}} = .044\ \text{in.}$$

Note: All values are in inches

1 in. = 25.4 mm

5.2.3 Comparisons with Previous Research

The measured transfer lengths reported by selected researchers are summarized in Table 5.3. Little data are available on the transfer length of 15.2 mm (0.6 in.) diameter strands in high performance (high strength) concrete. The results of Barrios and Burns (2) and Mitchell et al. (19) are comparable to, though slightly larger than, the average measured

transfer length of 14.3 in. in this study. The results of Bruce et al. (4) and Castrodale et al. (9) for 12.7 mm (0.5 in.) strands in high performance concrete also fall into the same general range of low transfer lengths. The transfer lengths reported in those studies that used 15.2 mm (0.6 in.) diameter strands in normal strength concrete are significantly higher than the results of this study. Note that the strand condition, an important variable affecting transfer length, is difficult to quantify in any of these tests. However, in this study and that of Barrios and Burns (2), the surface condition of the 15.2 mm (0.6 in.) diameter strands was rusty.

Table 5.3 Reported transfer lengths from previous research

	Strand Diameter mm (in.)	f'_{ci} MPa (psi)	**Transfer Length** (in.)
15.2 mm (0.6 in.) diameter strands			
Burdette et al. (1994) (7)	15.2 (0.6)	28.3– 37.6 (4,100–5,450)	(21–30)
Cousins et al. (1990) (10)	15.2 (0.6)	32.7–32.8 (4,740–4,750)	(44–68) [(1)]
Cousins et al. (1990) (10)	15.2 (0.6)	28.9–32.7 (4,190–4,740)	(22–39) [(2)]
Russell and Burns (1993) (23)	15.2 (0.6)	26.5–33.0 (3,850–4,790)	(41)
Lane (1992) (16)	15.2 (0.6)	29.9 (4,330)	(43) [(1)]
Lane (1992) (16)	15.2 (0.6)	29.9 (4,330)	(26) [(2)]
Kaar et al. (1963) (14)	15.2 (0.6)	11.4–34.5 (1,660–5,000)	(28–52)
High Performance Concrete			
Bruce et al. (1994) (4)	12.7 (0.5)	59.3–70.3 (8,600–10,200)	(21)
Castrodale et al. (1988) (9)	12.7 (0.5)	64.8 (9,400)	(11–19)
15.2 mm (0.6 in.) Diameter Strands AND High Performance Concrete			
Barrios and Burns (1994) (2)	15.2 (0.6)	54.3–63.0 (7,880–9,130)	(18–27) [(3)]
Mitchell et al. (1993) (19)	15.7 (0.62)	47.9 (6,950)	(17–21)

1 in. = 25.4 mm
[(1)] *Uncoated strands.*
[(2)] *Epoxy coated strands with grit.*
[(3)] *Finite element analysis by Baxi (3) reported transfer length of 18 in.*

5.2.4 Comparisons with Equations for Transfer Length

Several equations were used to predict transfer length for the specimen beams in this study. The values predicted by these equations are reported in Table 5.4. The actual equations may be found in Table 2.1. Calculations are based on measured material properties (i.e., companion concrete cylinder test results) where applicable. The effective prestress force, f_{se}, was assumed to be 1,360 MPa (197.0 ksi) at transfer, based on a calculated elastic shortening loss of 3.3% at the beam ends. All of the equations predicted transfer lengths significantly larger than the 14.3 in. average transfer length measured in this study.

Table 5.4 Calculated transfer lengths from selected equations

Equation	**Calculated Transfer Length** (in.)
AASHTO/ACI 318 (24, 6)	39.4
AASHTO/ACI 318 (Shear provision) (24, 6)	30.0
Martin and Scott (18)	48.0
Zia and Mostafa (26)	21.4
Cousins, Johnston, and Zia (10)	27.0 [(1)]
Russell and Burns (23)	59.1
Mitchell et al. (19)	26.6
Burdette, Deatherage, and Chew (7)	40.7
Buckner (FHWA) (5)	25.5 [(2)]

1 in. = 25.4 mm
Note: f_{se} = 1,360 MPa (197.0 ksi) at transfer.
[(1)] Assumed U'_t = 10.6 to account for rusted strand condition.
[(2)] Unsimplified form of Buckner's TL equation;
Assumed E_c = 6,000 ksi at transfer.

The AASHTO/ACI 318 equation for transfer length, which is actually an implicit part of the development length equation in the codes, predicted a transfer length of 39.4 inches. This calculated transfer length is 2.76 and 2.32 times the average and maximum values observed in this study. In this particular case, with high concrete strength and rusted 15.2 mm (0.6 in.) diameter strands, the code equation is clearly very conservative.

Although still conservative, the best predictions for transfer length came from the equations that include f'_{ci}, the concrete strength at transfer, or E_c, the modulus of elasticity at transfer, as a parameter. Zia and Mostafa's (26) equation predicted a transfer length of 21.4 in., larger than the average measured value by a factor of 1.50. The equation proposed by Mitchell et al. (19) predicted a transfer length of 26.6 in., 1.86 times the average measured value in this study. Buckner's (5) equation, which includes the concrete stiffness

at transfer, predicted a transfer length of 25.5 in., 1.78 times the measured value. Cousins, Johnston, and Zia's (10) analytical model, the only equation to include a factor for the strand condition, predicted a value of 27.0 in., 1.89 times the measured value. Note that the results of this equation are highly sensitive to the assumption of U'_t, the bond stress factor, which is dependent on the strand condition.

5.2.5 Problems and Sources of Error

The only significant problem in the transfer length measurements in this study was the scatter of data and the resulting lack of a well-defined strain plateau. This scatter is effectively the result of the use of a mechanical concrete surface strain gauge system. The possible sources of error that may have contributed to the scatter of data are listed below:

Bonding of DEMEC Target Discs—DEMEC target discs must be fully bonded to the concrete surface before initial readings are performed. Because of the low ambient temperature during the installation of points, the epoxy took longer to set than anticipated. As a result, certain points may not have completely bonded before initial readings were taken.

Temperature Fluctuation—Temperature fluctuations of the concrete surface between readings will induce apparent strains that will be incorporated into measurements. Though the ambient temperature was relatively constant during both sets of readings, the temperature of the concrete surface was likely changing because of the high temperature gradient between the beam and the surrounding air. This is especially a problem when instrumenting high strength concrete specimens at early ages because of the very high hydration temperatures.

Reading Errors—In an effort to increase repeatability of readings, initial and final measurements on each beam end were read by the same person. However, the DEMEC points were located approximately 300 mm (12 in.) from the ground, making the measurements difficult to read. The possibility of reading errors was therefore increased.

As mentioned in Section 3.5.1, the overall accuracy of the DEMEC system is reported to be approximately 16 microstrains (1). The accuracy may have been decreased by any of these factors.

5.3 DEVELOPMENT LENGTH TESTS

5.3.1 Determination of Development Length

The determination of a value for development length is an iterative procedure involving many experimental tests. Identical specimens must be tested with various embedment lengths and the modes of failure of each experimental test must be noted. The

development length is the embedment length at which either flexural or bond failure may theoretically occur. Tests with embedment lengths longer than the development length will result in flexural failures, and tests with embedment lengths shorter than the development length will result in bond failures.

In the series of experimental tests in this study, flexural failures were noted for embedment lengths of 163, 119, 102, and 78 in., and no bond failures were observed. As a result, an exact value for development length could not be determined. It can only be stated that for this test series the development length is *less than 78 in*.

5.3.2 Discussion of Moment Capacities

The ultimate moment capacity of the specimen cross section was calculated using two methods: the ACI 318 method (6), and a strain compatibility analysis. The moment capacity calculated using ACI 318 Equation (18-3), which is similar to AASHTO Equation (9-17), and a rectangular stress block approach is 4,644 kN-m (1,044 ft-kip). With the inclusion of a strength reduction factor of 0.90, the ACI moment capacity becomes 4,179 kN-m (940 ft-kip). Based on the strain compatibility analysis, the ultimate moment capacity is 5,206 kN-m (1,171 ft-kip). A complete moment-curvature analysis for the specimen cross section, based on the strain compatibility approach, may be found in Appendix D.

The maximum total moment for each test, M_{test}, and a comparison to calculated moment capacities may be found in Table 5.5. The maximum total moment for each test is the algebraic sum of the moment due to applied loads, moment caused by the test setup (i.e., spreader beam and bearing plates), and the beam self-weight.

Table 5.5 Measured and predicted moment capacities for development length tests

Test	M_{test} [(1)] kN-m (ft-kip)	$M_{u,ACI}$ kN-m (ft-kip)	$\frac{M_{test}}{M_{u,ACI}}$	$\phi M_{u,ACI}$ kN-m (ft-kip)	$\frac{M_{test}}{\phi M_{u,ACI}}$	$M_{u,analysis}$ ***kN-m (ft-kip)***	$\frac{M_{test}}{M_{u,analysis}}$
1-D1N-163	5,173 (1,163)	4,644 (1,044)	1.11	4,179 (940)	1.24	5,206 (1,171)	0.99
2-D1S-119	5,240 (1,178)	4,644 (1,044)	1.13	4,179 (940)	1.25	5,206 (1,171)	1.01
3-D2N-102	5,355 (1,204)	4,644 (1,044)	1.15	4,179 (940)	1.28	5,206 (1,171)	1.03
4-D2S-78	5,298 (1,191)	4,644 (1,044)	1.14	4,179 (940)	1.27	5,206 (1,171)	1.02

(1) M_{test} includes applied load, self-wt., and test setup moments.

Note: $M_{u,ACI}$ is calculated using ACI Eq. 18-3, which is similar to AASHTO Eq. 9-17.

As expected for a flexural failure, maximum moments exceeded the design moment capacities and reached the moment capacities computed by a detailed analysis. Maximum total moments were 11% to 15% larger than the capacity predicted by the ACI 318 method, and 24% to 28% larger than the capacity predicted by the ACI 318 method with the inclusion of a strength reduction factor. Maximum total moments for each test were within 3% of the moment capacity calculated by the strain compatibility approach.

5.3.3 Comparisons with Previous Research

Development lengths reported by selected researchers are summarized in Table 5.6. Only Mitchell et al. (19) have studied the development length of 15.2 mm (0.6 in.) diameter strands in high performance (high strength) concrete. They reported a development length of approximately 30 inches. Development lengths reported by other researchers (7, 10, 23) for 15.2 mm (0.6 in.) diameter strands in normal strength concretes (f'_c less than 55 MPa [8,000 psi]) generally range from 64 to 85 in., except for the 132 in. development length reported by Cousins et al. (10) for uncoated strands. These results generally agree with the findings of this study: a development length less than 78 in. for 15.2 mm (0.6 in.) diameter strands in high performance concrete.

Table 5.6 Reported development lengths from previous research

	Strand Diameter mm (in.)	f'_c MPa (psi)	**Development Length** (in.)
0.6 in. diameter strands			
Burdette et al. (1994) (7)	15.2 (0.6)	35.4–55.0 (5,130–7,980)	(85)
Cousins et al. (1990) (10)	15.2 (0.6)	45.8 (6,640)	(132) [(1)]
Cousins et al. (1990) (10)	15.2 (0.6)	45.8 (6,640)	(64) [(2)]
Russell and Burns (1993) (23)	15.2 (0.6)	43.9–51.3 (6,360–7,440)	(84) [(3)]
Russell and Burns (1993) (23)	15.2 (0.6)	48.4 (7,020)	(< 78) [(4)]
0.6 in. Diameter Strands* and *High Strength Concrete			
Mitchell et al. (1993) (19)	15.7 (0.62)	65.0 (9,430)	(30)

1 in. = 25.4 mm
[(1)] *Uncoated strands.*
[(2)] *Epoxy coated strands with grit.* [(3)] *AASHTO-type beams.*
[(4)] *Rectangular beams.*

5.3.4 Comparisons with Equations for Development Length

Development length for the Hoblitzell-Buckner beams was predicted using several equations. Calculated development lengths are summarized in Table 5.7. The actual equations are listed in Table 2.1. Since almost all of the equations significantly depend on the assumed value of f_{ps}, the ultimate stress in the strands, two calculations were performed with each equation. The first calculation assumed f_{ps} = 1,725 MPa (250.2) ksi, the value calculated by ACI 318 Equation (18-3). The second calculation assumed f_{ps} = 1,917 MPa (278.0 ksi), the ultimate stress in the strands calculated by a strain compatibility analysis based on measured material properties. For all calculations, the effective prestress force was assumed to be 1,264 MPa (183.3 ksi), based on prestress losses of 10% at the time of testing, calculated by the PCI General Method (21).

Table 5.7 Calculated development lengths from selected equations

Equation	**Calculated Development Length f_{ps} = 250.2 ksi** (in.)	**Calculated Development Length f_{ps} = 278.0 ksi** (in.)
AASHTO/ACI 318(24, 6)	79.5	96.2
Martin and Scott (18)	158.8	201.5
Zia and Mostafa (26)	86.4	86.4
Cousins, Johnston, and Zia (10)	41.8 (1)	47.9 (1)
Mitchell et al. (19)	50.1	59.8
Burdette, Deatherage, and Chew (7)	100.9	125.9
Buckner (FHWA) (5)	105.8 (2)	139.1

1 in. = 25.4 mm
Note: f_{se} = 1264 MPa (183.3 ksi) at time of flexural testing.
(1) Assumed U'_d = 4.55 to account for rusted strand condition.
(2) λ=2.0 for both cases; TL calculated using unsimplified equation (see Table 2.1).

The AASHTO/ACI 318 equation for development length predicted a value of 79.5 in. for f_{ps} = 1,725 MPa (250.2 ksi). This value is conservative compared to the results of this study, though the exact factor of safety is unknown. The calculated development length using the AASHTO/ACI 318 equation and f_{ps} = 1,917 MPa (278.0 ksi) was 96.2 inches. This value predicts the length of bond required to develop the *actual* stress in the strands at failure. This calculation is therefore more physically representative of the development length and is conservative by *at least* a factor of 1.23.

Calculated values for development length using other equations exhibited a large degree of scatter. Predicted development lengths ranged from 41.8 inches to 201.5 inches. The predicted development lengths from those equations that considered the effect of concrete strength (10, 19) ranged from 41.8 inches to 59.8 inches. It is impossible to determine the degree, if any, to which these equations are conservative.

Note that both the Burdette et al. (7) and Buckner (5) equations predict conservative values for development length compared to the measured values. Both equations essentially take the form of the AASHTO/ACI 318 equation, with a multiplier greater than 1.0 applied to the flexural bond length term. Since the AASHTO/ACI 318 equation is conservative to some degree, both the Burdette et al. and Buckner equations are clearly conservative with respect to the results of this study.

5.3.5 Problems and Sources of Error

The main deficiency in the test program was the inability to determine an exact value for development length. It would have been desirable to have at least one bond failure out of the four tests, so that a lower bond for the development length might be obtained. Unfortunately, tests performed with embedment lengths much lower than 78 in. would have fallen into the category of deep beams, since the depth of the cross section was 42 inches. This would have made the results of such tests questionable.

Significant measurement errors did not occur during the four development length tests. The only source of error occurred in the measurement of maximum top fiber concrete strains, as the measured maximum strains generally did not coincide with crack locations. The actual maximum top fiber strains, which would occur at the crack locations, may therefore have been somewhat higher than the reported values. Each test was stopped when the actual top fiber strain was felt to be very close to the crushing strain.

5.4 EFFECT OF VARIABLES

The effect of several variables on transfer and development length is discussed in Section 2.4. This study examined one specific combination of these variables. Large diameter strands (15.2 mm or 0.6 in.), with high initial prestress (1,404 MPa or 203.7 ksi) and flame-cut at release, would generally be expected to produce high transfer and development lengths. However, these effects were apparently outweighed in this case by the effects owing to high concrete strength (f'_{ci} = 48.5 MPa [7,040 psi] and f'_c = 90.7 MPa [13,160 psi]) and a rusted strand condition, resulting in a very low average transfer length (14.3 in.), and a reasonably short development length (less than 78 in.). These results verify the potential benefits of high performance concrete and roughened strand conditions for transfer and development length. Although the benefits of high concrete strength may be incorporated into empirical equations, once sufficient data are available the benefits caused by roughened strand conditions may be difficult to quantify.

CHAPTER 6. SUMMARY AND CONCLUSIONS

6.1 SUMMARY

This study examined the transfer and development length of 15.2 mm (0.6 in.) diameter prestressing strands at 51 mm (2.0 in.) spacing in fully bonded high strength rectangular beams. Specimen beams, called the Hoblitzell-Buckner beams, were 1,067 mm (42 in.) deep and 356 mm (14 in.) wide, and contained six 15.2 mm (0.6 in.) diameter strands at 51 mm (2.0 in.) spacing and cover. Nonprestressed compression reinforcement was provided in the specimens in the form of three #9 top bars, to raise the neutral axis in bending and to induce high strains in the strand. Concrete strengths were 48.5 MPa (7,040 psi) at transfer and 90.7 MPa (13,160 psi) at the time of development length testing. The strand condition was weathered or rusty.

Transfer length was determined by constructing a concrete strain profile at the level of the strand at transfer. The strain profile was constructed using the DEMEC mechanical strain gauge system in which small stainless steel discs are bonded to the concrete surface and small changes in distance between the points, or strains, are read using a mechanical strain gauge. All instrumentation and measurements for transfer length were performed during the fabrication process at the prestressing plant.

Development length was measured through an iterative process involving four full-scale flexural tests performed at the Phil M. Ferguson Structural Engineering Laboratory at The University of Texas at Austin. The Hoblitzell-Buckner beams were loaded with various embedment lengths, and the mode of failure in each test was monitored. Applied load, deflections, end slips, and top fiber concrete strains were measured continuously throughout each test. Crack patterns were documented in detail.

6.2 CONCLUSIONS

The following conclusions were drawn from this study:

1) The average transfer length for the 15.2 mm (0.6 in.) diameter strands in high performance concrete with a rusty surface condition is 14.3 inches.
2) The development length for the 15.2 mm (0.6 in.) diameter strands in high performance concrete with a rusty surface condition is less than 78 inches.
3) The AASHTO/ACI 318 Code equations for transfer and development length are conservative *in this case*. The code prediction for transfer length is conservative by a factor of 2.76. The degree to which the development length equation is conservative cannot be determined.
4) All proposed transfer length equations selected from the literature are conservative compared with the results of this study. Many of the development length equations proposed in the literature are conservative.

5) The following parameters significantly reduced transfer and development length in this study: high concrete strengths and rusted strand conditions.
6) Little data are available on transfer and development length of 15.2 mm (0.6 in.) diameter strands in high performance concrete. Significant amounts of research are needed as the use of these materials becomes standard in practice.

REFERENCES

1. Arrellaga, J. A., "Instrumentation Systems for Post-Tensioned Segmental Box Girder Bridges," Master's Thesis, The University of Texas at Austin, December 1991.

2. Barrios, A. O., "Behavior of High Strength Concrete Pretensioned Girders During Transfer of Prestressing Forces," Master's Thesis, The University of Texas at Austin, May 1994.

3. Baxi, A., and Burns, N. H., *Technical Memorandum No. 2*, Research Project 9-580, Center for Transportation Research (CTR), The University of Texas at Austin, March 1993.

4. Bruce, R. N., Martin, B. T., Russell, H. G., and Roller, J. J., "Feasibility Evaluation of Utilizing High-Strength Concrete in Design and Construction of Highway Bridge Structures," Research Report No. 282, Louisiana Transportation Research Center, January 1994.

5. Buckner, C. D., "An Analysis of Transfer and Development Lengths for Pretensioned Concrete Structures," Publication No. FHWA-RD-94-049, Federal Highway Administration (FHWA), December 1994.

6. *Building Code Requirements for Reinforced Concrete*, ACI 318-89, American Concrete Institute, 1989.

7. Burdette, E. G., Deatherage, J. H., and Chew, C. K., "Development Length and Lateral Spacing Requirements of Prestressing Strand for Prestressed Concrete Bridge Girders," *PCI Journal*, Vol. 39, No. 1, January/February 1994, pp. 70–83.

8. Carrasquillo, R. L., Nilson, A. H., and Slate, F. O., "Properties of High Strength Concrete Subject to Short-Term Loads," *ACI Journal*, Vol. 78, No. 3, May/June 1981, pp. 171–178.

9. Castrodale, R. W., Burns, N. H., and Kreger, M. E., "A Study of Pretensioned High Strength Concrete Girders in Composite Highway Bridges—Laboratory Tests," Research Report 381-3, CTR, The University of Texas at Austin, January 1988.

10. Cousins, T., Johnston, D., and Zia, P., "Transfer and Development Length of Epoxy Coated Prestressing Strand," *PCI Journal*, Vol. 35, No. 4, July/August 1990, pp. 92–103.

11. Hanson, N. W., "Influence of Surface Roughness of Prestressing Strand in Bond Performance," *PCI Journal*, Vol. 14, No. 1, January/February 1969, pp. 32–45.

12. Hanson, N. W., and Kaar, P. H., "Flexural Bond Tests of Pretensioned Prestressed Beams," *ACI Journal*, Vol. 55, No. 7, 1959, pp. 783–803.

13. Janney, J. R., "Nature of Bond in Pre-Tensioned, Prestressed Concrete," *ACI Journal*, Vol. 50, 1954, pp. 717–736.

14. Kaar, P. H., LaFraugh, R. W., and Mass, M. A., "Influence of Concrete Strength on Strand Transfer Length," *PCI Journal*, Vol. 8, No. 5, 1963, pp. 47–67.

15. Lane, S. N., "Development Length of Prestressing Strand," *Public Roads—A Journal of Highway Research and Development*, FHWA, Vol. 54, No. 2, September 1990, pp. 200–205.

16. Lane, S. N., "Transfer Lengths in Regular Prestressed Concrete Concentric Beams," *Public Roads—A Journal of Highway Research and Development*, FHWA, Vol. 56, No. 2, September 1992, pp. 67–71.

17. Lin, T. Y., and Burns, N. H., *Design of Prestressed Concrete Structures*, John Wiley and Sons, 1981.

18. Martin, L. D., and Scott, N. L., "Development of Prestressing Strand in Pretensioned Members," *ACI Journal*, Vol. 73, No. 8, 1976, pp. 453–456.

19. Mitchell, D., Cook, W. D., Khan, A. A., and Tham, T., "Influence of High Strength Concrete on Transfer and Development Length of Pretensioning Strand," *PCI Journal*, Vol. 38, No. 3, May/June 1993, pp. 52–66.

20. Nilson, A. H., *Design of Prestressed Concrete*, John Wiley and Sons, 1987.

21. *PCI Design Handbook*, Prestressed Concrete Institute, Third Edition, 1985.

22. Ralls, M. L., Ybanez, L., and Panak, J. J., "The New Texas U-Beam Bridges: An Aesthetic and Economical Design Solution," *PCI Journal*, Vol. 38, No. 5, September/October 1993, pp.20–29.

23. Russell, B. W., and Burns, N. H., *Design Guidelines for Transfer, Development, and Debonding of Large Diameter Seven Wire Strands in Pretensioned Concrete Girders*, Research Report 1210-5F, CTR, The University of Texas at Austin, January 1993.

24. *Standard Specifications for Highway Bridges*, American Association of State Highway and Transportation Officials, Washington, D.C., 1992.

25. Tabatabai, H., and Dickson, T. J., "The History of the Prestressing Strand Development Length Equation," *PCI Journal*, Vol. 38, No. 6, November/December 1993, pp. 64–75.

26. Zia, P., and Mostafa, T., "Development of Prestressing Strands," *PCI Journal*, Vol. 22, No. 5, 1977, pp. 54–65.

APPENDIX A

CONTRACTOR DRAWINGS FOR HOBLITZELL-BUCKNER BEAMS

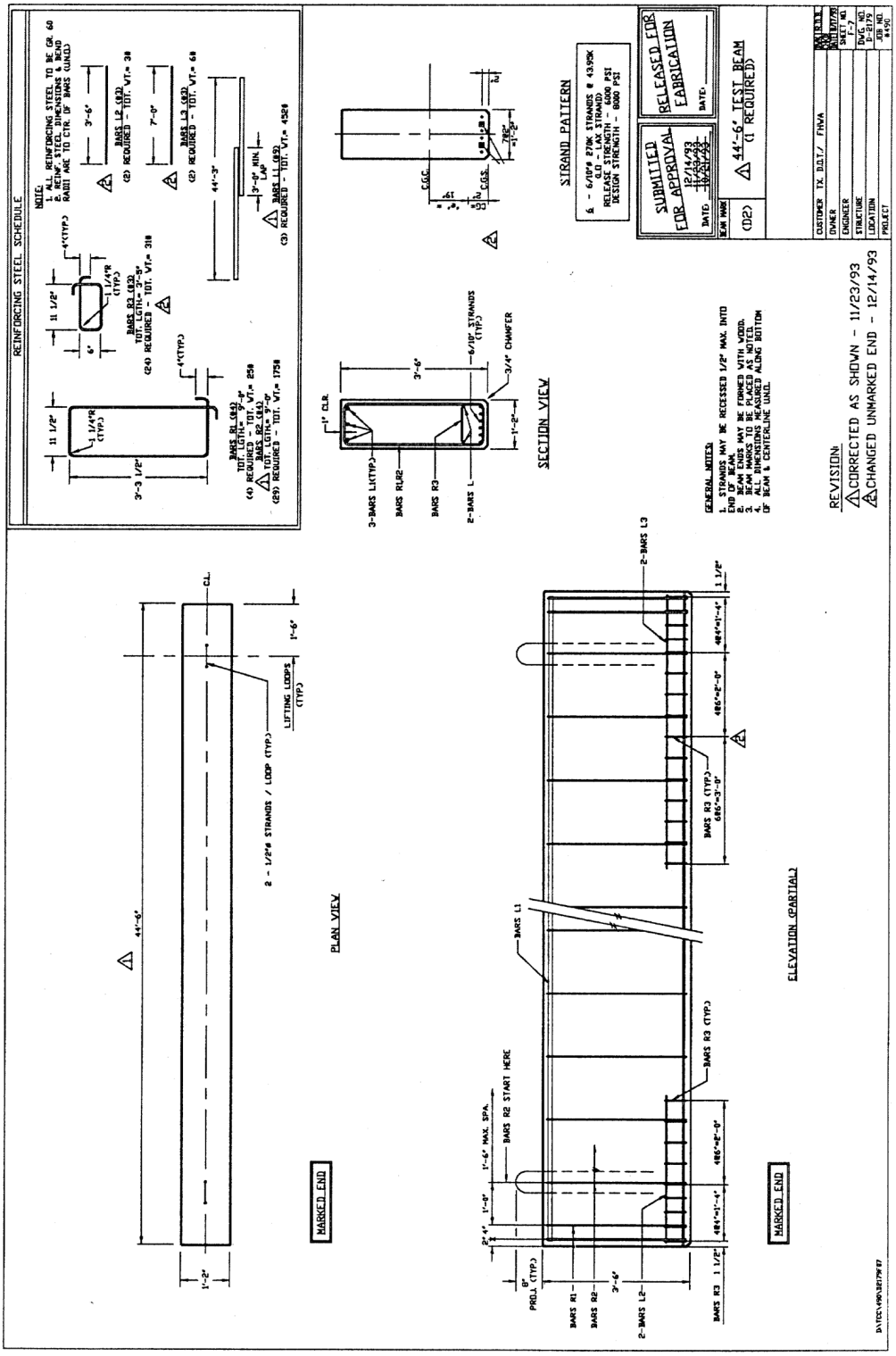

Figure A.1 Contractor drawing for test specimen beams

APPENDIX B

MATERIAL PROPERTY PLOTS

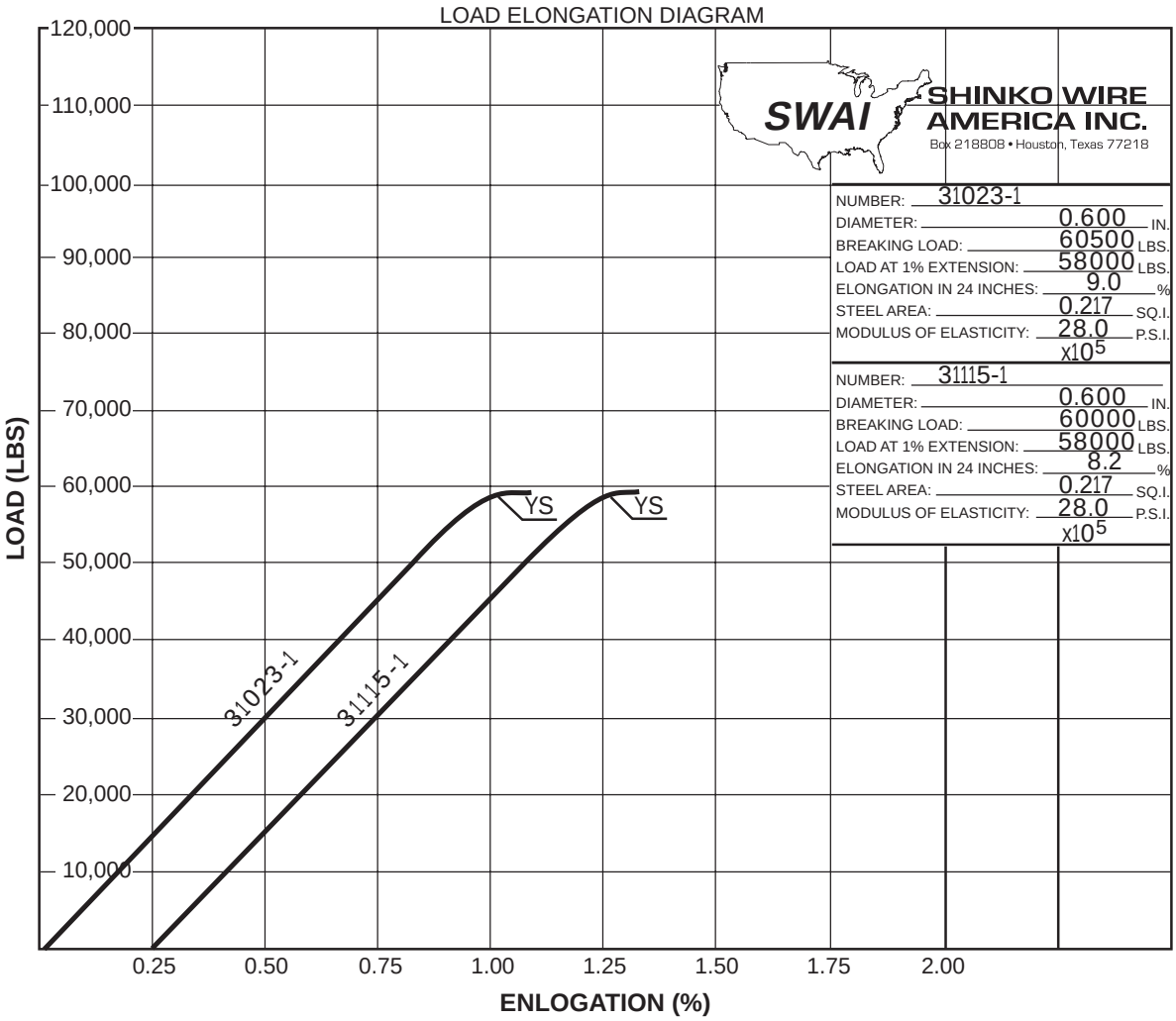

Figure B.1 Strand manufacturer tensile test results

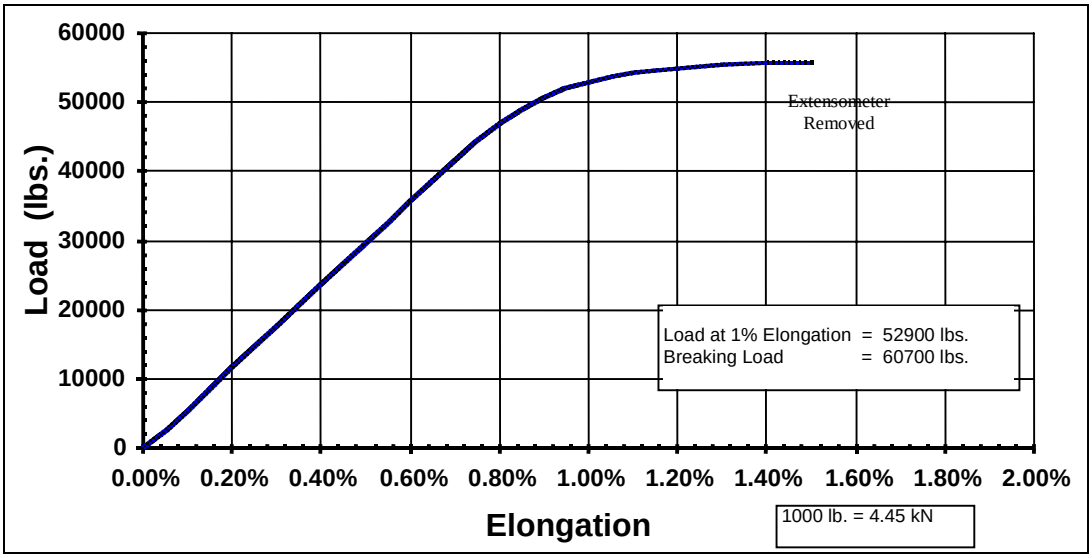

Figure B.2 CMRG tensile test results (Strand Sample 1)

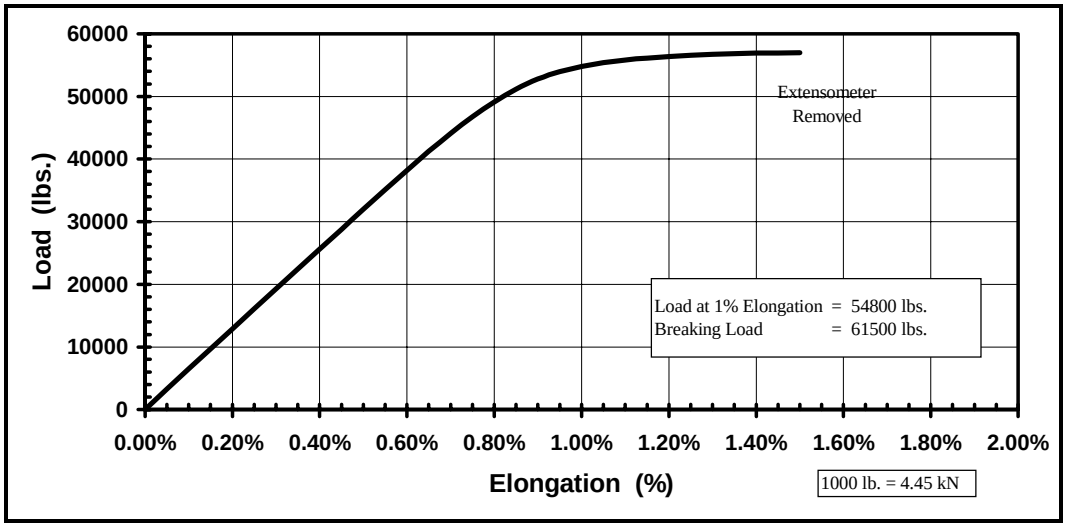

Figure B.3 CMRG tensile test results (Strand Sample 2)

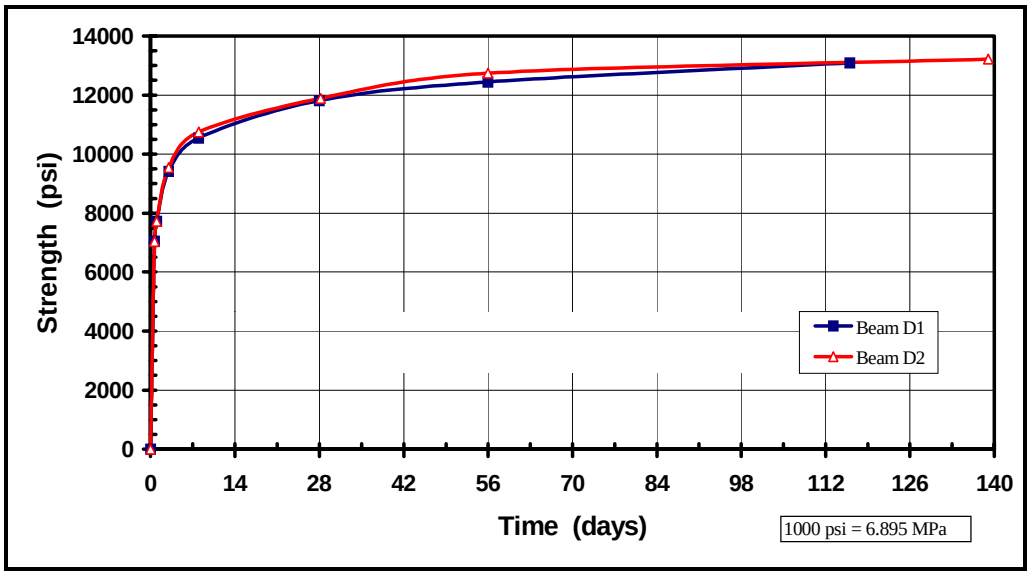

Figure B.4 Companion concrete cylinder compressive strength versus time

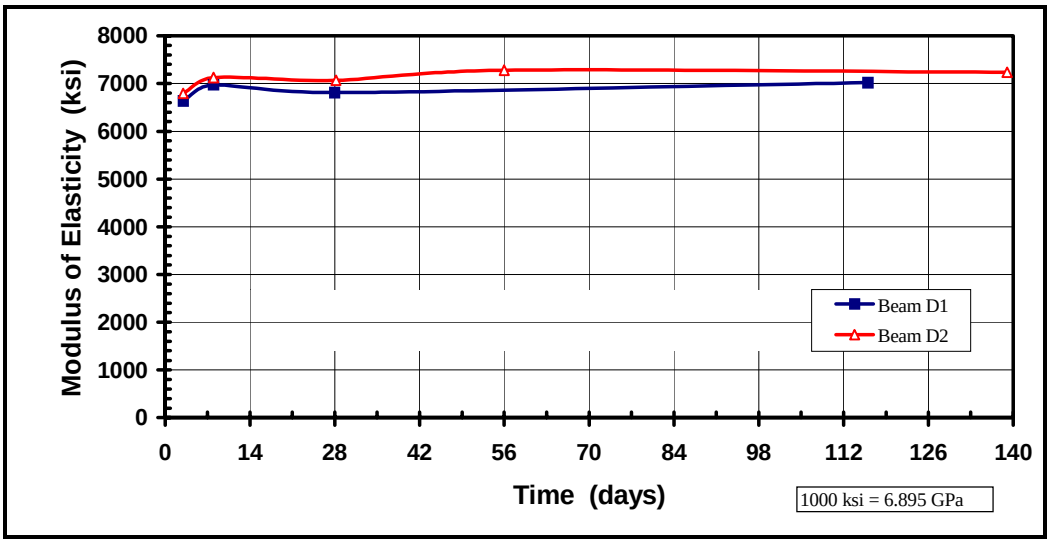

Figure B.5 Companion concrete cylinder modulus of elasticity versus time

APPENDIX C

DEVELOPMENT LENGTH TEST SETUPS

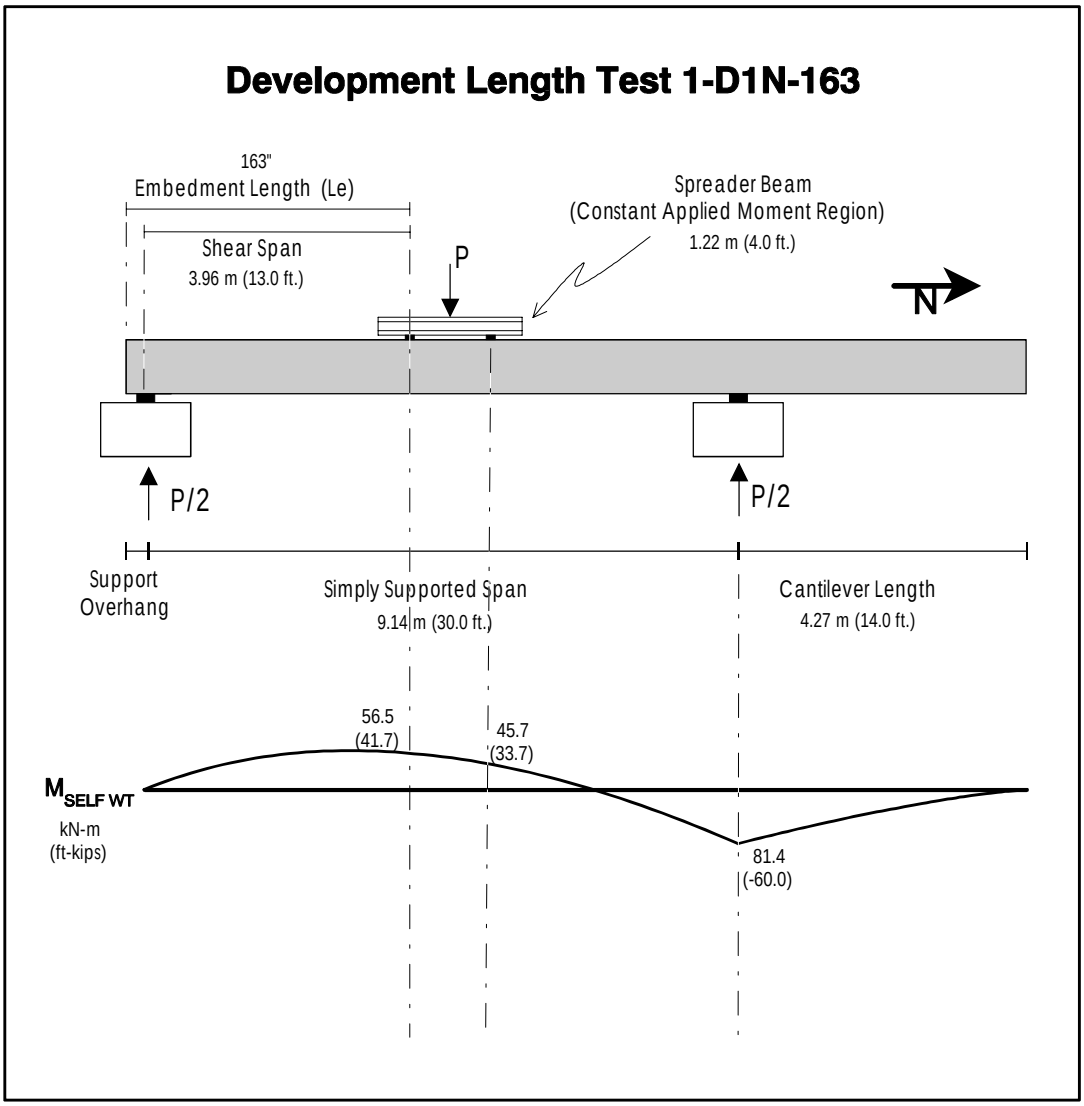

Figure C.1 Test 1-D1N-163 setup

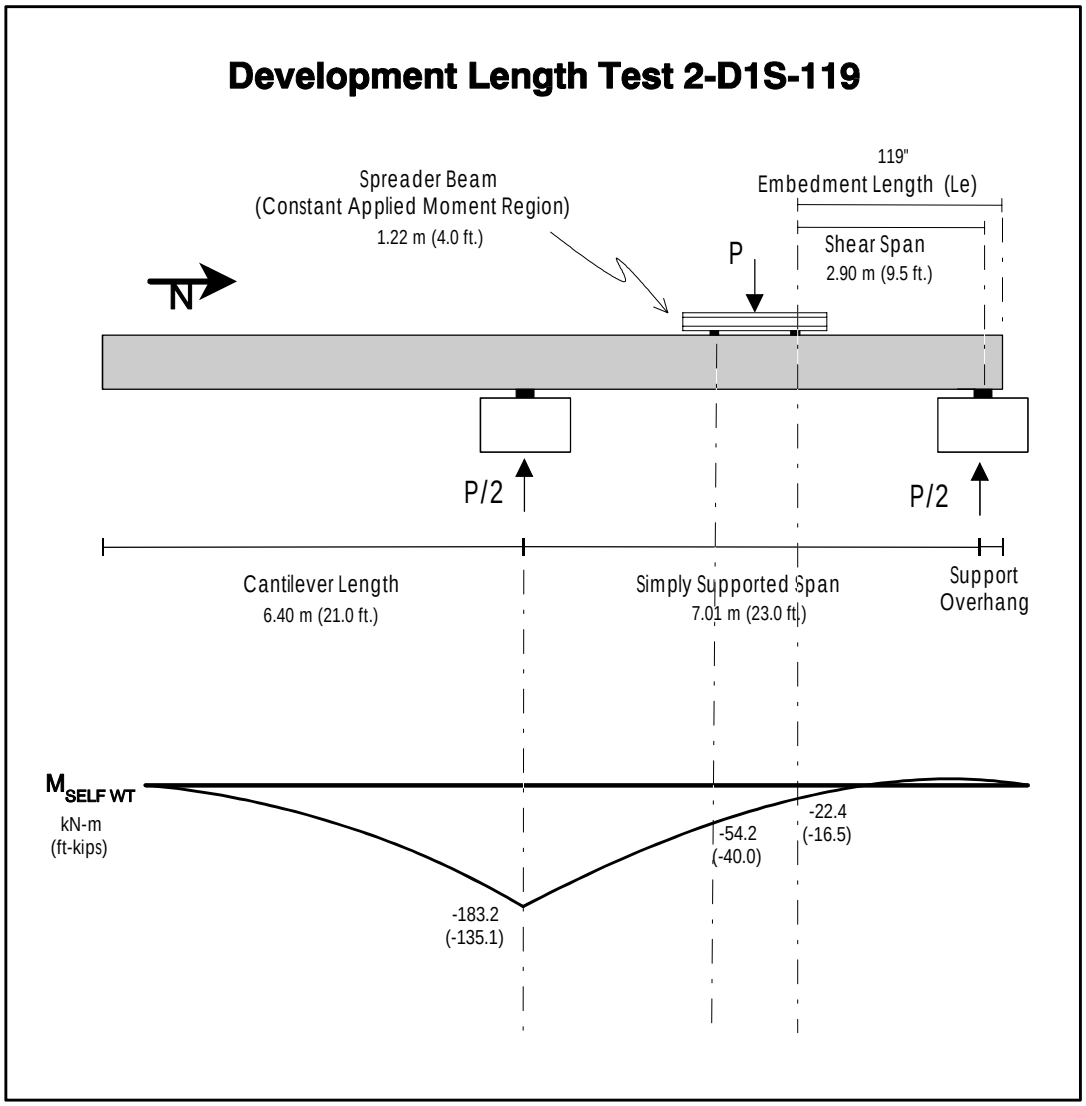

Figure C.2 Test 2-D1S-119 setup

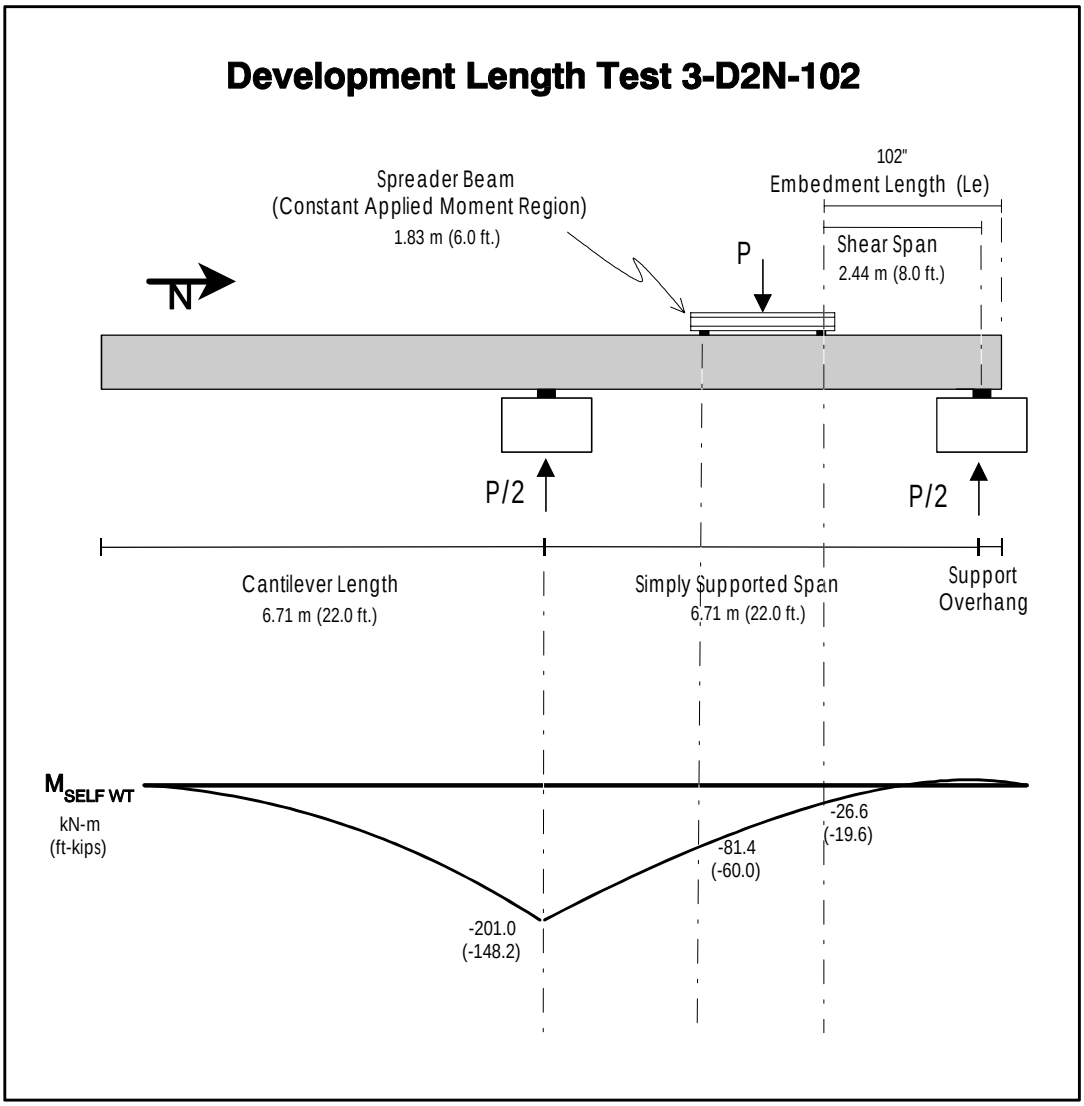

Figure C.3 Test 3-D2N-102 setup

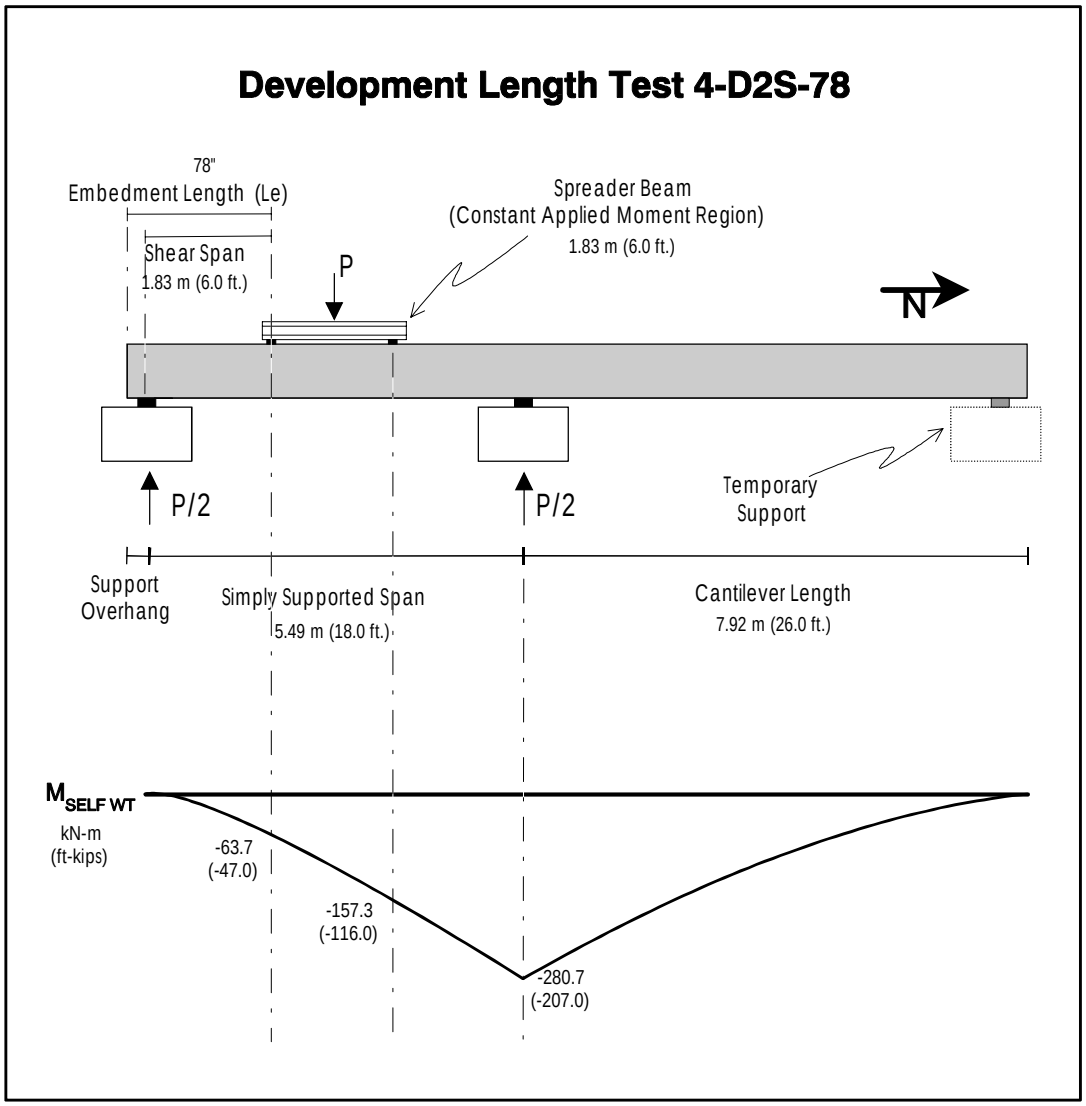

Figure C.4 Test 4-D2S-78 setup

APPENDIX D

MOMENT-CURVATURE SECTION ANALYSIS

A moment-curvature relationship was developed for the test specimen cross section on the basis of a strain-compatibility analysis. Specific details of the analysis procedure are discussed by Lin and Burns (17). The analysis is divided into two stages: before flexural cracking when elastic behavior is assumed, and after cracking when the actual stress-strain relationships of the materials are used. Results of the analysis are shown in Figure D.3 and Table D.1.

ASSUMPTIONS USED IN THE ANALYSIS:

Material Properties—Prestressing Steel

The assumed strand stress-strain relationship is shown in Figure D.1. The approximate equation is of the same form as that given by the PCI Handbook Section 11.2.5 (21), with modifications to accommodate the average measured strand properties reported in Section 3.3.1:

$$f_{ps}\ (\text{in ksi}) = \begin{cases} 28{,}000 \cdot \varepsilon_{ps} & \varepsilon_{ps} \le 0.008 \\ 279.6 - \dfrac{.0723}{\varepsilon_{ps} - .0067} & \varepsilon_{ps} > 0.008 \end{cases}$$

The assumed ultimate tensile strength of the strands is 1.928 GPa (279.6 ksi). The modulus of elasticity of the strands is taken as 193 GPa (28,000 ksi).

Material Properties—Concrete

The assumed concrete stress-strain curve, based on the Hognestad model, is shown in Figure D.2. The relationship is approximated by the equation:

$$f_c = f'_c \cdot \left[\frac{2 \cdot \varepsilon}{\varepsilon_0} - \left(\frac{\varepsilon}{\varepsilon_0} \right)^2 \right]$$

For this case, f'_c = 90.7 MPa (13,160 psi) and ε_0 = 0.003151.

The modulus of elasticity at the time of flexural testing is assumed to be 49.2 GPa (7,130 ksi), based on the material properties reported in Section 3.3.2. The modulus of rupture, f_r, is approximated as:

$$f_r = 10\sqrt{f'_c} = 1147 \text{ psi} = 7.909 \text{ MPa}$$

The coefficient in the preceding equation is based on the results of Carrasquillo, Nilson, and Slate (8) for high strength concrete.

Material Properties—Nonprestressed Steel

An idealized elastic, perfectly plastic stress-strain relationship is used for the nonprestressed compression steel. The yield strength is assumed to be 414 MPa (60 ksi), and the modulus of elasticity is assumed to be 200 GPa (29,000 ksi). The effects of strain hardening are neglected.

Transformed Section Properties

Transformed section properties are used in the elastic analysis prior to first cracking. The transformed section properties are as follows:

A = 388,000 mm^2 (601 in.^{2})
I = 37.9 x 10^9 mm^4 (91,110 in.^{4})
y_{bot} = 537.7 mm (21.17 in.)

Initial and Effective Prestress Force/Prestress Losses

An initial prestress force, f_{si}, of 1.405 GPa (203.7 ksi) is assumed based on measured elongations during actual stressing operations. Losses at the time of flexural testing are assumed to be 10%, resulting in an effective prestress force, f_{se}, of 1.264 GPa (183.3 ksi). Losses were calculated by the PCI General (Time-Step) Method (21).

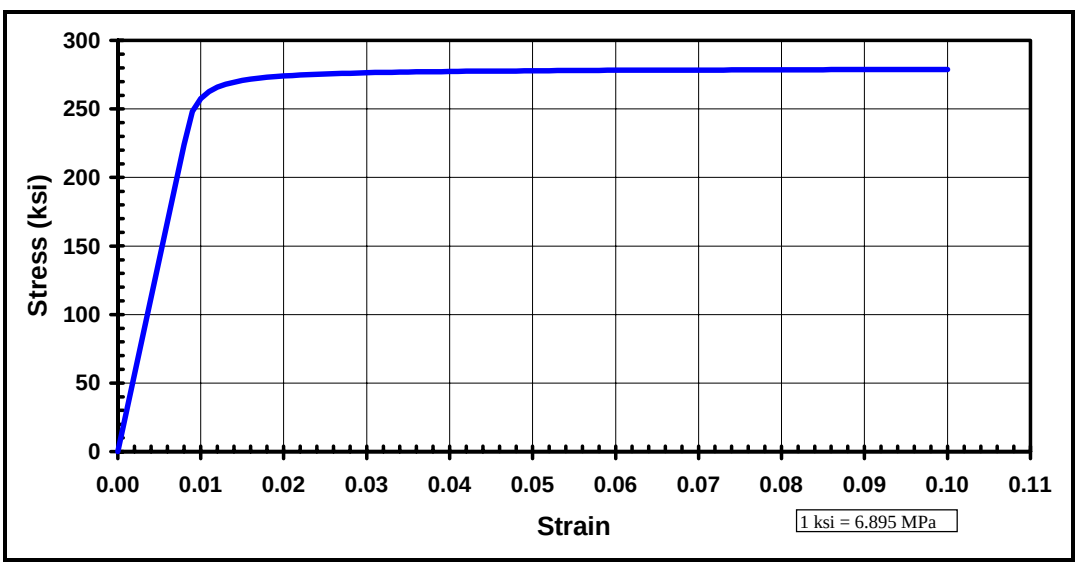

Figure D.1 Assumed strand stress-strain relationship

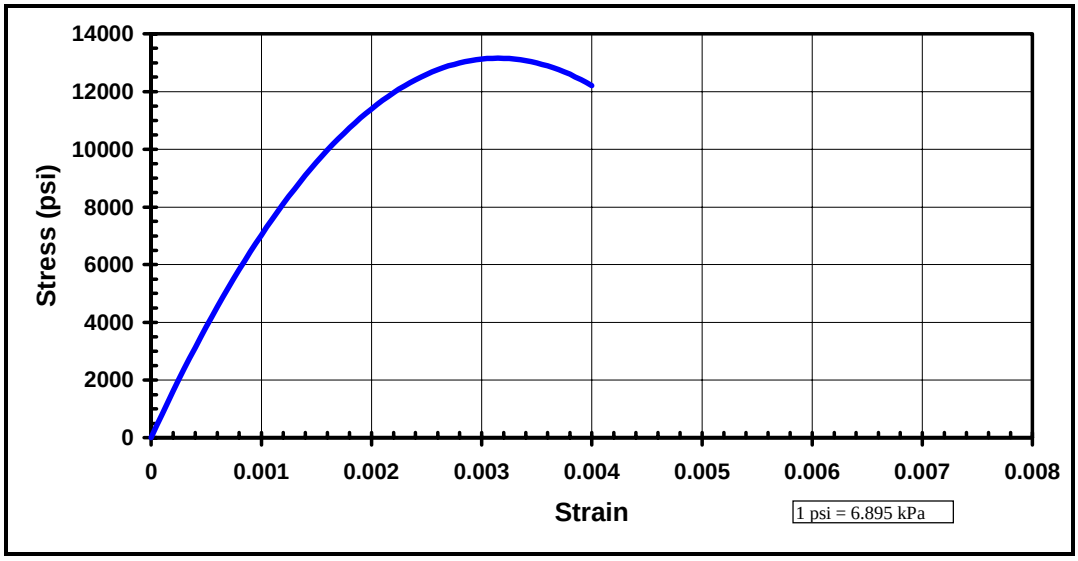

Figure D.2 Assumed concrete stress-strain relationship

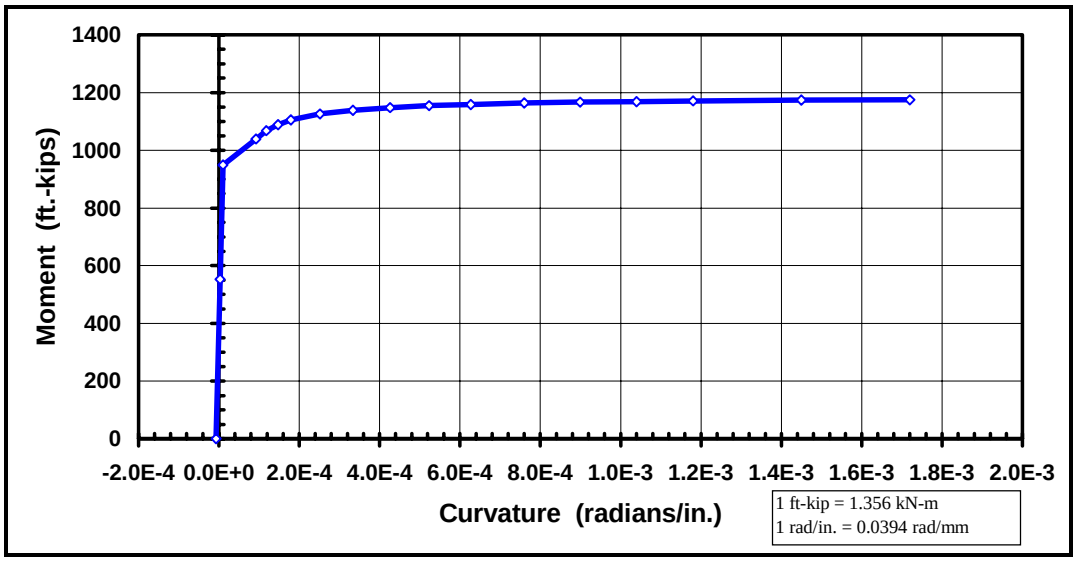

Figure D.3 Moment-curvature relationship for specimen cross section

Table D.1 Calculated moment-curvature points

ε_{top}	ϕ		M		ε_{ps}	f_{ps}		c	
(in./in.)	*(rad/mm)*	*(rad/in.)*	*(kN-m)*	*(ft-kips)*	*(%)*	*(MPa)*	*(ksi)*	*(mm)*	*(in.)*
-0.000080	-2.67E-07	-6.78E-06	0	0	0.655%	1264	183.3	301	11.86
0.000119	1.18E-07	2.99E-06	750	553	0.674%	1300	188.6	1016	40.00
0.000272	4.06E-07	1.03E-05	1287	949	0.688%	1327	192.5	670	26.38
0.000700	3.63E-06	9.22E-05	1409	1039	0.973%	1763	255.7	193	7.59
0.000800	4.65E-06	1.18E-04	1448	1068	1.060%	1802	261.3	172	6.79
0.000900	5.79E-06	1.47E-04	1477	1089	1.170%	1828	265.2	156	6.13
0.001000	7.05E-06	1.79E-04	1498	1105	1.290%	1847	267.9	142	5.59
0.001200	9.92E-06	2.52E-04	1527	1126	1.560%	1872	271.5	121	4.77
0.001400	1.31E-05	3.34E-04	1544	1139	1.870%	1886	273.6	106	4.19
0.001600	1.68E-05	4.26E-04	1557	1148	2.220%	1896	274.9	96	3.76
0.001800	2.06E-05	5.23E-04	1566	1155	2.590%	1902	275.8	87	3.44
0.002000	2.47E-05	6.27E-04	1572	1159	2.980%	1906	276.5	81	3.19
0.002250	2.99E-05	7.60E-04	1578	1164	3.490%	1910	277.0	75	2.96
0.002500	3.54E-05	8.99E-04	1582	1167	4.020%	1913	277.4	71	2.78
0.002750	4.09E-05	1.04E-03	1585	1169	4.550%	1915	277.7	67	2.65
0.003000	4.65E-05	1.18E-03	1588	1171	5.080%	1917	278.0	65	2.55
0.003500	5.71E-05	1.45E-03	1592	1174	6.130%	1919	278.3	61	2.41
0.004000	6.77E-05	1.72E-03	1593	1175	7.170%	1920	278.5	59	2.32

APPENDIX E

NOTATION

A	(Transformed) area of cross section
A_{strand}	Area of prestressing strand
B	Bond stress factor used in transfer length equation in Reference 10
d_b, D	Diameter of prestressing strand
E_c	Modulus of elasticity of concrete
E_{ci}	Modulus of elasticity of concrete at transfer
E_{ps}	Modulus of elasticity of prestressing strand
f_c	Stress in concrete
f_{ce}	Stress in concrete at level of strands (after losses)
f_{ps}, f^*_{su}	Stress in strands at failure
f_{pu}	Ultimate tensile strength of strands
f_r	Modulus of rupture of concrete
f_{se}	Stress in strands after losses
f_{si}	Stress in strands immediately before transfer
f'_c	Concrete compressive strength at 28 days
f'_{ci}	Concrete compressive strength at transfer
I	(Transformed) moment of inertia of cross section
L_b	Length of debonding for debonded strands
L_d	Development length of prestressing strands
L_e	Embedment length of prestressing strands
L_t	Transfer length of prestressing strands
M_{cr}	Cracking moment for cross section
M_{test}	Maximum total moment acting on cross section during testing
M_u	Moment capacity of cross section
n	Modular ratio of steel with respect to concrete
U'_d	Strand surface coefficient used in development length equation in Reference10
U'_t	Strand surface coefficient used in transfer length equation in Reference 10
V_u	Ultimate factored shear acting at a location along member
y_{bot}	Location of (transformed) centroid of cross section from bottom fiber
ε	Strain in concrete
ε_{ce}	Strain in concrete at level of strands (after losses)
ε_{se}	Strain in strands after losses (due to prestressing only)
ε_{si}	Strain in strands immediately before transfer
ε_0	Strain in concrete at compressive strength (f'_c)
ϕ	Strength reduction factor used in Reference 6